

ABSTRACT

GORSKI, JESSICA F. Deterministic, Dynamic Model Forecasts of Storm-Driven Erosion. (Under the direction of Casey Dietrich).

The U.S. Atlantic and Gulf coasts are vulnerable to storms, which can cause significant erosion of beaches and dunes that otherwise protect coastal communities. One example is Hurricane Ian (2022), which impacted Florida's Gulf coast and then again the southeast U.S. Atlantic coast, resulting in significant beach and dune scarping and breaches in multiple locations. Models can be used for real-time forecasts of storm-driven erosion, which can support decision-making, but are limited due to demands for computational resources and uncertainties in dynamic coastal systems. Current methods for erosion forecasts are based on empirical equations for wave run-up, which do not represent sediment transport during the storm, and on surrogate models, which also must rely on simplified representations of the system. However, with continued advancements in high-resolution geospatial data and computational efficiencies, there is an opportunity to apply morphodynamic models for deterministic forecasts of beach and dune erosion as a storm approaches the coast. Real-time morphodynamic model implementation is challenging because the framework must be accurate and efficient while maintaining versatility to account for forecast uncertainties. Additionally, the evaluation and post-processing for the model needs to effectively communicate the results, including the timing and scale of coastal change during an extreme event when temporal observations are unavailable.

In this study, we apply the state-of-art model eXtreme Beach (XBeach) to predict coastal erosion due to Hurricanes Michael (2018) and Ian (2022). Sandy beaches along the U.S. Atlantic and Gulf coasts are represented with thousands of one-dimensional transects, which are sampled for real-time forecasts based on the storms' tracks and projected landfall locations. The morphodynamic model is initialized with high-resolution digital elevation models of the present-day conditions and forced with hydrodynamics from high-resolution wave and circulation models, and its predictions are categorized based on impacts to the primary dune. A key contribution of this study is the semi-automation of the modeling system, so the modeling framework can be applied to different regions of the coast as the landfall location shifts.

To demonstrate this, forecasts for Ian (2022) were initiated several days before the initial landfall location in Punta Gorda, Florida, and continued as the track made a secondary landfall near Georgetown, South Carolina. About 1800 transects are selected for each of the 25 advisories. The simulations are monitored, evaluated, and visualized to communicate the XBeach predictions of coastal change. The framework produces results in less than an hour

and then publishes visualizations in less than 10 minutes. Results are compared spatially and temporally to qualitative post-Ian observations and total water level predictions. XBeach can predict dune impact compared to an established coastal change forecasting model while providing additional morphodynamic information not typically available, such as timing and magnitude of volume change. The addition of fully resolved ground surface information and morphodynamics in the model makes it possible to better understand the storm evolution and how that translates into erosion of beaches and dunes.

© Copyright 2023 by Jessica F. Gorski

All Rights Reserved

Deterministic, Dynamic Model Forecasts of Storm-Driven Erosion

by
Jessica F. Gorski

A thesis submitted to the Graduate Faculty of
North Carolina State University
in partial fulfillment of the
requirements for the Degree of
Master of Science

Civil Engineering

Raleigh, North Carolina
2023

APPROVED BY:

Elizabeth Sciaudone

Katherine Anarde

Rick Luettich

Casey Dietrich
Chair of Advisory Committee

DEDICATION

To my mom Eileen Gorski and sister Alicia Gorski.

For constantly supporting me and offering helpful advice, even if I do not always accept it.

BIOGRAPHY

Jessica Gorski was born in New Britain, Connecticut in 1999 to Eileen and Jozef Gorski. She graduated Plainville High School in 2017 before continuing her education at North Carolina State University. Following in the footsteps of her older sister, she decided to pursue a B.S. in engineering. During her undergraduate studies, she began participating in coastal engineering related research under the advice of then graduate student, Dr. Alireza Gharagozlou, and her now advisor, Dr. Casey Dietrich. She decided to continue her education at NCSU and pursue a M.S. in civil engineering with a focus in coastal engineering after completing her B.S. in May 2021. Outside of academia, she enjoys travel, dog walking, and playing volleyball with friends.

ACKNOWLEDGEMENTS

I would first like to thank my advisor Dr. Casey Dietrich for his encouragement, mentorship, and guidance over the past 4 years. I could not have asked for a better advisor and I am very thankful for all of the opportunities he has given me.

I would also like to thank my committee members for their contributions to my academic journey. Dr. Elizabeth Sciaudone first introduced me to coastal engineering and I could not be more appreciative. Dr. Katherine Anarde has been a great role model for me and Dr. Rick Luettich has shared invaluable knowledge and feedback.

I'd like to thank Dr. Alireza Gharagozlou for teaching me everything XBeach related. I appreciate his patience and willingness to meet at all hours of the night to help with code debugging or simulation errors. From the NOPP project, I'd like to thank Matt Bilskie, Robert Fiegelist, Davina Passeri, and RC Mickey for their collaboration and XBeach related advice.

I am also grateful for the coastal engineering team at NCSU for their support throughout both my undergraduate and graduate research. Thanks to Sophia, Lexi, Thomas, Tomás, Jenero, Johnathan, and many others for being a part of my life during my time at NCSU.

Lastly, I would like to thank my mother Eileen, my sister Alicia, and my extended family for their love and unwavering support. I am lucky to have such intelligent, independent, and successful women in my life. I cannot express the full extent of my gratitude. I would not be here without them.

TABLE OF CONTENTS

List of Tables	vii
List of Figures	viii
Chapter 1 INTRODUCTION	1
1.1 Funding Acknowledgment	7
Chapter 2 BACKGROUND	8
2.1 Descriptions of U.S. Coastal Regions	9
2.1.1 Digital Elevation Models	9
2.1.2 Transect Data	11
2.1.3 National Land Cover Database	13
2.2 Forecast Models	14
2.2.1 ADCIRC+SWAN	14
2.2.2 Total Water Level and Coastal Change Forecast Viewer	16
2.2.3 XBeach	18
2.3 Storms	18
2.3.1 Michael (2018)	19
2.3.2 Ian (2022)	20
2.4 Motivation	23
2.4.1 Remaining Questions	23
2.4.2 Objectives	25
Chapter 3 METHODS	26
3.1 Preparations Before Hurricane Season	26
3.1.1 Bed Friction Interpolation	28
3.1.2 Hindcast Transect Preparation	30
3.1.3 Forecast Transect Preparation	32
3.2 Preparations for Each Storm Advisory	34
3.2.1 Selection of Transects	34
3.2.2 Boundary and Initial Conditions	34
3.3 XBeach Modeling	36
3.3.1 Input Parameters	36
3.3.2 Computational Timing and Resources	39
3.4 Post-Processing and Visualization	39
3.4.1 Dune Crest Impact	40
3.4.2 Dune Crest Elevation and Percent Volume Change	42
3.4.3 Additional Hindcast Evaluations	43
3.4.4 Visualizing and Publishing Results	43
3.4.5 Total Water Level and Coastal Change Forecast Viewer Comparison	45
Chapter 4 Results and Discussion	46
4.1 Hindcast of Storm-Driven Erosion during Michael (2018)	47

4.1.1	Qualitative Assessment of Coastal Change	47
4.1.2	Quantitative Comparison to Post-Storm Ground Surface	49
4.2	Forecasts of Storm-Driven Erosion during Ian (2022)	51
4.2.1	Evolution of Erosion Predictions across Forecast Advisories	51
4.2.2	Erosion Predictions by Region	58
4.3	Discussion	74
4.3.1	Lessons Learned about Deterministic Forecasting	74
4.3.2	Lessons Learned about Beach/Dune Erosion during Storms	76
4.3.3	Remaining Challenges	78
Chapter 5	CONCLUSIONS AND FUTURE WORK	82
APPENDIX	91
Appendix A	Appendix	92
A.1	XBeach Parameters	92

LIST OF TABLES

Table 2.1	Bulk transect statistics calculated from the dataset (Mickey and Passeri, 2022). Beach width and volume are measured from shoreline to dune toe; dune width and volume are measured from dune toe to dune crest.	13
Table 3.1	NCLD2019 land classifications and corresponding Manning’s n values from Passeri et al. (2018, Table 1). The majority of the NCLD2019 classes have a corresponding C-CAP class, except the Woody and Emergent Herbaceous Wetlands, which use the most-similar C-CAP class possible (Palustrine and Estuarine Forested Wetlands for Woody Wetlands ($n = 0.15$) and Estuarine Emergent Wetland for Emergent Herbaceous Wetlands ($n = 0.05$)).	29
Table 3.2	Comparison between the computed transect characteristics with updated ground surface information and the previously identified characteristics from the Mickey and Passeri (2022) dataset. These statistics only include the 39 transects selected for the hindcast simulation of Michael. The dune crest elevation is the vertical height above the MWL at the selected dune crest index. The beach width and dune width are the cross-shore distances from the shoreline to the dune toe and from the dune toe to the dune crest, respectively. Similarly, the beach and dune volumes are the sub-aerial cross-shore volumes from the shoreline to dune toe and from dune toe to dune crest, respectively. The total volume is the sub-aerial cross-shore volume from the shoreline to the dune crest.	32
Table 3.3	XBeach parameters changed from their default values for the Michael and Ian simulations. Most of these parameters were calibrated in van der Lugt et al. (2019), and <code>wbcevarreduce</code> was calibrated in McCall et al. (2023) . . .	38
Table 4.1	Numbers of predicted vs observed impacts at transects during Michael. Impacts are defined as a change in dune crest elevation of larger than 0.2 m. Impacts are quantified at the XBeach transect locations, by using results from the nearest CCHP transect. Colors correspond to the profiles plotted in Figure 4.2.	49

LIST OF FIGURES

Figure 1.1	Example from the Total Water Level and Coastal Change Forecast Viewer showing a daily forecast of coastal erosion. The colored dots represent 16 coastal regions, each with hundreds of 1D transects of the beach/dune system. The colors signify the maximum impact category for the region: (green) dune impacts unlikely, (yellow) potential dune erosion, (orange) predicted overwash, or (red) potential inundation (U.S. Geological Survey, 2023b).	3
Figure 2.1	Pre-2018 and post-Michael (October 2018) DEM (National Geodetic Survey, 2016; OCM Partners, 2010, 2015, 2018) extents for the Florida Panhandle including Mexico Beach and Cape San Blas. The elevations (m) are displayed above satellite imagery for the area.	10
Figure 2.2	Map of the U.S. with red points representing offshore transect locations. The smaller satellite image in the upper left corner displays transect 1595 from southwestern Florida as an example depiction of transect length and orientation.	11
Figure 2.3	Cross-shore transects from (left) Massachusetts, (center) North Carolina, and (right) Florida. The x -axis is the distance (m) from offshore and the y -axis is elevation NAVD88 (m). The figures include the entire transect length however, we will focus on storm impacts in the subaerial portion.	12
Figure 2.4	Screen capture of CERA website for Hurricane Ian (2022) NHC Advisory 22 (0900 UTC 28 September). Colors indicate forecasted water elevation from ADCIRC+SWAN model with dark red signaling water heights above 3 m (NAVD88) (Coastal Emergency Risks Assessment, 2019)	15
Figure 2.5	Screen capture from the Total Water Level and Coastal Change Forecast Viewer website. Site 3972 from Region 4 (southwest Florida) and forecast 0600 UTC 27 September (during Ian (2022)) is selected to display the TWL and associated storm impact prediction. On the map to the left, transects are colored green (dune impact unlikely), yellow (potential dune erosion), orange (potential overwash), or red (potential inundation) depending on the predicted dune impact at that location. On the right, the solid blue line is the TWL, the cyan band is the 95% confidence range, and the dotted blue line is the mean water level (no runup). The dune crest and toe are represented by the solid and dotted tan lines respectively. The hourly predicted water levels are plotted with respect to time and cross-shore space. The color of the profile changes from tan to match the predicted dune impact regime (U.S. Geological Survey, 2023b,c).	17
Figure 2.6	Temporal evolution of Michael intensity from the National Weather Service (Beven et al., 2019b). The icons along the track are labeled with the date, time, maximum sustained wind speed, and the corresponding hurricane category. Reproduced from National Weather Service (2019).	19

Figure 2.7	Figure from Tropical Cyclone Report for Ian published by the National Hurricane Center (Bucci et al., 2023a). The still images show time snaps from a remote camera capturing the storm surge inundation in Fort Myers, FL. Credit: Max Olson.	21
Figure 2.8	Map of Lee County post-Ian erosion conditions from the Florida Department of Environmental Protection Hurricane Ian & Hurricane Nicole Preliminary Post-Storm Beach Conditions and Coastal Impact Report (Clark et al., 2022)	22
Figure 3.1	Morphological modeling workflow for real-time forecasting.	27
Figure 3.2	Cross-shore bed friction values for two 1D profiles. Each point represents a node in the profile that has been assigned a Manning’s n value based on its land classification. Transect 3653 is located on Cape San Blas and transect 3644 is located on St. Vincent Island (both on the Florida Gulf coast).	28
Figure 3.3	Mickey and Passeri (2022) and updated cross-shore transect elevations with red and blue markers indicating the selected dune crest and toe locations respectively. Transect 3643 is located on St. Vincent Island and transect 3664 is located near Mexico Beach.	33
Figure 3.4	Comparison between NOAA stations, ADCIRC+SWAN water levels interpolated at the NOAA station, and XBeach water levels at the offshore boundary for the closest nearby transect. NOAA Stations 8725110- Naples Florida (left) on the southwest Florida coast and Station 8661070- Springmaid Pier, SC (right). Note that NOAA station 8725110 failed as the storm made landfall (National Oceanic and Atmospheric Administration, 2023e).	35
Figure 3.5	Simplified schematic of the two dune impact categories. The initial profile (dotted black), modeled profile (black), and water levels (blue) are represented as lines in the figure. The red star indicates the initial dune crest index where the water levels will be evaluated; this initial dune crest can be lowered during the simulation.	41
Figure 3.6	Screen capture from the public website displaying the forecast results for Ian. Each icon represents a transect, and the colors indicate the dune impact prediction for that forecast (red for ‘overwash/inundation’ or impact, green for ‘swash/collision’ or no impact). Transect 4074 is selected to show the interactive feature of the map, which provides the location coordinates, dune impact prediction, and a link to the corresponding plotted result on the GitHub repository.	44
Figure 4.1	CCHP and XBeach impact prediction maps for Michael. Red indicates regions of ‘impact’ predictions and white indicates regions of ‘no impact’ predictions.	48

Figure 4.2	Map of predicted vs observed impacts for Michael (with colors to match the categories in Table 4.1). Transects in blue and orange represent matches between predictions and observations, whereas transects in yellow and purple represent mismatches. Labels indicate the selected transects for further analyses (Figure 4.3).	50
Figure 4.3	Examples of XBeach results compared to the observed post-Michael lidar data. Each figure is labeled by the transect ID (with locations shown in Figure 4.2) and the impact comparison category.	52
Figure 4.4	Accuracy of hydrodynamic predictions from the hindcast-from-forecasts reanalysis, with subfigures: (upper) contours of ADCIRC peak water levels (m NAVD88) near Fort Myers compared with peaks from (left) gauge observations (m NAVD88) and (right) high water marks (m NAVD88); and (lower) scatter plot of ADCIRC peak water levels vs observed peaks (gauges and high water marks).	54
Figure 4.5	a) Track for hindcast reanalysis compared to NHC best track. b) Dune impact predictions for hindcast simulation where green transects represent ‘no impact’ or ‘collision’ predictions, and red transects represent ‘impact’ or ‘overwash/inundation’ predictions.	55
Figure 4.6	Comparison of XBeach-predicted dune impacts between the forecasts and hindcast. The colored bars represent the percentage of transects in each impact category: no impact (orange), match (blue), forecast greater (pink), or hindcast greater (yellow).	55
Figure 4.7	Dune impact predictions for Ian forecasts. The approximately 1800 transects are categorized as either ‘impacted’ when water reaches the dune crest (red) or ‘not impacted’ when water levels do not reach the crest index (green).	57
Figure 4.8	For southwest Florida, comparison of predicted dune impacts between XBeach and TWLCCFV forecasts. The colored bars represent the percentage of transects in each impact category: (orange) no impact, (blue) match, (pink) XBeach greater, or (yellow) TWLCCFV greater.	59
Figure 4.9	For southwest Florida, forecasts of dune impacts for advisories: (first row) 1800 UTC 24 September, (second row) 0000 UTC 25 September, (third row) 1800 UTC 27 September, and (fourth row) 1200 UTC 29 September. Dune impacts are shown for: (first column) the TWLCCFV forecast and (second column) the XBeach forecast, as well as (third column) a comparison between the two. For the two forecast frameworks (first and second columns), the transects are colored based on no predicted dune impacts (green) or predicted dune impacts (red). For the comparison (third column), the transects are colored based on the dune impact category: no impact (orange), match (blue), XBeach greater (pink), or TWLCCFV greater (yellow).	61

Figure 4.10	XBeach erosion predictions for transect T4074 located on Estero Island adjacent to the Fort Myers Fishing Pier. Times include: 2300 UTC 27 September, 0500 UTC 28 September, 1000 UTC 28 September, 2200 UTC 28 September, 2300 UTC 29 September, and 1600 UTC 2 October. The grey line is the initial XBeach profile and the tan area is the predicted bed levels at a specific time step. The water levels in XBeach are represented as a purple line, and the TWLCCFV predicted TWL (with associated 95% confidence band) are included as a horizontal blue line across the profile.	63
Figure 4.11	Post-Ian aerial photo from NOAA (National Oceanic and Atmospheric Administration, 2022) with the pre- and post-storm survey profiles plotted near transect T4074. The post-Ian aerial photo of the observed coastal change includes two lines depicting where the profiles are located in relation to the shoreline and one another. Above the aerial photo, there are two plots – the surveyed transect (left) and the XBeach transect (right). The plots are limited to the same extent, although the XBeach profile continues much further compared to the surveyed profile.	65
Figure 4.12	For southeast Florida, comparison of predicted dune impacts between XBeach and TWLCCFV forecasts. The colored bars represent the percentage of transects in each impact category: no impact (orange), match (blue), XBeach greater (pink), or TWLCCFV greater (yellow).	66
Figure 4.13	For southeast Florida, forecasts of dune impacts for advisories: (first row) 0000 UTC 24 September, (second row) 1200 UTC 28 September, and (third row) 1200 UTC 29 September. Dune impacts are shown for: (first column) the TWLCCFV forecast and (second column) the XBeach forecast, as well as (third column) a comparison between the two. For the two forecast frameworks (first and second columns), the transects are colored based on no predicted dune impacts (green) or predicted dune impacts (red). For the comparison (third column), the transects are colored based on forecast impact categories: no impact (orange), match (blue), XBeach greater (pink), or TWLCCFV greater (yellow).	68
Figure 4.14	XBeach results at 6 time snaps during the 1200 UTC 28 September forecast for transect 2656 located in South Beach, FL. Times include: 0900 UTC 28 September, 0000 UTC 29 September, 1300 UTC 29 September, 1100 UTC 30 September, 1200 UTC 1 October, and 1800 UTC 2 October. The grey line is the initial XBeach profile and the tan area is the predicted bed levels at a specific time step. The water levels in XBeach are represented as a purple line and the TWLCCFV predicted TWL (with associated 95% confidence band) are included as a horizontal blue line across the profile.	69
Figure 4.15	For the southeast U.S., comparison of predicted dune impacts between XBeach and TWLCCFV forecasts. The colored bars represent the percentage of transects in each forecast impact category: no impact (orange), match (blue), XBeach greater (pink), and TWLCCFV (yellow).	70

Figure 4.16	For the southeast U.S., forecasts of dune impacts for advisories: (first row) 0000 UTC 24 September, (second row) 1200 UTC 26 September, and (third row) 1200 UTC 28 September. Dune impacts are shown for: (first column) the TWLCCFV forecast and (second column) the XBeach forecast, as well as (third column) a comparison between the two. For the two forecast frameworks (first and second columns), the transects are colored based on no predicted dune impact (green) or predicted dune impact (red). For the comparison (third column), the transects are colored based on the dune impact category: (orange) no impact, (blue) match, (pink) XBeach greater, or (yellow) TWLCCFV greater.	72
Figure 4.17	XBeach results at six time snaps during the 0000 UTC 28 September forecast for transect 1173 located on Oak Island NC. Times include: 2000 UTC 28 September, 1900 UTC 29 September, 0800 UTC 30 September, 1900 UTC 30 September, 0200 UTC 1 October, and 0000 UTC 3 October. The grey line is the initial XBeach profile and the tan area is the predicted bed levels at a specific time step. The water levels in XBeach are represented as a purple line and the TWLCCFV predicted TWL (with associated 95% confidence band) are included as a horizontal blue line across the profile.	73
Figure 4.18	Timing of dune impact, represented as hours relative to Ian’s initial landfall in southwest Florida at 2000 UTC 28 September. Panels identify the timing of dune impact via thresholds of: (a) when water levels reach the dune crest, or (b) when the dune crest elevation is changed by more than 0.2 m. Lighter colors indicate impacts predicted closer to the observed landfall. Negative or blue colors indicate dune impacts before 0000 UTC 28 September, and positive or red colors indicate dune impacts after the initial landfall.	78
Figure 4.19	Water level time series in NAVD88 for forecasts or observations at 0000 UTC 27 September. The dashed lines are from the TWLCCFV api, with the blue and black color indicating the hourly TWL and ‘tidewindsetup’ forecasts respectively (U.S. Geological Survey, 2023b). Observational water levels from Station 8725110- Naples, FL are included in green (before damage during the peak of Ian). The red and pink lines are ADCIRC forecasted water levels at the tide gauge and a location closer to shore (-82.0335,26.436) respectively. XBeach water elevations at the offshore origin in yellow and at the shoreline in orange for the closest transect to the tide gauge (T4071).	81

CHAPTER

1

INTRODUCTION

Tropical cyclones pose a major threat to the United States, especially given recent climate trends. Nearly 40 percent of the U.S. population lives in coastal counties, despite the coast representing less than 10 percent of the nation’s landmass (excluding Alaska; National Oceanic and Atmospheric Administration, 2023b). More than 128 million people are susceptible to coastal hazards, including tropical cyclones, which caused 6,697 deaths and more than \$ 1.1 trillion in damages between 1980 and 2021 (National Oceanic and Atmospheric Administration, 2023c). Impacts from tropical cyclones will only be exacerbated by recent climate trends. Sea level rise, “very likely” caused by human activity, will result in higher coastal inundation, while tropical cyclone rainfall and global intensities are projected to increase (Knutson, 2023). Additionally, the portion of high-intensity cyclones (category 4 or 5 hurricanes) is projected to increase in the future (Knutson, 2023). With these projections, the millions of coastal residents and trillions of goods and services produced annually by coastal counties are at risk.

Tropical cyclones induce storm surges and wave run-ups as coastal hazards. Storm surge occurs when winds push water toward and onshore so that water surface elevations rise above the normal astronomical tidal range (National Hurricane Center, 2021). The level of storm surge depends on the intensity and speed of the storm, as well as the characteristics of the coastal system. For example, the storm surge in southwest Florida for Ian (2022) was between 3 to 5 m, which led to widespread inland flooding and directly caused 41 casualties (Bucci

et al., 2023a), whereas the storm surge in southeast Florida for Nicole (2022), just a month after Ian, was less than 2 m and had no directly related casualties (Beven and Alaka, 2023). Wave run-up also contributes to the total water level at the coast. Wave run-up is the breaking of waves onshore and subsequent increase in water surface elevation onto the beach face relative to the still water level (U.S. Geological Survey, 2023c). Wave run-up depends on multiple beach and wave properties, including beach slope and wave height. Recent studies have found wave run-up can be responsible for more than 70% of total water level during times of predicted dune erosion (Stockdon et al., 2023). Understanding both storm surge and wave run-up components is essential for accurate predictions of risk along the coast.

These hazards affect beaches and dunes, which are often the last line of defense between coastal communities and intense tropical cyclone conditions. Coastal dunes act as a barrier for storm surges and wave run-ups, preventing the water from spilling over the dune and affecting the infrastructure or property behind them. However, during a tropical cyclone, the hydrodynamics can severely erode the beach and dune faces and occasionally overtop the dune crest (Ruggiero et al., 2001). As high-intensity storms become more frequent and coastal inundation levels rise with relative sea level changes (Knutson, 2023), the likelihood of significant beach and dune erosion increases (U.S. Geological Survey, 2023a). Repeated high-erosion events can leave regions of the coast vulnerable to the next high-intensity tropical cyclone or extreme event (U.S. Geological Survey, 2023a). The ability to predict coastal response to storm impact and forecast vulnerability along the coast in real-time would be beneficial for emergency decision-makers and local stakeholders who may be affected by the results.

There are multiple methods for predicting storm impact, but each method requires different input information, produces different metrics for predicted erosion, and comes with its own limitations. The most common method to predict coastal erosion is empirical analysis (e.g. Ruggiero et al., 2001; Sallenger, 2000; Stockdon et al., 2006). This method uses empirical equations for wave run-up to predict total water level (TWL). The equations require information about the beach (e.g. slope β) and storm characteristics (e.g. wave height H , length L , and period T). This TWL calculation can be done once with peak storm characteristics or multiple times at preferred intervals (e.g. hourly or daily). Then the computed TWL can be compared to the dune crest and toe elevations to predict the storm impact regime. The four impact regimes include swash (TWL < dune toe elevation), collision (dune toe elevation < TWL < dune crest elevation), overwash (TWL > dune crest elevation), and inundation (tides/surge > dune crest elevation) (Sallenger, 2000). In the collision regime, the dune face is eroded, but still acts as a barrier to inland flooding. Whereas in the overwash or inundation regimes, the water elevations raise above the dune crest, and the dune is unable to prevent the water from spilling past the dune (Sherwood et al., 2022). These storm impact predictions based on empirical

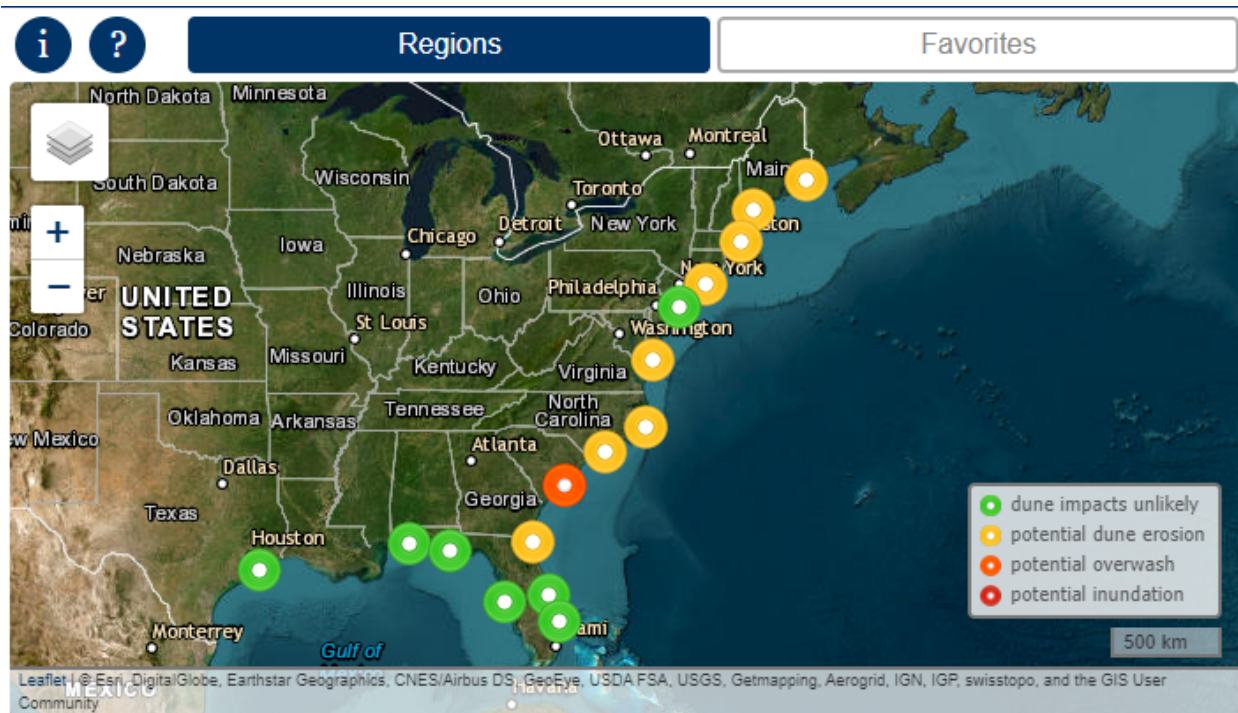


Figure 1.1: Example from the Total Water Level and Coastal Change Forecast Viewer showing a daily forecast of coastal erosion. The colored dots represent 16 coastal regions, each with hundreds of 1D transects of the beach/dune system. The colors signify the maximum impact category for the region: (green) dune impacts unlikely, (yellow) potential dune erosion, (orange) predicted overwash, or (red) potential inundation (U.S. Geological Survey, 2023b).

calculations are computationally efficient and require minimal information about the beach or storm conditions.

Recently, this empirical approach has been used in a forecast system along the U.S. Gulf and Atlantic coasts. The Total Water Level and Coastal Change Forecast Viewer (TWLCCFV, Stockdon et al., 2023; U.S. Geological Survey, 2023b) predicts TWL dune impacts on hundreds of 1D transects. It uses the empirical equations from Stockdon et al. (2006) to predict the hourly total water level and associated storm impact category relative to the transect characteristics. The TWLCCFV assumes a static, idealized profile throughout the forecast. The Stockdon et al. (2006) storm scaling model can accurately predict about 50-60% of dune erosion events, as opposed to a 33% accuracy if the predictions were assigned by random chance (Stockdon et al., 2023).

However, the empirical approach has limitations, especially in how it represents the ground surface. The Stockdon et al. (2006) empirical parameterization considers the beach slope β and the dune crest and toe elevations, but disregards the sub-aqueous or beach face features

that could affect nearshore morphology are not considered. Also, the profile characteristics remain static throughout the forecast. Thus TWL predictions would not be aware of dune crest lowering or dune face erosion that occurred previously in the storm. Stockdon et al. (2023) states “the largest source of uncertainty is a static representation of coastal morphology (beach slope).”

To combat this uncertainty, a dynamic ground surface can be included via 1D or 2D morphological models. The eXtreme Beach model (XBeach, Roelvink et al., 2009) can produce high-fidelity morphodynamic predictions of sediment transport throughout an extreme event (e.g. Splinter and Palmsten, 2012; Splinter et al., 2014). In a study by Vousdoukas et al. (2012), an XBeach 1D model was calibrated for Faro Beach, Portugal, with thousands of simulations. The calibrated model achieved ‘satisfactory’ skill scores for predicting morphology. The final step was implementing the model to forecast storm impacts for 5-, 25-, and 50-year return period extreme events, which showed regional vulnerability over the 1-km study area. XBeach 1D models are able to capture similar dynamic profile evolution as 2D models, but much faster and with fewer computational costs. They also require less ground surface information, reducing the amount of storage required. Depending on the duration of the storm and the size of the profile, simulations can require about 20 to 30 minutes in comparison to the hours required for 2D models. While XBeach is used widely, other morphological models (e.g. CSHORE (Johnson et al., 2012; Kobayashi, 2016) or SBEACH (Larson and Kraus, 1989)) can produce similar results according to model comparisons studies (Harter and Figlus, 2017; Kalligeris et al., 2020; Simmons et al., 2019).

Morphological models can also use 2D domains, which incorporate alongshore sediment transport not considered in 1D models. This translates into a more robust representation of the erosion processes. Multiple studies have validated the accuracy of XBeach 2D models (e.g. Gharagozlou et al., 2020; Passeri et al., 2018; Schweiger et al., 2020; van der Lugt et al., 2019) and demonstrated their use for different modeling applications. van der Lugt et al. (2019) used two 2D domains on the U.S. Atlantic coast to predict storm-driven erosion during two historical events. The models achieve ‘good’ to ‘excellent’ scores and are able to produce an observed breach in one of the domains. This would not be possible without the high-resolution domain representation and 2D sediment transport computations. Aside from XBeach, other 2D morphological models like Delft3D (Canizares and Irish, 2008; Cho et al., 2012; Roelvink and Banning, 1994) can achieve similar accuracy for morphodynamic predictions.

Dynamic, deterministic models (like XBeach) are not typically implemented for real-time forecasting because they require significant information about the coastal system and storm and considerable computational resources. In addition to high-resolution ground surface information, a full time series of wave properties and water levels are required for the model to

build a full wave spectra. Uncertainties in these initial and boundary conditions propagate through the model and can result in additional error (Baart et al., 2016). Fundamental equations for hydraulics, such as wave breaking (e.g. Roelvink, 1993), and sediment transport (e.g. Galappatti and Vreugdenhil, 1985) are solved to compute how wave energy propagates through the domain and how that affects the morphology of the profile. These computations are done at each grid cell in the domain for each time step of the model, making the 2D models very computationally expensive (e.g. Baart et al., 2011). They can take hours and numerous computational resources to complete. The additional computational time is a concern when timely forecasts are essential for coastal decision making. With recent advancements in technology, there is an opportunity to implement high-resolution XBeach models for real-time forecasting (Sherwood et al., 2022).

When studies have used XBeach 1D models to forecast erosion (e.g. Baart et al., 2016; Harley et al., 2011; Vousdoukas et al., 2012), the study area is typically restricted to a set location with a limited number of profiles. Vousdoukas et al. (2012) forecasted hypothetical storm impacts for selected return periods, and did an extensive calibration with the high-resolution observational data available at 6 survey locations in their study area. This level of calibration would not be possible without high-resolution pre- and post-storm elevation data, and even then, the calibrated parameters may only be applicable within the 1-km study area (Simmons et al., 2019). Also, their ‘forecast’ was not done in real-time or with a real event, so efficiency or uncertainty considerations were minimized. Harley et al. (2011) did a calibration for two 1D profiles, and then the calibrated model was used to forecast two storm events and assessed to understand how well it performed. In both cases, by only considering a specific region with a handful of 1D transects, the parameters and findings may only be applicable in the original locations.

Another approach is training a surrogate model to emulate a morphological model or dune impacts (Beuzen et al., 2019a,b; Gharagozlou et al., 2022; Jager et al., 2018; Santos et al., 2019, e.g.). This method requires significant computational resources to train the library, but it is very efficient when implemented in real-time. To train the surrogate library, synthetic profiles resembling the original training location and a realistic set of synthetic storms are applied as initial conditions for hundreds of representative morphological model simulations. The surrogate model then attempts to emulate the deterministic model results and produce the same level of accuracy as the morphological model would more efficiently for future storms. Although the surrogate model produces dynamic results, a lot of computation time and analysis is required before it can be used to predict storm impacts. Depending on the amount of complexity and number of principal components, the training library could require hundreds of morphological model simulations before any validation is possible. Additionally,

the surrogate model is only applicable to the training location. Either multiple emulators or a much larger training library would be required to represent a wider region. The last limitation is the simplification of the system as a whole. Storm and ground surface conditions are reduced to principle components to reduce the training complexity, therefore certain storm characteristics or profile features may not be included. To achieve deterministic and dynamic forecasts of storm-driven erosion, a morphological model is required.

Thus, there are several challenges to deterministic modeling over a large area, such as: accurate model calibration while maintaining versatility for different regions, efficient model framework for submitting hundreds of simulations, and effective evaluation and communication of model results. However, with advancements in computational efficiency and high-resolution data availability as a result of technological improvements, these challenges no longer prevent the implementation of real-time deterministic, dynamic morphological modeling. High-performance computing allows for parallelization, which significantly reduces forecast lead time. High-resolution ground surface observations have become more widely accessible through public databases and cloud storage. There is an opportunity to expand our morphological modeling beyond a set location or a handful of transects to achieve a wider understanding of erosion forecasting along the U.S. Atlantic and Gulf coasts. We first have to develop a computationally efficient, morphological modeling framework to accurately predict storm-driven erosion through hundreds of XBeach 1D models and communicate the erosion predictions effectively to potentially unfamiliar audiences.

Then, with this development, we can investigate questions related to creating an accurate and efficient modeling framework for coastal erosion, and improving our understanding of morphodynamics during extreme events. Questions related to model performance include: How well will uncalibrated parameters perform for predictions of erosion during a large, impactful storm? Because these predictions will be made in real-time, how efficient is the forecast modeling framework? After the results are completed, the modeling framework also needs to effectively communicate predicted erosion along the coast. One potential erosion metric is a binary dune impact classification. How accurate and effective is the binary dune impact categorization, and how do other models compare using this metric?

Then with the established modeling framework, we will consider: How do forecast predictions change across advisories, and how do we compare to what really happened given the limited observational data available? Real-time forecasts often do not have observational data, so the forecast model comparison may be the best way to understand erosion trends along the coast. The forecast models likely have a different method of representing ground surface information compared to the dynamic bed in XBeach. How do additional ground surface information and morphodynamics affect our forecast predictions?

The goal of this research is to develop an effective forecast method for storm-driven erosion, and then use the forecasts to learn more about storm-driven coastal erosion. We anticipate the model framework will achieve both accurate and efficient predictions of coastal erosion. It is hypothesized that the dynamic morphology component in the 1D XBeach models will change the predictions of dune impacts compared to other forecast methods and provide more information about the temporal evolution of the profile not typically available through observations. The morphodynamic information can be used to draw larger conclusions about erosion and coastal change during other extreme events.

1.1 Funding Acknowledgment

This research was funded by the National Oceanic Partnership Program (NOPP), a national collaboration to support and advance ocean science research. This partnership between federal agencies, industry, and academia aims to enhance our understanding of ocean systems through technology development.

CHAPTER

2

BACKGROUND

This research will examine questions about storm-driven erosion along the U.S. Atlantic and Gulf coasts. Understanding storm-driven erosion can help inform coastal decision-makers and local stakeholders about potential risks to beach and dune systems, which are often the last line of defense between storm waves and surges and coastal communities and infrastructure. Researchers have strived to evaluate and quantify storm-driven erosion, to better understand the morphodynamic processes and identify regions of vulnerability. Models can aid in these evaluations, by simulating nearshore morphodynamics to represent the system's response to storm forcings. However, coastal erosion is a complex process that can be affected by many factors, and additional complexity is added when attempting to make predictions in real time.

In this chapter, we examine elements that led to this research. First, we investigate the U.S. Atlantic and Gulf coasts through spatially varying elevations, cross-shore profiles of the coast, and land cover information. This ground surface data will be used by the models as initial conditions or as a comparison for predictive accuracy. Next, we describe the models used to predict extreme event conditions, such as waves or storm surges, during Hurricanes Michael (2018) and Ian (2022). These storms are described in detail, including their paths, storm characteristics through time, and the resulting impacts to the U.S. coast. Lastly, we will discuss some of the remaining questions that motivated this research and the key objectives this research will address.

2.1 Descriptions of U.S. Coastal Regions

To understand the erosion of beaches and dunes during coastal storms, this research will focus on forecasts for storms that affect the U.S. Gulf and Atlantic coasts. These coasts stretch approximately 6000 km from Texas through Maine, and they are characterized mostly by sandy beach and dune systems. To understand how these systems are affected by storms, we need descriptions of their ground-surface and land-cover conditions, ideally in the days immediately preceding and following each storm. These descriptions can be obtained from digital elevation models (DEM) derived from lidar observations, as well as land-use land-cover (LULC) datasets derived from Landsat satellite imagery. There are extensive DEMs and land-cover datasets to describe the U.S. Gulf and Atlantic coasts, and here we describe the data most applicable to this research.

2.1.1 Digital Elevation Models

Digital Elevation Models (DEMs) are representations of the bare Earth surface, excluding additional surface objects such as vegetation or other surface objects (USGS, 2023). DEMs can be used in multiple applications, including estimating storm-driven erosion and morphological modeling (Mitasova et al., 1996). Morphological models use high-resolution DEMs to represent nearshore initial ground surface conditions by interpolating the pre-storm elevation values onto different meshes or grids. Post-storm DEMs also play a key role in validating model results. Erosion of beaches and dunes is often evaluated using metrics, like dune crest elevation change and change in volume, that rely on DEMs to provide spatially varying elevation data in both the alongshore and cross-shore directions.

For model validation in this research, we will focus on a specific stretch of coast along the Florida panhandle near Mexico Beach, and we will use elevation data that represents the best possible understanding of the ground surface before and after the hurricane season of 2018. The pre-2018 DEM was created by combining three topography and bathymetry lidar datasets from 2010, 2015, and 2016 (Figure 2.1, National Geodetic Survey, 2016; OCM Partners, 2010, 2015, 2018). The 2010 and 2015 lidar data were completed by the Joint Airborne Lidar Bathymetry Technical Center of Expertise (JALBTCX) for the U.S. Army Corps of Engineers (USACE) National Coastal Mapping Program. The 2010 point cloud extends from the western edge of the Alabama coast to the coastline immediately south of Tallahassee, FL. The 2010 lidar points have a vertical accuracy of 0.15 m and an estimated point spacing of 2 m. The 2015 point cloud covers from Destin to Mexico Beach and from Clearwater to Naples on the Florida Gulf Coast. The 2015 lidar points have a vertical accuracy of 0.095 m and an estimated point spacing of 0.35 m. The NOAA National Geodetic Survey collected the 2016 lidar covering St.

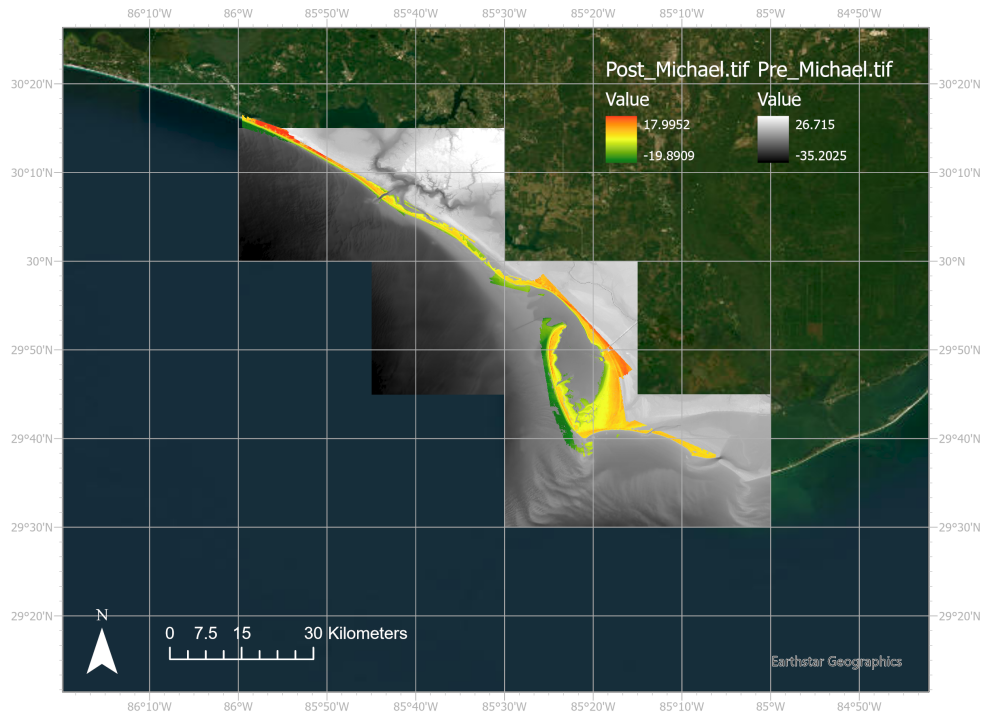


Figure 2.1: Pre-2018 and post-Michael (October 2018) DEM (National Geodetic Survey, 2016; OCM Partners, 2010, 2015, 2018) extents for the Florida Panhandle including Mexico Beach and Cape San Blas. The elevations (m) are displayed above satellite imagery for the area.

Joseph Bay, south of Mexico Beach, with a vertical accuracy of 0.15 m and a point spacing of 0.25 m. The lidar datasets were combined, trimmed to the area of interest between Panama City Beach and St. Joseph Bay, and converted into a single digital surface model with priority given to the most recently collected elevation points. This creation of a pre-Michael DEM was completed by Chris Amante, and the data were made available via Google Drive.

After the 2018 hurricane season, the USACE collected lidar data along the shoreline from the eastern edge of Alabama to the coast south of Tallahassee, on behalf of the Federal Emergency Management Agency (FEMA) to assess recent changes in ground surface elevation. The points have an estimated point spacing of 0.35 m and a vertical accuracy of 0.1 m. The lidar point cloud was then processed and converted to a digital surface model with a 1-m horizontal resolution and a vertical datum in NAVD88.

For forecasting future storms, it is important to start with datasets to describe the present-day conditions for coastal regions. Unlike the year-specific DEMs described above, the Continuously Updated Digital Elevation Model (CUDEM, CIRES, 2014) is regularly edited and amended to include the most recent available ground surface elevations for the U.S. Atlantic and Gulf coasts, as well as some small stretches of the northwest. The CUDEM has a 1/9th arc (approx. 3

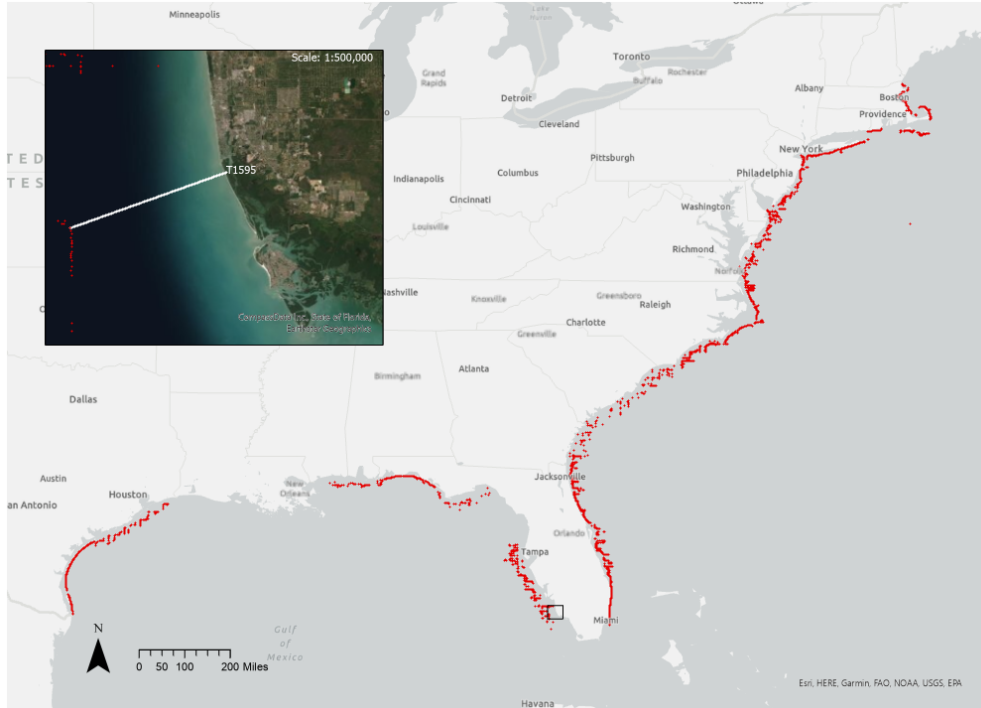


Figure 2.2: Map of the U.S. with red points representing offshore transect locations. The smaller satellite image in the upper left corner displays transect 1595 from southwestern Florida as an example depiction of transect length and orientation.

m) resolution nearshore and a 1/3rd arc (approx. 10 m) resolution offshore and is split into 0.25 decimal degree tiles. The date for each tile ranges from 2014 to 2022, depending on when the data was collected. The CUDEM is used in a number of research products, including the transect dataset described in the next section. Digital Coast, managed by NOAA, is a user-friendly way to select and download CUDEM tiles based on the requested projection and spatial extent from the interactive map.

2.1.2 Transect Data

An example of a CUDEM-related research product is a database of approximately 4000 cross-shore transects generated along the U.S. Atlantic and Gulf coasts (Mickey and Passeri, 2022). The transects have an alongshore resolution of 0.5 to 2.5 km and a cross-shore resolution of 10 m offshore to 2.5 m nearshore. For each transect, the topography was interpolated from the most-recent high-resolution lidar topography, which was then stitched with the CUDEM topo-bathy data to create a seamless transect of the coast from an offshore -20 m depth to a variable distance past the foredune. Thus each profile has a different position, length, and cross-shore resolution. The dataset also includes a number of characteristics for each transect,

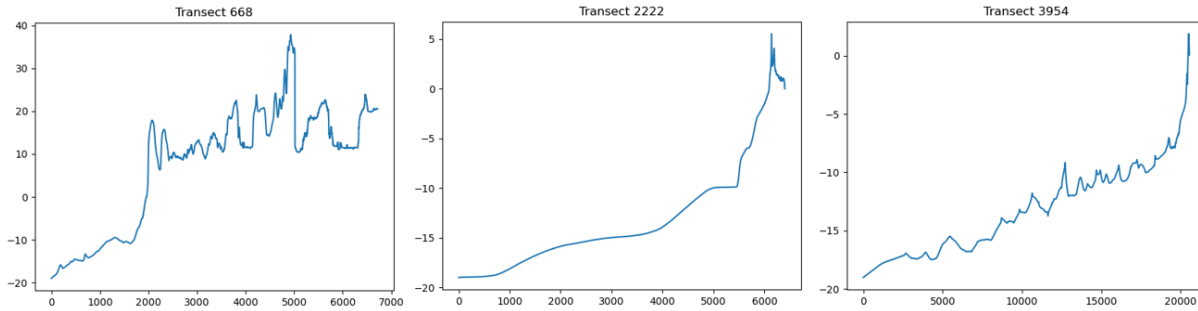


Figure 2.3: Cross-shore transects from (left) Massachusetts, (center) North Carolina, and (right) Florida. The x -axis is the distance (m) from offshore and the y -axis is elevation NAVD88 (m). The figures include the entire transect length however, we will focus on storm impacts in the subaerial portion.

such as beach slope, dune crest elevation, and dune volume, that are of general interest and will be used in future model studies. Aside from deterministic morphological modeling, this dataset is directly applicable to any science related to sandy coastlines.

Figure 2.3 contains three example transects from different regions of the U.S. Atlantic and Gulf coasts that include unique topographic landforms represented through the profile elevations. Transect 668 is located on the Massachusetts coast inside Cape Cod bay, just south of the Manomet Bluffs. This transect is about 7 km long with a steep nearshore bathymetry and expansive subaerial coverage stretching 5 km past the shoreline. Dune width and volume for transect 668 are 81 m and 1196 m^3 , respectively. The transect has a dune crest higher than 17 m (NAVD88) and a maximum elevation of nearly 40 m (NAVD88). Transect 2222 is located on a barrier island in the Outer Banks of North Carolina. Unlike the previous transect, this transect 2222 has shallower nearshore bathymetry that reaches -20 m depth approximately 6 km from the shoreline and has a maximum dune crest and elevation of about 5.5 m (NAVD88). Dune width and volume for transect 2222 are 7 m and 31 m^3 , respectively. Transect 3954, located on the southern Gulf coast of Florida, has the lowest dune crest of less than 2 m (NAVD88) and stretches more than 20 km offshore to reach a -20 m depth. Dune width and volume for transect 3954 are 12 m and 21 m^3 , respectively. These transects display the drastic differences between different regions of the coast. These differences will affect how they respond during extreme storm events.

By taking a step back and looking at this transect dataset holistically, we can glimpse the complexity of the U.S. Atlantic and Gulf coasts. Transect statistics – such as dune crest elevations, beach and dune widths and volumes, and nearshore slopes – show a wide range of values (Table 2.1). When comparing these bulk statistics, the averages are generally greater than their

Table 2.1: Bulk transect statistics calculated from the dataset (Mickey and Passeri, 2022). Beach width and volume are measured from shoreline to dune toe; dune width and volume are measured from dune toe to dune crest.

	maximum	minimum	median	average
Dune Crest Elevation (m (NAVD88))	56	0.79	4.4	4.8
Beach Width (m)	2200	1.74	36.2	48.8
Dune Width (m)	465	1.67	15.0	21.6
Beach Volume (m ³)	8790	2.06	53.9	83.1
Dune Volume (m ³)	2960	1.57	53.8	87.6
Total Volume (m ³)	8830	5.46	124.0	171.0

corresponding median values, implying the mean values are slightly skewed by the upper end of the range. The average beach volume, measured from the shoreline to the dune toe, is smaller than the average dune volume, measured from the dune toe to the dune crest. The total volume includes the beach and dune volumes from the shoreline to the dune crest. The transect width statistics are not as close in value, with an average beach width of approximately double the average dune width. In general, these statistics highlight the transect diversities and encourage the use of spatially varying elevation data to represent the nearshore topographic features.

2.1.3 National Land Cover Database

The National Land Cover Database (NLCD), maintained by USGS and the Multi-Resolution Land Characteristics Consortium (MRLC), provides publicly accessible land cover and land cover change information derived from Landsat imagery for the entire continental United States (Multi-Resolution Land Characteristics Consortium, 2019). The original NLCD was released in 1992, and since 2001, the database has been updated every 2-3 years to monitor and observe the national landscape. The NLCD has a 30-m resolution where each pixel is categorized based on a 16-class system, including an open water class and different subsets of developed land categories ranging from open space to high intensity, using a modified version of the Anderson Classification System (Anderson et al., 1976). The most recent product released, the NLCD 2019, builds on accuracy improvements from the 2016 release and includes historical impervious surface information dating back to 2001 to highlight land development over the past several years. The NLCD 2019 includes the U.S. Atlantic and Gulf coasts and can provide our models with information on impervious surfaces, vegetation, and other influential factors.

2.2 Forecast Models

Hurricane forecasting continues to improve as new technologies allow us to better understand and predict the potential progression of the storm and the response of the coastal system.

This section will describe the forecasting models used to predict and evaluate the magnitude, timing, and extent of storm-driven flooding and erosion. Each of these models has its own limitations, which lead to motivating research questions described at the end of this chapter.

2.2.1 ADCIRC+SWAN

ADvanced CIRCulation (ADCIRC; Luetlich et al., 1992; Westerink et al., 2008) is a large-scale circulation model that can be applied for predictions of tides and wind-driven circulation in coastal regions, both for everyday and storm conditions, and both during real storms and for synthetic storm conditions for possible future conditions (Blanton and Luetlich, 2008; Fleming et al., 2008). ADCIRC uses an unstructured, finite-element mesh to solve modified forms of shallow water equations for the conservation of mass and momentum, both spatially and temporally. Water surface elevations and depth-averaged velocities are computed by discretely solving the generalized wave continuity equation (GWCE) and conservation of momentum equation, respectively, at each finite element vertex. Depending on the ground surface elevation, the modeled water surface elevations and depth-averaged velocities nearshore may result in flooding or inundation of low-lying coastal areas. ADCIRC can be coupled with Simulating WAVes Nearshore (SWAN Booi et al., 1999) to give a more complete picture of the nearshore water conditions. SWAN is a phase-averaged spectral wave model that solves the wave action density equation to predict wave height, peak period, peak direction, and other important wave characteristics. When tightly coupled, ADCIRC+SWAN share the same unstructured mesh and parallel computing structure which facilitates inter-model communication (Dietrich et al., 2011b). This coupled approach produces high-fidelity nearshore wave and water level predictions that have been well validated through numerous studies (Dietrich et al., 2018; Thomas et al., 2019).

Researchers have automated the implementation of ADCIRC+SWAN models for real-time forecasting of storm surge and coastal flooding. One such automation is the ADCIRC Surge Guidance System (ASGS), which uses wind advisories published every 6 hours by the National Hurricane Center (NHC) as forcing to predictions of tides, winds, and water surface elevations as the storm develops off the coast. The ASGS results are visualized and made public on the Coastal Emergency Risks Assessment (2019, CERA) website to help inform coastal stakeholders and decision-makers, such as local or federal government agencies (Figure 2.4). The ASGS system was successful in forecasting storm surge for numerous historical storms – including

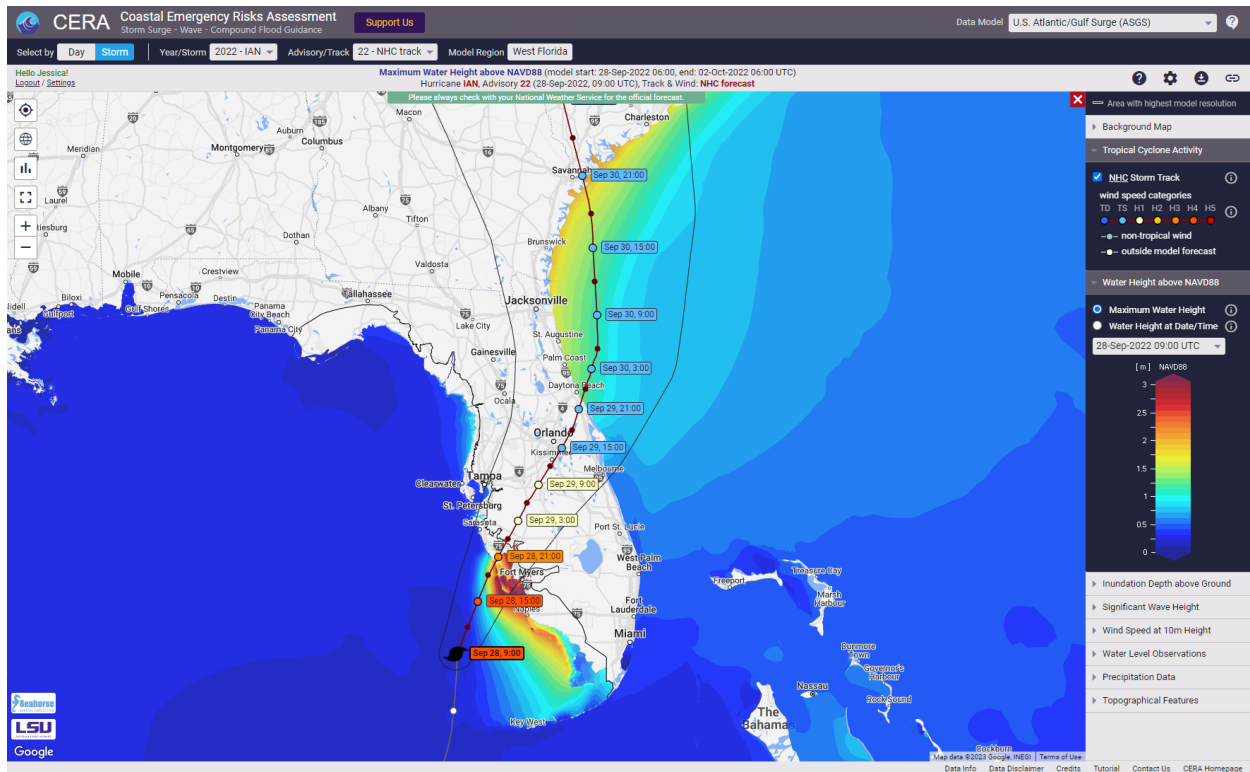


Figure 2.4: Screen capture of CERA website for Hurricane Ian (2022) NHC Advisory 22 (0900 UTC 28 September). Colors indicate forecasted water elevation from ADCIRC+SWAN model with dark red signaling water heights above 3 m (NAVD88) (Coastal Emergency Risks Assessment, 2019)

Micheal (2018), Irene (2011), and Katrina (2005) – that have affected coastal environments and configurations along the U.S. Atlantic and Gulf coasts (Bilskie et al., 2020; Blanton et al., 2012; Fleming et al., 2008). The CERA Historical Storm Surge Archive contains data for more than 50 tropical cyclones from the last 20 years, and the archive continues to be updated with the most recent forecasts for each hurricane season (CERA Historical Storm Archive, 2023).

The ADCIRC Prediction System (APS) at the University of North Carolina (UNC) Chapel Hill uses a similar automated approach to produce high-resolution predictions of storm-driven flooding, winds, and wave information in real-time. The APS can receive atmospheric forcing from multiple sources, including the Coupled Ocean/Atmosphere Mesoscale Prediction System (COAMPS) created by the Naval Research Laboratory (Bilskie et al., 2022; Chen et al., 2003). With each available COAMPS forecast every 6 hours, the APS downloads and converts the atmospheric products into a format compatible with ADCIRC, and then automatically begins forecasting potential conditions. The APS relies on computing resources at multiple institutions, including the Renaissance Computing Institute (RENCI), which handles the computations for

the frequent APS forecasts and visualizes the results in a public web service.

While the coupled ADCIRC+SWAN can produce robust predictions of nearshore waves and water levels across large domains, the topography and bathymetry within the model are static. ADCIRC+SWAN is not intended to predict storm-driven erosion and therefore does not attempt to alter the initial ground surface or estimate sediment transport. Instead, its hydrodynamic predictions can be implemented as boundary forcing in other models, both theoretical or dynamic, on smaller domains that are intended for storm-driven erosion forecasting. The following models describe how the wave properties and water surface elevation can be incorporated into a morphological modeling framework.

2.2.2 Total Water Level and Coastal Change Forecast Viewer

The Total Water Level and Coastal Change Forecast Viewer (TWLCCFV; U.S. Geological Survey, 2023b) is a forecasting tool created for the USGS National Assessment of Coastal Change Hazards project in collaboration with the National Oceanic and Atmospheric Association (NOAA) / National Weather Service (NWS) and the National Center for Environmental Protection (NCEP) (Figure 2.5). The viewer displays the hourly predicted total water level, composed of tides, surge, and runup, and the corresponding impact regime, based on the profile characteristics. Tides and surge are predicted by either the (Extratropical) Surge and Tide Operations Forecast Systems ((E)STOFS) (National Oceanic and Atmospheric Administration, 2021), an experimental ADCIRC-based model run by NOAA, or the Probabilistic Surge (P-Surge, National Oceanic and Atmospheric Administration, 2023d) model from the NHC. The decision of whether to use ESTOFS or P-Surge for the water level component of the forecast is left to the discretion of local forecasters. The Nearshore Wave Prediction System (NWPS National Oceanic and Atmospheric Administration, 2023a), a SWAN-based model that obtains its boundary conditions from a global WaveWatch III model (WW3), provides the wave height and peak period required to empirically calculate runup (Stockdon et al., 2006).

Simplified cross-shore transects, generated using beach characteristics from recent lidar topography, provide the beach slope for runup calculations in the total water level. The transects also provide dune elevations for categorizing coastal change. Storm impact is categorized as swash (dune impacts unlikely), collision (potential dune erosion), overwash (potential overwash), or inundation (potential) depending on the current dune crest and toe elevations compared to the predicted high and low water levels (Sallenger, 2000). The storm impact regimes are defined by the predicted total water level (R_{High}) or storm surge (R_{Low}) relative to the dune crest (D_{High}) and dune toe elevations (D_{Low}). The viewer displays the collective transect impact regime predictions by color where green, yellow, orange, and red represent swash (R_{High}

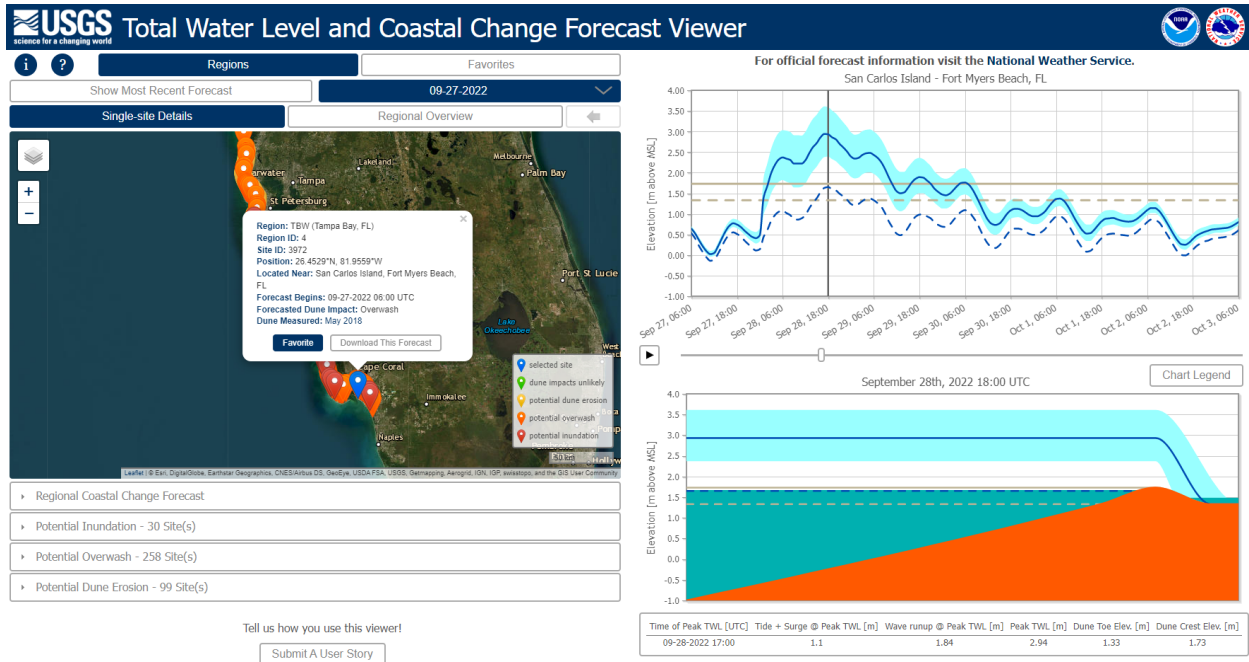


Figure 2.5: Screen capture from the Total Water Level and Coastal Change Forecast Viewer website. Site 3972 from Region 4 (southwest Florida) and forecast 0600 UTC 27 September (during Ian (2022)) is selected to display the TWL and associated storm impact prediction. On the map to the left, transects are colored green (dune impact unlikely), yellow (potential dune erosion), orange (potential overwash), or red (potential inundation) depending on the predicted dune impact at that location. On the right, the solid blue line is the TWL, the cyan band is the 95% confidence range, and the dotted blue line is the mean water level (no runup). The dune crest and toe are represented by the solid and dotted tan lines respectively. The hourly predicted water levels are plotted with respect to time and cross-shore space. The color of the profile changes from tan to match the predicted dune impact regime (U.S. Geological Survey, 2023b,c).

$< D_{Low}$), collision ($D_{High} > R_{High} > D_{Low}$), overwash ($R_{High} > D_{High}$, $R_{Low} < D_{High}$) and inundation ($R_{Low} > D_{High}$) respectively (Figure 2.5). Users can select individual transects on the map to watch an animation of the predicted total water level time series alongside a representative profile.

The TWLCCFV can provide fast, hourly predictions of total water levels with an associated impact category, but it has limitations. First, the empirical formula for runup within the total water level uses simplified transects that do not include potentially significant ground surface features. Secondly, the impact regime predictions assume the transect characteristics are static throughout the storm duration. Pre-storm dune crest and toe elevations are compared to the hourly total water levels to assign an impact regime, but the system does not consider if the beach or dune has been eroded in previous time steps. These deterministic and dynamic

limitations of this approach lead to further questions that will be described later in this chapter.

2.2.3 XBeach

The eXtreme Beach model (XBeach, Roelvink et al., 2009) is a hydrodynamic and morphological model for sandy coastal environments during storms. XBeach has a non-hydrostatic mode that solves the nonlinear shallow water wave equation with pressure correction to fully resolve individual wave propagation and decay, a stationary mode that solves wave-averaged equations, and a surfbeat mode that resolves the long waves associated with a short-wave envelope. The computed hydrodynamic conditions, specifically the wave and current critical velocities, are used in the default transport formulations to calculate bed and suspended load transport (van Thiel de Vries, 2010). XBeach morphodynamics can also account for avalanching, breaching, and hard structure or vegetation effects.

Studies have demonstrated the XBeach model is capable of producing robust, high-resolution, two-dimensional predictions of storm-driven sediment transport and nearshore morphodynamics (e.g. Gharagozlou et al., 2020). Although the XBeach 2D models are able to produce high-accuracy results, the simulations are computationally intensive and require high-resolution topographic and bathymetric data.

To reduce computational expenses, there is an option to run XBeach in surfbeat mode along a singular transect in one dimension. Using similar equations and physics as the 2D model, XBeach 1D predicts sediment transport in the cross-shore direction without solving for alongshore components. These XBeach 1D models have been used for real-time forecasting and hazard predictions (Harley et al., 2011; Vousdoukas et al., 2012), but the implementation of this modeling approach is often restricted to a specific location or a limited number of designated profiles.

2.3 Storms

This thesis will focus on two major hurricanes, both of which made their original U.S. landfalls on the Gulf coast of Florida. The events resulted in significant erosion and large-scale damage to coastal communities. The sections for each storm below will elaborate on features of the landfall regions, storm paths, and observations of resulting impacts.

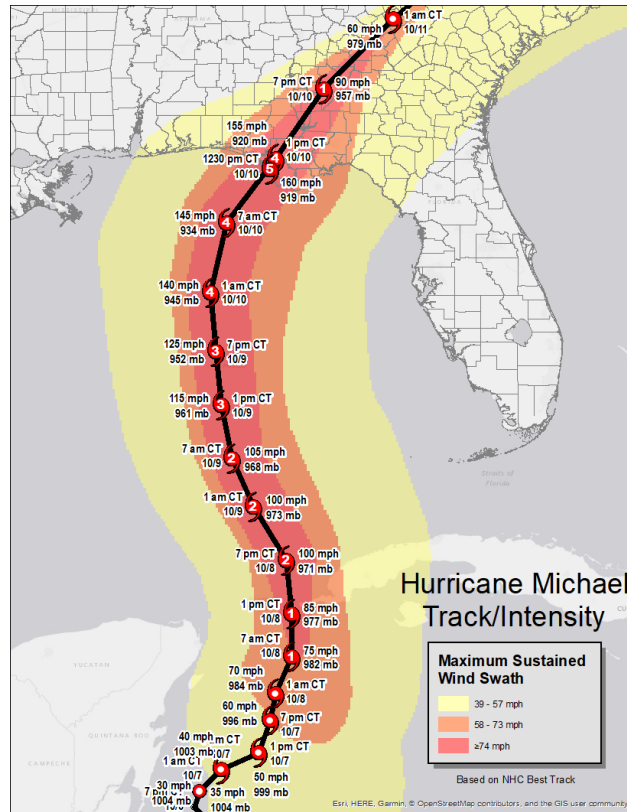


Figure 2.6: Temporal evolution of Michael intensity from the National Weather Service (Beven et al., 2019b). The icons along the track are labeled with the date, time, maximum sustained wind speed, and the corresponding hurricane category. Reproduced from National Weather Service (2019).

2.3.1 Michael (2018)

Michael originated in the southwest Caribbean, combining with the remnants of Tropical Storm Kirk (Beven et al., 2019a), about 320 km north of Panama on 6 October 2018 (National Weather Service, 2019). The tropical storm made its way north as it intensified and eventually made landfall near Mexico Beach, FL, as a Category-5 hurricane at 1730 UTC 10 October. The rapid intensification of this storm resulted in an abrupt peak of storm surge, wind velocities, and wave energy (Figure 2.7). When Michael made landfall on the Florida Panhandle, the maximum sustained wind speed at the Tyndall Air Force Base was 72 m/s and the nearby Mexico Beach area experienced about 3 m of storm surge (National Weather Service, 2019). Michael then continued to weaken as the eye of the storm moved north and eventually transitioned to an extratropical event in North Carolina by 0000 UTC 12 October (Beven et al., 2019a).

Focusing specifically on coastal change, this event resulted in several beach locations experiencing dune overwash, where the water overtops the dune crest, and inundation, where

the dunes are almost completely removed leaving the back shore vulnerable to storm impacts. Bay County, which contains the landfall location near Mexico Beach, reported approximately 952,530 m³ of erosion with a net volume loss of 529,357 m³ (Water Resource Management, 2019). Similarly, Gulf County to the southeast of the landfall reported a total eroded volume of 2,310,030 m³ a net volume loss of 1,484,090 m³ (Water Resource Management, 2019). A breach was formed at a narrow spot along Cape San Blas, leaving the roadway connecting the T.H. Stone Memorial St. Joseph Peninsula State Park to the mainland out of commission. The 60-m gap had an average depth of about 2 m with one location experiencing a nearly 14-m change in elevation from a 9-m dune elevation to a -4.5-m channel (Water Resource Management, 2019).

This storm was selected as a validating test case for this thesis because of the challenges associated with the rapid intensification of the storm and the notable coastal change observed after the storm. The post-storm lidar taken only days after landfall was converted to a digital elevation model for erosion/deposition analysis and replaces the existing CUDEM elevation data representing pre-Michael conditions. Unlike other historical storms, the recent post-storm data gives a clearer understanding of observed coastal impacts. This will facilitate model comparisons, such as dune crest elevation change and percent of dune volume change discussed in the methodology section.

2.3.2 Ian (2022)

Ian originated from a tropical wave off the west coast of Africa from 14-15 September and continued across the Atlantic for 6 days until it reached the Windward Islands on 21 September (Bucci et al., 2023a). The system organized to form a tropical depression at 0600 UTC 23 September approximately 150 km northeast of Aruba and advanced to a tropical storm at 0000 UTC 24 September, located southeast of Jamaica. Ian's core turned northwestward and intensified rapidly, resulting in Ian officially gaining hurricane status at 0600 UTC 26 September near Grand Cayman Island. Intensification continued as Ian approached Cuba and made its first landfall as a category-3 hurricane at 830 UTC 27 September near La Coloma. Ian entered the southeastern Gulf of Mexico at 1400 UTC 27 September and reached its peak intensity of 72 m/s at 1200 UTC 28 September, making Ian a category-5 hurricane. Slightly weakened, Ian made a second landfall near Punta Gorda, Florida at 2035 UTC 28 September with an estimated intensity of 64 m/s and continued northeastward across the Florida peninsula. The system entered the Atlantic near Cape Canaveral, FL, as a tropical storm at 1200 UTC 29 September and began to strengthen as it moved northward toward the South Carolina coast. The final landfall near Georgetown, SC occurred at 1805 UTC 30 September with a 36-m/s intensity, and Ian became an extratropical cyclone over North Carolina by 0000 UTC 1 October.



Figure 2.7: Figure from Tropical Cyclone Report for Ian published by the National Hurricane Center (Bucci et al., 2023a). The still images show time snaps from a remote camera capturing the storm surge inundation in Fort Myers, FL. Credit: Max Olson.

Observed storm surge during Hurricane Ian is well-documented due to the deployment of tide gauges and water level sensors, and surveys of high water marks. Peak inundation, measured near Fort Myers Beach, was 3 to 4.5 m above the ground level (AGL), which is validated by video evidence of waves and storm surge covering a camera mounted 3.5 m above the ground (Figure 2.7) (Bucci et al., 2023a). Sanibel Island in Florida saw maximum inundation levels of nearly 4 m resulting in structural damage to the Sanibel causeway and visible breaches in NOAA post-storm aerial imagery. Tampa Bay, located to the left of the storm track and originally anticipated to be the landfall location of early track advisories, experienced a drawdown of about 1.3 m below the Mean Lower Low Water (MLLW) as water levels receded below normal levels. For the U.S. Atlantic coast, Volusia County, FL, and Georgetown, SC, had maximum inundation levels of 1 to 1.5 m and 1.2 to 1.8 m, respectively. Rainfall also contributed to the coastal flooding with more than 68 cm recorded in Grove City, FL near the storm landfall and 25 to 50 cm in central and eastern Florida (Bucci et al., 2023a).

Ian is the third-costliest hurricane on record in the U.S. after causing an estimated \$112.9

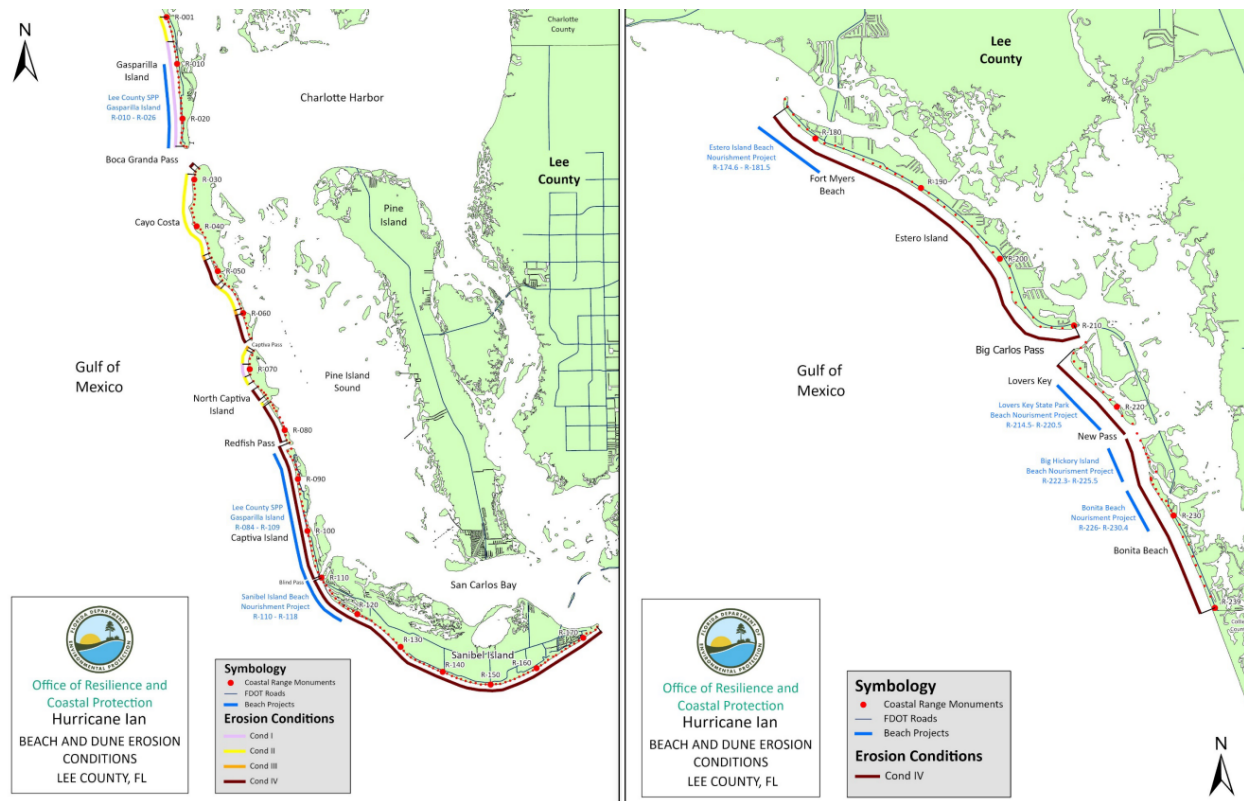


Figure 2.8: Map of Lee County post-Ian erosion conditions from the Florida Department of Environmental Protection Hurricane Ian & Hurricane Nicole Preliminary Post-Storm Beach Conditions and Coastal Impact Report (Clark et al., 2022)

billion worth of total damage, \$109.5 billion in Florida alone (Bucci et al., 2023a). Lee County saw impacts to more than 52,000 structures, where about 5,000 were destroyed and 14,000 had major damage. More than 9.6 million people lost power between 28 September and 1 October. In addition to the direct damages caused by Ian, this event also produced 15 tornadoes that resulted in an estimated \$2 million worth of property damage. Predicting the landfall location for this event was challenging because the storm track ran parallel to the coastline, where small changes in the heading can significantly alter the path. Consensus models – such as HCCA, the United Kingdom Met Office global model (EGRI), and the COAMPS-TC model (CTCI) – outperformed the official NHC forecasts, with CTCI providing the best 72- and 96-hr guidance of the consensus models (Bucci et al., 2023a).

It is difficult to quantify the storm-driven erosion and coastal change caused by Ian alone because Nicole (2022) made landfall along the southeast Atlantic coast about 1 month following Ian. Thus any surveys taken after November 2022 may be affected by the impact of Nicole. The Florida Department of Environmental Protection combined the impacts from Ian and Nicole into a singular preliminary post-storm report and described the observed erosion

for several counties along the east and southwest coast of Florida (Clark et al., 2022). Beach conditions are categorized on a scale from I to IV, where condition I is minor beach erosion and IV is major dune erosion or complete dune removal. Range or reference monuments, spaced approximately every 300-m, are classified based on the previously described beach erosion condition scale to describe the storm impact for that region. Lee (Figure 2.8) and Collier Counties in the southwest coast and St. Johns, Flagler, Volusia, Brevard, and Indian River Counties on the east coast had multiple ranges classified as condition IV or major dune erosion. Surrounding counties – such as Sarasota, Charlotte, St. Lucie, and Martin – saw a minimum of minor beach erosion with some regions experiencing moderate dune erosion and beach profile lowering (category III) (Clark et al., 2022). It is important to note that the conditions for counties on the Florida east coast include the impact from both Ian and Nicole in their evaluation. Post-storm elevation data are not yet available for storm-driven erosion analysis, but aerial photos published by NOAA show the impacts and widespread damage caused by Ian (National Oceanic and Atmospheric Administration, 2022).

2.4 Motivation

There are remaining questions about beach and dune erosion during extreme events along the U.S. Atlantic and Gulf coasts. These questions will motivate the research objectives in this thesis.

2.4.1 Remaining Questions

The initial set of questions pertains to the predictive capabilities of a morphological modeling framework applied on 1D transects along the entire U.S. Atlantic and Gulf coasts. It is common for morphological models to be applied in 1D transects, but typically for specific limited coastlines (Harley et al., 2011; Vousdoukas et al., 2012), and typically with calibration for a specific location. It would be impossible to calibrate transects along the entire U.S. coast, so we aim to use a ‘default’ input parameter set for all transects. *How will these uncalibrated parameters perform for predictions of erosion during a large, impactful storm like Michael?* Via a detailed hindcast of Michael and comparisons to post-storm observations of the eroded beaches and dunes of the Florida panhandle, we will evaluate the accuracy of the XBeach model with default parameters. Then, turning to forecast applications, the erosion predictions must be communicated in a way that emphasizes the potential ‘failure’ of the beach and dune system as a protection. We aim to use a simplified version of the Sallenger (2000) regimes, in which we will use a binary categorization of whether the waves and water levels affect the

dune crest (overwash, inundation) or not (swash, collision). *How accurate and effective is the binary dune impact categorization, and how do other forecasts compare using this metric?* It is anticipated that the 1D Michael simulations will verify that the selected model and parameters are applicable for the U.S. Atlantic and Gulf coast and produce accurate predictions of dune impact compared to observed elevation changes. This is likely a result of improved ground surface information and improvements to the XBeach 1D infragravity wave formulation. The Michael validation will justify the XBeach 1D model implementation for real-time forecasting of beach and dune erosion during an anticipated hurricane event.

The next set of questions involves the computational efficiency and modeling framework of the forecasting system. XBeach has been implemented for real-time forecasting (Baart et al., 2003, 2016; Harley et al., 2011; Voudoukas et al., 2012), but previous studies have focused on predetermined locations with a limited number of transects or domain size. By expanding the modeled area of interest beyond a set location, track uncertainties can affect where and how much storm-driven erosion is predicted in each advisory. *How do forecast predictions change across advisories, and how do we compare to what really happened given the limited observational data available?* Forecasts are expected to be heavily influenced by variations in advisories because each advisory will provide different boundary conditions into the model. A comparison will demonstrate that forecast accuracy improves as track uncertainty decreases. By increasing the number of modeled 1D transects, there is a potential that this could affect the efficiency of the forecasts. *How efficient is real-time morphological modeling?* We hypothesize that the additional transects will not cause a significant decrease in the forecasting efficiency because the simulations are submitted to a HPC system simultaneously with a maximum time allotment to ensure timely predictions.

The final set of questions involves what we can learn about coastal erosion during extreme events, based on the morphological modeling forecasts of Ian. Current erosion prediction methods attempt to reduce modeling complexity and save computation expenses by either producing static erosion forecasts or using simplified profile representations (Sallenger, 2000). These simplifications do not capture potentially significant subaqueous features and do not account for morphodynamics throughout the storm duration. A dynamic, deterministic morphological model is required to represent the complex nearshore features and temporal evolution of the profile. Assuming predictive accuracy through previous validation, we will quantify the addition of dynamic morphology about storm-driven erosion along the U.S. Atlantic and Gulf coast. *How do additional ground surface information and morphodynamics affect our forecast predictions?* Through comparisons to similar impact forecasts, we expect the nearshore ground surface information and dynamic morphology to affect the timing and scale of beach and dune erosion. XBeach forecasts of Ian will improve our understanding of erosion along the

U.S. Atlantic and Gulf coast by providing hourly predictions of beach and dune responses to extreme event conditions when temporal cross-shore observations are not available.

2.4.2 Objectives

By validating and implementing a deterministic, dynamic model system to forecast erosion during extreme storm events, we can expand upon and better understand the existing predictive capabilities for nearshore morphology. The following objectives will be completed:

1. *Demonstrate 1D XBeach is capable of accurately predicting storm-driven erosion.* A hind-cast simulation for Michael will be compared to observed post-storm elevations to evaluate how well the model performs.
2. *Forecast storm-driven erosion during Ian.* This includes developing a semi-automated model framework to run hundreds of storm simulations depending on the anticipated location and radius of storm impact.
3. *Evaluate and communicate the erosion forecast results.* Using familiar metrics like the Storm Impact Scale (Sallenger, 2000), create an effective way to spatially display the 1D results for each advisory. Assess the hundreds of model results through qualitative and quantitative post-storm analysis.
4. *Verify that the addition of dynamic morphology affects our forecasting capabilities.* Due to a lack of spatial and temporal elevation change data, the Total Water Level and Coastal Change Forecast Viewer provides hourly static impact predictions to determine the value of including the morphodynamic component.

By the end of this research, we will have a better understanding of storm-driven erosion and how to best estimate risk of hurricane impact.

CHAPTER

3

METHODS

This chapter describes the data preparation and computational framework used to model storm-driven erosion along the U.S. Atlantic and Gulf coast for both Michael (2018) and Ian (2022). Each section of this chapter discusses a major step within the morphological modeling process (outlined in Figure 3.1). The process varies slightly depending on whether the simulation is a hindcast intended for validation or a forecast intended for real-time predictions. However, both Michael and Ian simulations undergo a pre-storm ground surface information update, a boundary and initial condition interpolation, and XBeach simulations with the same parameters and computational resources. The steps and methods described in this chapter will provide more information about the model results and performance metrics.

3.1 Preparations Before Hurricane Season

Each XBeach simulation requires a unique set of input files for each transect. Some of these inputs are storm-specific, such as the wave parameters and water levels at the offshore boundary, and thus, for real-time forecasts, they must be developed during the storm. But other inputs are specific only to the transect, such as the ground surface elevations along the profile. These inputs can be developed before hurricane season.

The initial ground surface is represented by a 1D grid with variable cross-shore resolution

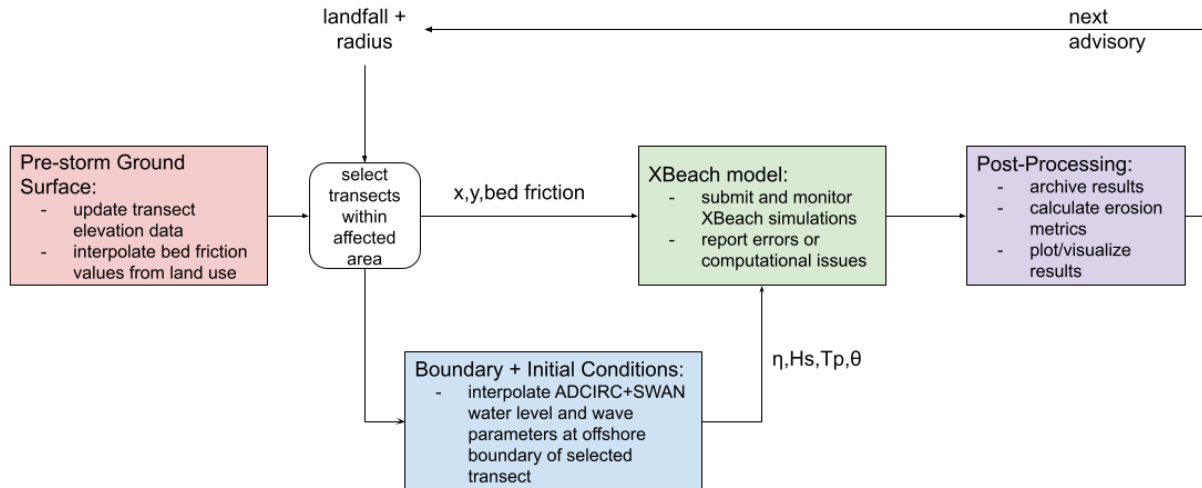


Figure 3.1: Morphological modeling workflow for real-time forecasting.

and corresponding elevation and bed friction values at each grid cell. The 1D grid is described by the cross-shore distance of each computational point from the offshore boundary and the angle of the overall profile from east. Elevation and bed friction values are then interpolated onto the grid from the best-available pre-storm ground surface data. Starting with a recently published cross-shore profile dataset for the U.S. Atlantic and Gulf coast (Mickey and Passeri, 2022, described in Chapter 2), modifications and additions to the existing transects are made before the hurricane season, and then the transects are saved for future use.

The goal of this process is to develop a set of XBeach input files that describe the ground-surface elevation and other characteristics for each transect. The nearly 4000 transects within the dataset (Mickey and Passeri, 2022) are converted to tab-delimited text files to represent the ground surface within the XBeach model. The x -file contains the cross-shore distance in meters from the offshore boundary to each gridpoint, and the y -file contains the corresponding elevations, either from topographic lidar or the stitched CUDEM. Additional profile characteristics – such as dune crest elevation, dune width, dune volume beach width, beach volume, and beach slope – are stored in a separate information file for future use during post-processing and result analysis. Folders, named with the assigned arbitrary ID, are created for each transect to contain all of the prepared input files – including the x - and y -files, the interpolated bed-friction coefficient file, and a figure of the cross-shore profile. In later stages, the interpolated wave and water-level time series, as well as the XBeach parameters file, will be added to the folder for each simulation. The following subsections will describe how the required transect files for the XBeach model are prepared.

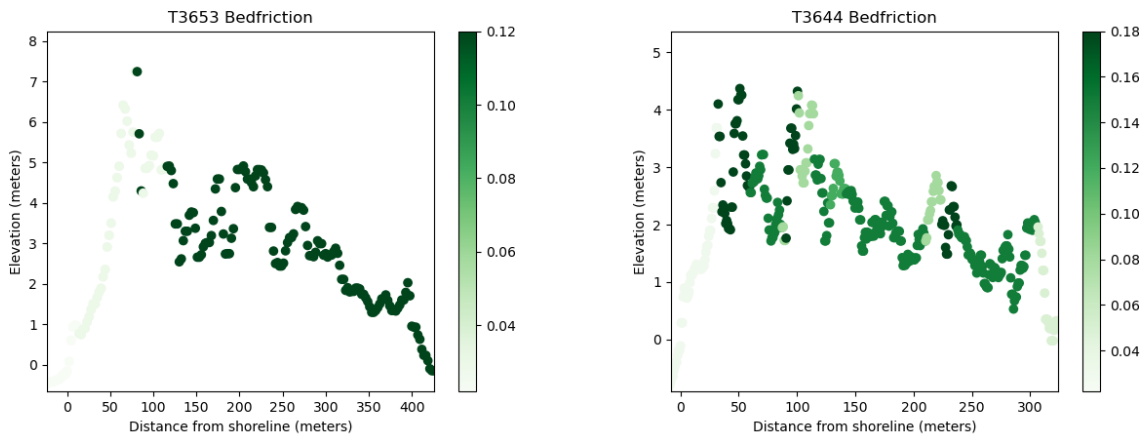


Figure 3.2: Cross-shore bed friction values for two 1D profiles. Each point represents a node in the profile that has been assigned a Manning’s n value based on its land classification. Transect 3653 is located on Cape San Blas and transect 3644 is located on St. Vincent Island (both on the Florida Gulf coast).

3.1.1 Bed Friction Interpolation

Recent studies have shown that spatially varying bed-friction values based on land cover classifications can improve morphological modeling predictions by more accurately representing overwashing and breaching (Passeri et al., 2018). The dataset from Mickey and Passeri (2022) does not include bed-friction values for the transects, so they were added as part of this research. For every transect along the U.S. Atlantic and Gulf coast, land-use classifications were interpolated from the NLCD2019 30-m resolution raster (USGS, 2019) onto the 1D cross-shore grid. The sampled land classifications were converted to a Manning’s n bed-friction factor at each grid cell using tables derived for C-CAP classes utilized in previous numerical modeling studies (Dietrich et al., 2011a; Passeri et al., 2018). Values for bed-friction factors range from $n = 0.022$ in open water to $n = 0.18$ in highly-developed areas, which can drastically affect the computed sediment transport. The spatially varying bed-friction coefficients corresponding to a specific 1D transect are saved in a tab-delimited text file and stored for future XBeach simulations. These bed-friction values can be updated using the same process when new land use data becomes available.

The transects in Figure 3.2 display the interpolated bed friction values for two transects located on the Florida Panhandle. Transect 3653 represents a mainly residential portion of Cape San Blas that is classified as ‘low to medium intensity development’ for a majority of its sub-aerial gridcells. The corresponding classification (Manning’s $n = 0.12$) is typically assigned to regions with mixed vegetation and single-family housing units (Multi-Resolution

Table 3.1: NCLD2019 land classifications and corresponding Manning’s n values from Passeri et al. (2018, Table 1). The majority of the NCLD2019 classes have a corresponding C-CAP class, except the Woody and Emergent Herbaceous Wetlands, which use the most-similar C-CAP class possible (Palustrine and Estuarine Forested Wetlands for Woody Wetlands ($n = 0.15$) and Estuarine Emergent Wetland for Emergent Herbaceous Wetlands ($n = 0.05$)).

NLCD2019 Class	Manning’s n
High Development	0.12
Medium Development	0.12
Low Development	0.12
Open Space Development	0.035
Cultivated Crops	0.1
Pasture/Hay	0.05
Grassland/Herbaceous	0.035
Deciduous Forest	0.16
Evergreen Forest	0.18
Mixed Forest	0.17
Scrub/Shrub	0.08
Woody Wetlands	0.15
Emergent Herbaceous Wetlands	0.05
Barren Land	0.03
Open Water	0.022

Land Characteristics Consortium, 2019). The portion of the transect representing the beach is classified as barren land ($n = 0.03$). Transect 3644 is southeast of transect 3653, located on the highly vegetated St. Vincent Island. The sub-aerial gridcells are classified as Evergreen Forest ($n = 0.18$), Woody Wetlands ($n = 0.15$), Scrub/Shrub ($n = 0.08$), Emergent Herbaceous Wetlands ($n = 0.05$), and Barren Land ($n = 0.03$). The cross-shore interpolated land classifications for both transects match qualitatively to aerial images of the locations. The green-scale bed friction values in Figure 3.2 show how the mainly residential and mainly vegetated transects differ spatially in the cross-shore. Although the transects are less than 30 km apart, they have different land classifications. In general, a majority of transects across the U.S. Atlantic and Gulf coasts have two or more land classifications that could affect the sediment transport properties. Interpolating the most-recently available land classification information from the NLCD2019 will improve our understanding of the pre-storm ground surface and translate into improved model accuracy.

3.1.2 Hindcast Transect Preparation

For our hindcast of Michael (2018), we start with a small subset of transects from Mickey and Passeri (2022). However, these transects must be updated to represent the pre-storm conditions along the Florida panhandle. These updates include a re-interpolation of the ground surface elevations, as well as a recalculation of transect characteristics (e.g. dune crest elevation, beach width, dune volume, etc.).

Of the approximately 4000 transects in the Mickey and Passeri (2022) dataset, 39 transects were selected for the hindcast simulations of Michael based on their location within extents of the best-available pre-Michael DEM (Figure 2.1). The existing transect dataset uses the most recent (later than 2018) topography and bathymetry data to assign ground-surface elevations in the cross-shore, so interpolation is required to reassign the elevations to better represent the beach conditions in 2018 prior to Michael. For each selected transect, the interpolation process starts with a conversion from UTM Easting and Northing to latitude and longitude using the *pyproj* package in Python (*pyproj* 2023). Next, the pre-Michael DEM is sampled using the nearest-neighbor technique at each grid cell through the *rasterio* Python package (*rasterio* 2023). The pre-Michael sampled elevations are saved as tab-delineated text files, which will be specified as the depth file used in the hindcast simulation. The same sampling process is repeated for the post-Michael lidar data (Figure 2.1), but null values are assigned to gridcells that are not within the lidar extents. The newly interpolated post-storm elevation data is stored for future analysis. At the end of this process, all 39 transects have an updated *y*-file with the best-available pre-Michael ground surface elevations for the hindcast simulations.

However, with this updated topography and bathymetry, the transect information provided by the Mickey and Passeri (2022) dataset may not be representative of the transect features. The shoreline locations, dune crests, and dune toes are then updated to reflect the new ground surface information. This process can be difficult to automate given the diverse transect topography for the 39 profiles and requires some manual supervision. To start, the shoreline is automatically selected as the first location on the transect where the elevation values become positive, or the zero-crossing point. This selection is fairly straightforward and does not require any manual adjustments or supervision. Next, the dune crest selection is semi-automated where the Python script allows the user to manually adjust the original dune crest selection if the automated selection is not accurate. The dune crest is placed automatically at the first peak of the transect that is above 2 m. This threshold was selected to avoid small beach-face features from being selected as the initial dune crest. After the automated selection, the updated transect elevations are plotted from the selected shoreline to several meters past the maximum elevation of the profile with a red star indicating where the dune crest is initially placed. The Python script then uses `matplotlib.pyplot.ginput` to allow the user to override the dune crest selection by right-clicking on a desired location or accept and proceed to the next profile by hitting enter. By right-clicking on the plot, the plot returns the exact coordinates of the selection however, it may not land exactly on a grid cell point. To find the closest grid cell to the user selection, the selected x -coordinate (in meters from offshore) is subtracted from cross-shore distances and the grid cell with the minimum difference is set as the newly selected dune crest index. The dune crest elevation will be the corresponding y -value at the selected dune crest index. With the dune crest selected, a straight line is created from the crest to the shoreline. The dune toe is automatically placed on the transect at the location of the maximum perpendicular distance between the transect elevations and the straight line. The updated shoreline, dune crest, and dune toe will be used to compute the same transect characteristics and statistics from Table 2.1.

The previous and updated information for the 39 selected transects is included side-by-side in Table 3.2. The updated dune crest elevations are similar to the Mickey and Passeri (2022) dataset dune crests with the updated average only about 10 cm less than the previous average. However, the remaining transect characteristics, such as beach and dune widths or volumes, are less similar. The updated widths and volumes are often about half the size of the minima, medians, averages, and maxima from the transect dataset. The reason for this drastic difference is more apparent when the data are plotted (e.g. Figure 3.3). The updated elevations (gray) represent pre-Michael conditions however, the Mickey and Passeri (2022) dataset (dotted, black) use post-Michael lidar data as the most recent topography. This results in different dune crest and toe positions, and thus affects the updated width and volume

Table 3.2: Comparison between the computed transect characteristics with updated ground surface information and the previously identified characteristics from the Mickey and Passeri (2022) dataset. These statistics only include the 39 transects selected for the hindcast simulation of Michael. The dune crest elevation is the vertical height above the MWL at the selected dune crest index. The beach width and dune width are the cross-shore distances from the shoreline to the dune toe and from the dune toe to the dune crest, respectively. Similarly, the beach and dune volumes are the sub-aerial cross-shore volumes from the shoreline to dune toe and from dune toe to dune crest, respectively. The total volume is the sub-aerial cross-shore volume from the shoreline to the dune crest.

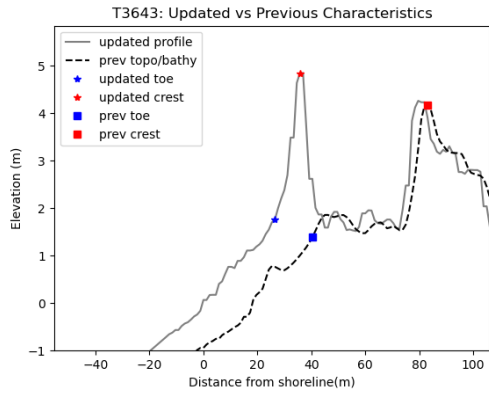
Characteristic	Units	Mickey and Passeri (2022)				Updated for pre-2018			
		Min	Mdn	Avg	Max	Min	Mdn	Avg	Max
Dune Crest Elevation	m	2.15	3.65	4.41	11.34	1.72	3.96	4.31	13.86
Beach Width	m	13.17	55.10	69.33	243.87	1.42	25.09	25.02	46.43
Dune Width	m	6.38	16.05	24.07	84.11	1.07	7.94	9.39	24.57
Beach Volume	m^3	10.47	64.90	89.36	414.92	0.01	29.82	31.66	67.62
Dune Volume	m^3	17.15	53.93	78.24	410.04	2.05	19.87	30.51	206.75
Total Volume	m^3	31.59	123.89	167.59	600.93	3.05	55.37	62.17	256.13

calculations. Transect 3643 (Figure 3.3a) shows the updated dune crest is more than 40 m closer to the shoreline and the updated dune toe is only about 20 m from the dune crest, whereas the previously selected dune crest and toe are more than 40 m apart. Thus the dune width for this transect has been reduced by about half from the previous transect information. Similarly, transect 3664 (Figure 3.3b) has an updated dune toe nearly 80 m closer to the shore than the previous dune toe, resulting in a much shorter updated beach width. In both cases, the longer beach and dune widths also affect the computed volumes because there is more cross-shore volume being included over the longer distances. This analysis and comparison between the previous and updated transect information gives us a better understanding of the initial ground surface before Michael and verifies that updating the transect elevations for this hindcast was necessary to represent pre-storm conditions. This dune crest, dune toe, and shoreline selection and transect characteristic computation process can be repeated if and when the transect elevations need to be updated.

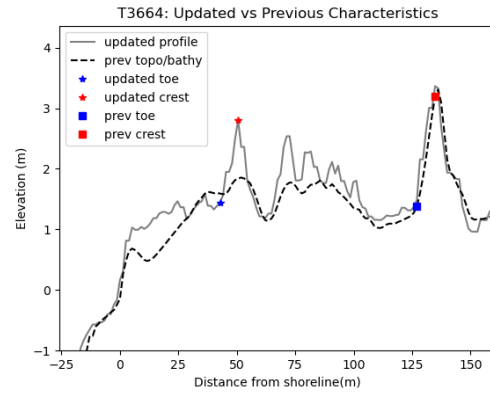
3.1.3 Forecast Transect Preparation

Our forecast simulations will use subsets of the nearly 4000 transects from Mickey and Passeri (2022). These transects can be pre-processed to provide input files for XBeach, as described earlier. However, for this study, this dataset was extended to include additional transects along the south Texas coast.

The nearly 4000 transects cover a majority of the sandy beaches along the U.S. Atlantic and



(a) T3643: St. Vincent Island, FL



(b) T3664: Mexico Beach, FL

Figure 3.3: Mickey and Passeri (2022) and updated cross-shore transect elevations with red and blue markers indicating the selected dune crest and toe locations respectively. Transect 3643 is located on St. Vincent Island and transect 3664 is located near Mexico Beach.

Gulf coasts, but the southern region of the Texas coast near Corpus Cristi was not included in the Mickey and Passeri (2022) dataset. Thus, transects were added in this research to represent this region. Starting with a Texas coastline shapefile (Himmelstoss et al., 2017), the “Line to Point” tool in ArcGIS was used to generate shoreline points at an alongshore resolution of 0.5 km, starting at the southern tip of the Texas coast. The 126 shoreline points were exported to a Python script, where 1D cross-shore grids were created perpendicular to the shoreline. The offshore origin was set approximately 3 km from the shoreline, and the grid was built toward the shore based on the linearly varying cross-shore resolution. The offshore resolution starts at 10 m, transitions to a 2-m resolution onshore, and returns to a 4-m resolution landward of the dune. The transects are about 3.3 km in length with 650 cross-shore nodes.

The CUDEM is interpolated to assign elevation data to the 650 cross-shore nodes of the 126 newly created transects. Following the same process described earlier, land use classifications are interpolated from the NLCD2019 30-m resolution raster and converted to bed-friction coefficients. Similar to the published transect dataset (Mickey and Passeri, 2022), profile characteristics are calculated and stored for future analysis. Shoreline, dune crest, and dune toe selection is fully automated using the methods described above (except the dune crest selection is used without manual user adjustment). With the selected shoreline and dune features, transect information like beach width and dune volume are calculated and stored in a separate file for every transect. The computed transect information can be used in future post-processing to evaluate how much erosion has taken place. These additional 126 transects and corresponding files are added to the stored folders for real-time forecasting.

3.2 Preparations for Each Storm Advisory

For each XBeach simulation, the storm-specific inputs must be developed during each advisory. For the hindcast of Michael, there is just one ‘advisory’ – the best-possible hindcast simulation. But for forecasts of Ian, simulations were run for multiple advisories over a week-long period as the storm approached the U.S. Gulf and Atlantic coasts. For each advisory, a subset of transects must be selected to cover the coastal regions likely to be affected by the storm. Then, for each transect, hydrodynamic forcings must be interpolated and applied as offshore boundary conditions.

3.2.1 Selection of Transects

Transects are selected for real-time forecasting based on the user-specified landfall location and radius of interest. After initiating the C-shell script in the NCSU high-performance computing (HPC) system, the script prompts the user to input the anticipated landfall location in latitude and longitude coordinates and the radius of interest in kilometers. This establishes the extent desired for modeling. The script then loops through the transect offshore coordinates and creates a list of transect IDs within the desired modeling extents. The selected transects are then copied into a folder for forecast simulations and boundary condition interpolation begins. This process is currently semi-automated. It requires the user to select the anticipated landfall location and adjust this location to account for changes in the storm track. There are other possible selection methods however, the user-specified semi-automated approach is efficient and flexible. This will be discussed further in Chapter 4.

3.2.2 Boundary and Initial Conditions

During each advisory, the forecast simulations can represent the storm via hydrodynamic forcings at the offshore boundaries. The goal is for XBeach to apply water surface elevations to represent the effects of tides and storm surge, and also to apply a wave spectra constructed from a series of parameters like significant wave height, period, direction, etc. (Roelvink et al., 2010). To achieve these boundary forcings, the user must provide input files with time series of water levels and wave parameters, distinct for every profile. These input files must follow the same formatting described in the XBeach user manual (Roelvink et al., 2010).

For this study, the wave parameters and water levels are provided by the coupled AD-CIRC+SWAN simulations (Chapter 2.2) from either the best-available hindcast or the most recent forecast simulation. XBeach applies the boundary forcing at the offshore origin of the profile. This location is typically several kilometers from the shoreline at an approximate water

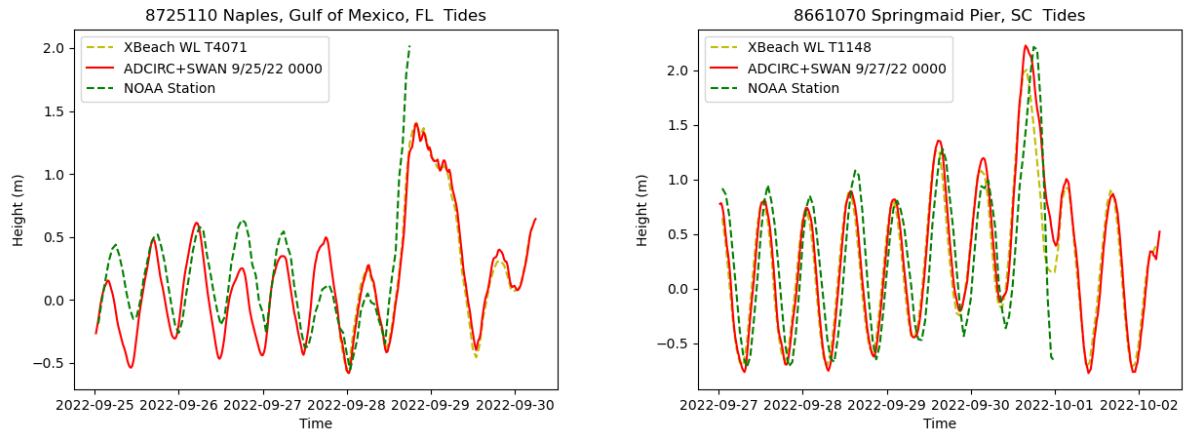


Figure 3.4: Comparison between NOAA stations, ADCIRC+SWAN water levels interpolated at the NOAA station, and XBeach water levels at the offshore boundary for the closest nearby transect. NOAA Stations 8725110- Naples Florida (left) on the southwest Florida coast and Station 8661070- Springmaid Pier, SC (right). Note that NOAA station 8725110 failed as the storm made landfall (National Oceanic and Atmospheric Administration, 2023e).

depth of 20 m to allow waves to enter the computational domain without any bottom friction effects. At the offshore origin of each selected transect, the time series for wave height (H_s), wave period (T_p), wave direction (θ), and water level (ζ) are interpolated from the ADCIRC+SWAN results using the area-weighted average of three surrounding mesh vertices. This interpolation is performed by using a Python script, and it requires about 10 min for approximately 1800 interpolation locations and a typical simulation duration of 5 days.

For the hindcast of Michael, the ADCIRC+SWAN results were provided at a frequency of every 10 minutes to represent the rapid intensification and steep peak of the wave and water level conditions. Time series interpolation began when the offshore wave heights reached 0.01 m to ensure non-zero wave values. Similarly, the water level time series is saved to a tab-delimited text file with each line containing the simulation time in seconds starting from zero and the associated water level in meters. Although the XBeach model is provided with wave properties for a JONSWAP spectrum and water levels every 10 minutes, the output time step is set to hourly to reduce the resulting file sizes and computation times. The simulation is ended at the last provided time step of boundary conditions. For example, for transect 3664 near Mexico Beach, the simulation starts at 1800 UTC October 4 when the offshore wave height was 0.05 m, and it ends at 1200 UTC October 11, for a total duration of just over 160 hours around the storm's landfall. This duration is the same as the other 38 profiles, which indicates all locations achieved the minimum threshold for wave heights at the start of the ADCIRC+SWAN simulation.

For forecasts of Ian, the ADCIRC+SWAN predictions were provided at a frequency of every 20 minutes to reduce file sizes and reduce computational expense. Time series interpolation begins the first hour that the wave conditions reach a threshold of 0.5 m or higher. This 0.5-m value was selected to reduce unnecessary computation time and ensure non-zero wave values that may cause model instability. This may affect the length of the XBeach simulation because the interpolation may start several time steps after the ADCIRC+SWAN simulation. For example, transect 890 on the northeast Florida coast begins interpolation for the 0000 UTC 28 September forecast 22 days and 19 hours after the ADCIRC start date (including spinup). This is when wave heights at the offshore boundary of T890 reach 0.5 m. The next transect T891, about 1 km north of T890, begins interpolation 2 hours later than T890 because this location does not yet hit the minimum threshold. This means the length of the simulation for T891 (123 hours) is 2 hours shorter than T890 (125 hours). The XBeach simulations output results every hour, so therefore it is essential that the simulation does not begin in between hours. This will facilitate conversion between XBeach model time and wall clock time and allow for dynamic comparisons to other hourly forecasting models, such as the TWLCCFV. Similar to the hindcast files for Michael, the wave and water level time series data for each Ian simulation is saved in the appropriate, tab-delineated file format described in the XBeach manual.

3.3 XBeach Modeling

By this step in the modeling framework, the selected transect folders with updated ground surface information have been copied to a modeling directory and the necessary boundary conditions have been interpolated. The XBeach model requires a parameter file for each simulation to help locate the input files and adjust the model formulations to better predict storm-driven erosion. Using a C-shell script, the 1D XBeach models are submitted to a high-performance computing (HPC) system and monitored to ensure they are running properly. This section will describe what input parameters are specified within the XBeach models for Michael and Ian, and how the computational resources are allotted and supervised for each simulation.

3.3.1 Input Parameters

The XBeach manual lists more than 300 parameters that can be adjusted within a set range or with specific keywords to alter the model results. Given this large number of potential parameters, it is typical for default values to be used for most parameters. However, calibration of a few parameters can be useful to better represent erosion in a specific location. This calibration

is done by selecting a test case where pre- and post-storm data are available and evaluating how the adjusted parameters improve or worsen model skill to select the best-possible model setting for future modeling applications (e.g. Simmons et al., 2019; Vousdoukas et al., 2012). Some examples of parameters that are often adjusted from their default values include wet_{slp} , Γ , α , β , and f_{acAs} (Kalligeris et al., 2020). The descriptions for these parameters are available in Table 3.3. Most studies show that parameter calibration improves model skill, but the calibration process is typically limited to specific locations where observations are available.

In this research, considering the diversity of the 4000 profiles along the entire U.S. Atlantic and Gulf coasts, it would be difficult to calibrate the XBeach parameters so that the results will be equally applicable at any location. Thus, for versatility reasons, the majority of the possible XBeach parameters will not be changed from their default values. This approach prevents over-calibration to a specific location, which could reduce model skill in other regions. For example, transects on the Gulf coast of Texas may respond differently to an extreme event compared to transects in the northeast on the Atlantic coast. These different responses can be a result of several different beach and dune properties (i.e. grain size). However, by tuning parameters to strictly improve XBeach results in one location, there could be negative effects on the model results elsewhere. To avoid over-calibration for Ian, which traveled from the southwest Gulf coast of Florida to the northeast Atlantic coast of South Carolina, a single set of parameters is selected for all modeled locations.

A few parameters were changed from their default values, based on calibration for two locations along the U.S. Atlantic and Gulf coasts (van der Lugt et al., 2019). The first location is Fire Island, NY, which was affected by Hurricane Sandy in 2012, and the second location is Matanzas Inlet, FL, which was affected by Hurricane Matthew in 2016. These calibration sites are located within our overall study area, so the selected parameters should be applicable to my forecast and hindcast XBeach models. The parameters were calibrated to best represent the significant erosion at both locations caused by extreme events. Both Fire Island and Matanzas are thin barrier islands that experienced dune erosion and some breaching as a result of storm surge and wave action. The XBeach models for these two locations achieved “reasonably good” skill scores for bed level change (Wilderness 0.55, Matanzas 0.4) and crest level change (Wilderness 0.64, Matanzas 0.60) (van der Lugt et al., 2019). Although the two locations are separated on the U.S. Atlantic coast, the shared set of parameters was able to predict significant storm-driven erosion with accuracy. In addition to the calibrated parameters, a new XBeach version was compiled and implemented to improve the 1D results. XBeach version 5924 has a new parameter wb_{cevar} that addresses the overestimation of infragravity wave heights in 1D XBeach models (McCall et al., 2023). The default 1D wave directional spreading coefficient

is assigned in addition to the van der Lugt et al. (2019) parameters, which were calibrated by comparing 1D and 2D model performance. There is a much better agreement between the 1D and 2D models and between 1D models and observations with the inclusion of `wbcevarreduce` (McCall et al., 2023).

Table 3.3: XBeach parameters changed from their default values for the Michael and Ian simulations. Most of these parameters were calibrated in van der Lugt et al. (2019), and `wbcevarreduce` was calibrated in McCall et al. (2023)

XBeach Parameter	Value	Default	Description
<code>wetslp</code>	0.18	0.3	Critical avalanching slope under water (dz/dx and dz/dy)
<code>beta</code>	0.08	0.1	Breaker slope coefficient in roller model
<code>facSk</code>	0.15	0.1	Calibration factor time averaged flows due to wave skewness
<code>facAs</code>	0.25	0.1	Calibration factor time averaged flows due to wave asymmetry
<code>gamma</code>	0.46	0.55	Breaker parameter in baldock or roelvink formulation
<code>gamma2</code>	0.34	0.3	End of breaking parameter in roelvink daly formulation
<code>alpha</code>	1.38	1.0	Wave dissipation coefficient in roelvink formulation
<code>alfaD50</code>	0.4	0	Sensitivity to grain size
<code>dynamicroughness</code>	1	0	Switch to decrease bed friction with increased erosion
<code>wbcevarreduce</code>	0.3	0.3	1D wave directional spreading coefficient

A list of the calibrated parameters from the van der Lugt et al. (2019) study, applied to the Michael and Ian simulations, can be found in Table 3.3. In addition to these calibrated parameters, there are two model settings adjusted for real-time forecasting applications. First, a `morfac` value of 5 is used to accelerate the computational time required for the models. This will improve the efficiency of the XBeach simulations and produce results faster than a default `morfac` value of unity. Second, a back wall boundary condition was used. During our model development, several XBeach tests for Michael were completely removing all subaerial sediment from the profile when the dune was inundated, resulting in submerged profiles and model instability. Multiple solutions were attempted to remediate this, including non-erodible layers and locked water levels at the back boundary. However, test results showed a back wall boundary condition was the most effective way to avoid unrealistic profile removal. The back wall boundary still allows for water to overwash or inundate the profile and remove sediment from the dune, however, the water cannot flow freely out of the back boundary. The wall boundary condition does not appear to affect the model’s ability to predict storm-driven erosion, as demonstrated by the Michael results in the next chapter. Further analysis and calibration will be considered for future work. The full set of specified XBeach parameters, including file names for transect-specific ground surface information or boundary conditions,

are saved as a text file in the selected profile's folder in preparation for modeling.

3.3.2 Computational Timing and Resources

With all files prepared, the 1D XBeach models can be submitted to high-performance computing (HPC) cores. A C-shell script loops through the selected transect folders and submits all of the jobs to the queue. The 1D XBeach runs require far fewer computational resources compared to 2D simulations, and they are typically finished in a fraction of the time. Each 1D model requests two computational cores, one for computations and the other for writing model output and a maximum wall clock time of one or two hours. For the hindcast of Michael, all simulations finished within the maximum 60-min wall clock time. For Ian's forecasts, an additional hour buffer was added to the maximum wall clock time to account for potentially long simulations with several days to model. Although the jobs were given a maximum run time of 2 hr, most jobs were completed within 30 min due to wave interpolation thresholds.

As the XBeach jobs filtered through the ccee queue on the NCSU Hazel HPC cluster, the runs were monitored for potential errors or issues. Typically when a 1D XBeach job has been running for more than an hour, there is an instability or problem that requires attention. Any unstable simulation is removed from the queue and investigated to find the source of the issue, if possible. Throughout the model computation, the XBeach results are saved to a netCDF output file that contains spatial and temporal model results. When a job is successfully completed, a file titled 'FINISHED' is created to verify that the simulation was run to completion. Immediately following the completion of successful or removal of unsuccessful models, the results are processed and visualized. The next section will describe how the results are prepared for further analysis.

3.4 Post-Processing and Visualization

This section will describe what erosion metrics are used to evaluate the XBeach results and how the forecasts are visualized to represent the predicted coastal change during extreme events. It is essential to effectively communicate erosion predictions, especially to local stakeholders in coastal communities who may not be familiar with morphological models, so multiple erosion metrics are selected to qualitatively and quantitatively represent forecast results. Dune crest impact will be a major focus of both our hindcast validation and forecast evaluation. Simplifying results to binary dune impact categories can facilitate risk communication and allow for comparison to other categorical forecast methods (e.g. TWLCCFV, U.S. Geological Survey, 2023b). Additionally, dune crest elevation change and percent volume change are

computed to supplement the qualitative dune impact information and provide quantitative metrics for predicted sub-aerial coastal change.

Hindcast simulations from Michael undergo additional analysis to verify the methodology produces accurate results and the erosion metrics are effective in representing the predictions. This validation is necessary to ensure the implementation of the forecasting framework will be successful. Because observational lidar data are not available for the Ian forecasts, the XBeach dune impact predictions are compared spatially and temporally to the closest nearby TWLCCFV site predictions. This qualitative comparison will be used to assess how dynamic morphology and high-resolution ground surface data affect dune impact predictions. The final step of post-processing is visualizing and publishing the figures and data to a website/repository. Users can access the cross-shore plots of the forecasted transects and spatial maps of the erosion metrics for each advisory.

3.4.1 Dune Crest Impact

Dunes are often our last line of defense between storm conditions and important coastal infrastructure. When water begins to overwash and flow past the dune, the coastal communities behind the dunes become vulnerable to the extreme event. Dunes are represented in the transect dataset (Mickey and Passeri, 2022), which includes transects with typical alongshore spacings of 0.5 to 2.5 km. To consider erosion along the entire continuous coast, each transect must represent the expected vulnerability not only at its 1D location, but also in its surrounding area. A comparison of pre- and post-storm dune crest elevations at each transect may be too precise, given the uncertainties in both observations and models, and may also be impossible, given the lack of data in real time. Thus, we investigate the use of a binary dune impact metric, which may reduce the complexity of the results and make the predictions more accessible to a wider audience.

A binary dune impact metric, which categorizes transect results by whether or not water reached or passed the dune crest, can identify vulnerable locations. The ‘no impact’ category (or swash/collision regime according to the Sallenger (2000) Storm Impact Scale) signifies a location where high water levels likely eroded the beach and dune face, but the maximum water level did not reach or pass the dune crest. The ‘impact’ category (or overwash/inundation) signifies when water does reach the dune crest and likely results in more sub-aerial erosion of the profile (e.g. Figure 3.5). This categorization is evaluated in the XBeach predictions by identifying if water reaches the specified dune crest index at any point throughout the storm. All predicted dune impacts are stored (1 for impact, 0 for no impact) in a list of metrics to be used for future visualization.

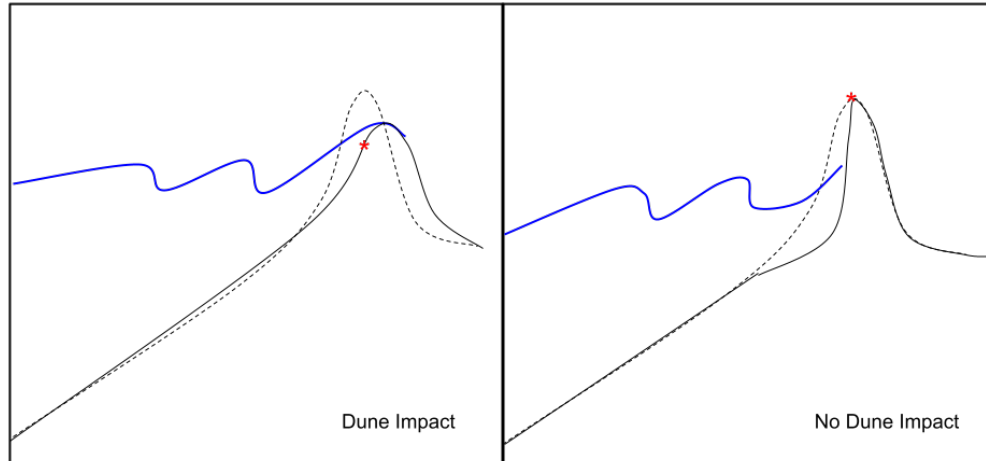


Figure 3.5: Simplified schematic of the two dune impact categories. The initial profile (dotted black), modeled profile (black), and water levels (blue) are represented as lines in the figure. The red star indicates the initial dune crest index where the water levels will be evaluated; this initial dune crest can be lowered during the simulation.

To evaluate how effective the dune impact metric is, Michael impact predictions are compared to post-storm observations to verify the accuracy of the categorization. For each selected transect (39 for Michael), the water elevations at the dune crest are investigated to decide if the profile saw dune impacts or not. Then, the post-Michael lidar data are categorized depending on change in dune crest elevation, because we do not have observations of temporal water level information at the dune crest. A transect is considered to have been overwashed or inundated if the observed lidar elevation, at the cross-shore location of the initial dune crest, is lowered by over 0.2 m. If not, the transect is assumed to have ‘no impacted.’ Using the observed dune impacts as truth, the XBeach dune impacts can be compared to understand how well the models predicted vulnerable locations.

It is important to note that the dynamic morphology in the XBeach model allows erosion to occur throughout the simulation, which could result in dune lowering. The proceeding beach and dune erosion could affect if and when the dune is predicted to be impacted in the model. In contrast, the TWLCCFV uses static and idealized profiles that do not change throughout their forecasts. The hourly predictions switch between swash, collision, overwash, and inundation depending on the water elevation relative to the fixed dune crest and toe (refer to Figure 2.5). A comparison between the two forecast methods can be useful to understand the role morphodynamics play in the prediction of dune impacts. More information on this will be provided later in this section.

3.4.2 Dune Crest Elevation and Percent Volume Change

Although the binary dune impact prediction is a good indicator of locations where significant erosion is predicted, quantifiable metrics provide a range of values to establish a scale within each category. Quantities like dune crest elevation change and percent volume change help to determine the magnitude of predicted erosion. These quantities can be computed without post-storm elevation data, which makes these metrics easy to implement for real-time XBeach forecast evaluation.

Dune crest elevation change is calculated by taking the difference between the initial profile dune crest elevation and the final modeled profile elevation at the same cross-shore location. This information is useful because it tells us how much erosion of the dune has taken place during the storm and how vulnerable this location would be if another extreme event would occur before the dune has recovered. However, dune crest elevation change is not restricted to locations where dune impact is predicted. Dune faces can scarp and avalanche as a result of the dynamic morphology throughout the storm and cause dune crest lowering without water spilling over the top. By computing dune crest elevation change at both 'impact' and 'no impact' locations, there is a better understanding of where dune crests are lowered without overwash, which could leave those regions susceptible to future storm impacts if dune crest elevations are unable to recover before the next storm (e.g. Nicole one month after Ian).

Percent volume change is also calculated because this metric includes erosion that occurs on the beach face, whereas the other two metrics focus on the dune. Percent volume is computed by taking the absolute difference between the initial and final volumes and dividing it by the initial volume. The initial and final volumes are calculated from the shoreline to the dune crest. Starting at the shoreline, the elevation for each point on the profile is multiplied by the distance between points and added to the sum. However, because the spacing between points can vary, the distance is computed from the midpoints between the last and next points. The final sum for both the initial and final profiles is essentially the area of the profile above the mean water level from the shoreline to the dune crest with units of m^3/m . By dividing the difference by the initial volume, the value is dimensionless and scaled by the size of the profile before any change occurs. This will prevent large volume differences from high-volume beaches and dunes from skewing the data. Limiting the percent volume change calculation from the shoreline to the dune crest ensures that sand is conserved within this portion of the profile and only volume moving in or out of this boundary is represented in the final value.

3.4.3 Additional Hindcast Evaluations

The available post-storm lidar data for Michael makes it possible to compute model skill and assess the predictive accuracy alongside the other erosion metrics. This will give a full picture of how well the model performs and how well the metrics represent the observed coastal change. The Brier Skill Score (*BSS*) is a commonly used metric to determine the accuracy of morphological models, and it is computed using the following equation:

$$BSS = 1 - \frac{\sum_{i=1}^N (\Delta z_{o,i} - \Delta z_{p,i})^2}{\sum_{i=1}^N (\Delta z_{o,i})^2} \quad (3.1)$$

where Δz_o is the difference between pre- and post-Michael elevations and Δz_p is the difference between pre-Michael and XBeach predicted elevations. The *BSS* has an associated scale to categorize the model results into ‘bad’ ($BSS < 0.0$), ‘poor’ ($0.0 < BSS < 0.3$), ‘reasonable’ ($0.3 < BSS < 0.6$), ‘good’ ($0.6 < BSS < 0.8$), and ‘excellent’ ($0.8 < BSS < 1.0$).

There are a few limitations of the *BSS*. First, it tends to favor under-prediction of storm-driven erosion (Bosboom et al., 2014). Second, in a forecast application with significant uncertainties in initial conditions and storm forcings, it is difficult to achieve good and excellent scores. For our application, any positive *BSS* (alongside visual and other metric agreements) is considered successful. The results for Michael will include the computed *BSS* in the information at the top of the plots, but it will not be a major focus of the evaluation because it is not applicable for forecasts which do not have observational data available. Visualizations and other qualitative information will give a holistic understanding of the model results in addition to the *BSS*.

3.4.4 Visualizing and Publishing Results

Visualizations are essential for communicating predictions of storm-driven erosion, especially considering the amount of spatial and temporal data for each set of XBeach simulations. Plotting or visualizing the results and representative metrics makes it easier to interpret the predictions at different scales. Spatial maps of dune impact, dune crest elevation change, and percent volume change show regions of the coast where significant erosion is predicted. At a smaller scale, individual cross-shore plots with the initial and final profiles can be used to understand how high-resolution ground surface information can affect the resulting morphology after a storm. Taking this one step further, temporal plots of the individual XBeach results provide dynamic information throughout the storm duration that is not typically available through observational data. For the Ian forecasts, spatial and individual plots were automatically created and uploaded to a public website in real-time to inform others about predicted

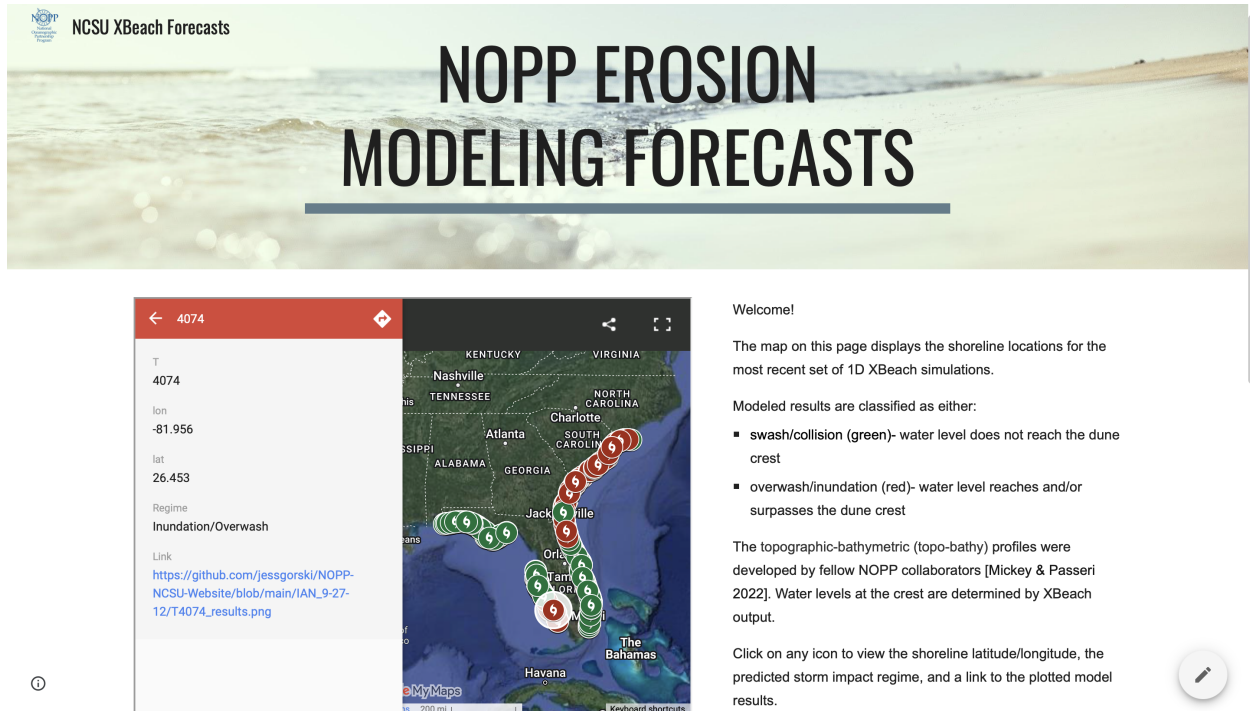


Figure 3.6: Screen capture from the public website displaying the forecast results for Ian. Each icon represents a transect, and the colors indicate the dune impact prediction for that forecast (red for 'overwash/inundation' or impact, green for 'swash/collision' or no impact). Transect 4074 is selected to show the interactive feature of the map, which provides the location coordinates, dune impact prediction, and a link to the corresponding plotted result on the GitHub repository.

coastal change and potentially vulnerable locations.

Plotted results are automatically uploaded to an online GitHub repository after the Python plotting code has successfully finished. The csh code used to prepare the files, submit the jobs, and plot the results has a final line that syncs the advisory results folder in Linux to a GitHub repository. While the upload to GitHub is automated, the website is manually updated with recent advisory information. First, the advisory folder for the plotted results on GitHub is linked under the specific storm's drop-down menu (Ian in this case). Next, the stored CSV file containing the shoreline location and erosion metrics for all approx 1800 simulations is added to an interactive map on the page. The map allows users to select the icons and follow the provided links to the corresponding cross-shore plot in the repository (e.g. T4074 for advisory 1200 UTC 27 September in Figure 3.6). This is repeated for each advisory so the website is up-to-date with the most recent forecasts available. The website makes it easy to interact with the data and view the forecast results.

3.4.5 Total Water Level and Coastal Change Forecast Viewer Comparison

Due to a lack of observational elevation data for Ian, the XBeach results are compared to another coastal change forecast model to assess the temporal differences between the predictions. The TWLCCFV (U.S. Geological Survey, 2023b), described in more detail in chapter 2, produces hourly predictions of coastal change along the U.S. Atlantic and Gulf coast. The simplified profiles being used in their forecasts are often located within a few meters alongshore of the transects being modeled by XBeach. By comparing the TWLCCFV hourly predicted impacts to the closest transect used by XBeach, we can assess how the dynamic morphology affects the predicted impacts. Using the TWLCCFV Application Programming Interface (API), the forecast impact regimes are downloaded by region, and the hourly total water levels are downloaded by site/profile. However, there are cases where every region is not modeled for each advisory. Therefore, XBeach-predicted impacts can only be compared in regions where the TWLCCFV has an available forecast. When a region forecast is available, the predicted impacts within that area are spatially plotted using the same color system to indicate collision (or no impact, green) versus overwash or inundation (or impact, red). Because neither XBeach nor TWLCCFV can be considered as truth or observed, the XBeach results are categorized by their predicted impact relative to the TWLCCFV prediction.

Individual transects near the path of Ian are then selected for further analysis. Using the same TWLCCFV API, hourly total water level predictions from the closest neighboring profile are plotted alongside the dynamic XBeach results at each time step. The plot includes the initial profile in grey for reference, the XBeach modeled bed-level and water surface elevations at each node, and the predicted TWL and associated confidence band represented as horizontal lines. The time snap plots will be analyzed to understand how the deterministic morphodynamics within the XBeach model changes the prediction. Further discussion about this comparison will be included in the next chapter.

CHAPTER

4

RESULTS AND DISCUSSION

The performance of the erosion prediction framework is assessed in two stages. First, the framework is deployed for hindcast simulations of Michael along the Florida Gulf coast. This hindcast uses a limited number of transects, but otherwise, the framework is deployed with full automation, by using hydrodynamic predictions from a SWAN+ADCIRC simulation as forcing for erosion predictions by XBeach. Results are compared qualitatively to the Coastal Change Hazards Portal (CCHP, U.S. Geological Survey, 2016), to assess whether the framework is predicting erosion impacts (overwash/inundation) in a reasonable way. Results are also compared quantitatively to the observed post-storm ground surface, to evaluate the ability of the framework to predict changes to the beach and dune. This analysis will determine if the framework produces reliable results and can be implemented for real-time forecasting.

Then, the framework is deployed for forecasts of Ian as it progressed toward and across Florida and then toward the U.S. Atlantic coast. An overview of the storm's progression will investigate how track uncertainties can affect the predictive accuracy of the morphological models and highlight regions of the U.S. coast that were most susceptible to beach and dune erosion. Then, focusing on three regions of the coast, transects are selected to compare the morphodynamic model predictions to the hourly Total Water Level and Coastal Change Forecast Viewer predictions (TWLCCFV U.S. Geological Survey, 2023b). The following discussion will evaluate the efficiency and effectiveness of the modeling framework and examine how

these results can improve our current understanding of storm-driven erosion.

4.1 Hindcast of Storm-Driven Erosion during Michael (2018)

Michael intensified rapidly as it traveled north across the Gulf of Mexico. When it made landfall near Mexico Beach at 1730 UTC 10 October, it was a Category-5 hurricane with an observed storm surge of about 3 m (National Weather Service, 2019). This surge and the storm waves caused the erosion of millions of cubic meters of sand from the beaches and dunes on the Florida Gulf coast. Michael is a strong validation test case to evaluate the performance of our modeling framework.

For this hindcast, 39 transects were selected within a 60-km radius of the observed landfall location, and then their elevation data were re-interpolated from the pre-storm DEM (Figure 2.1). Hydrodynamic conditions from a SWAN+ADCIRC hindcast were interpolated at the transect offshore boundaries, but only for the time period when the significant wave heights were above a specified threshold. Using the default threshold of 0.01 m, about 160 hr (6.5 days) were identified for computation, ranging from 1800 UTC 4 October to 1200 UTC 11 October. The simulations were submitted in bulk with a requested allocation of two computational cores per simulation and a maximum run time of 1 hr. The average run time for all Michael simulations was approximately 20 minutes, with maximum and minimum run times of 48.5 and 7 minutes, respectively. The following results will investigate how our models predict the observed coastal change and how well the erosion metrics, such as predicted dune impact or dune crests elevation change, communicate risk or vulnerability at the modeled locations.

4.1.1 Qualitative Assessment of Coastal Change

We first verify that a binary description of dune crest changes can qualitatively represent coastal vulnerability. The use of coarse ‘bins’ for predicted erosion is typical, and they are often based on the impact regimes described by Sallenger (2000). The Coastal Change Hazards Portal (CCHP; U.S. Geological Survey, 2016), which is similar to the Total Water Level and Coastal Change Forecast Viewer (TWLCCFV), uses P-Surge (National Oceanic and Atmospheric Administration, 2023d) and WAVEWATCH III (National Oceanic and Atmospheric Administration, 2023f) as hydrodynamic inputs to empirical equations to predict the probabilities of collision, overwash, and inundation on static profiles along the coast (Figure 4.1, left). The predicted regimes are plotted parallel to the coastline, with the probabilities of collision closest to the coast and probabilities of inundation the furthest. If all three regimes are shown in dark red for a given transect, then it is likely that the region will experience inundation, and if some of the regimes

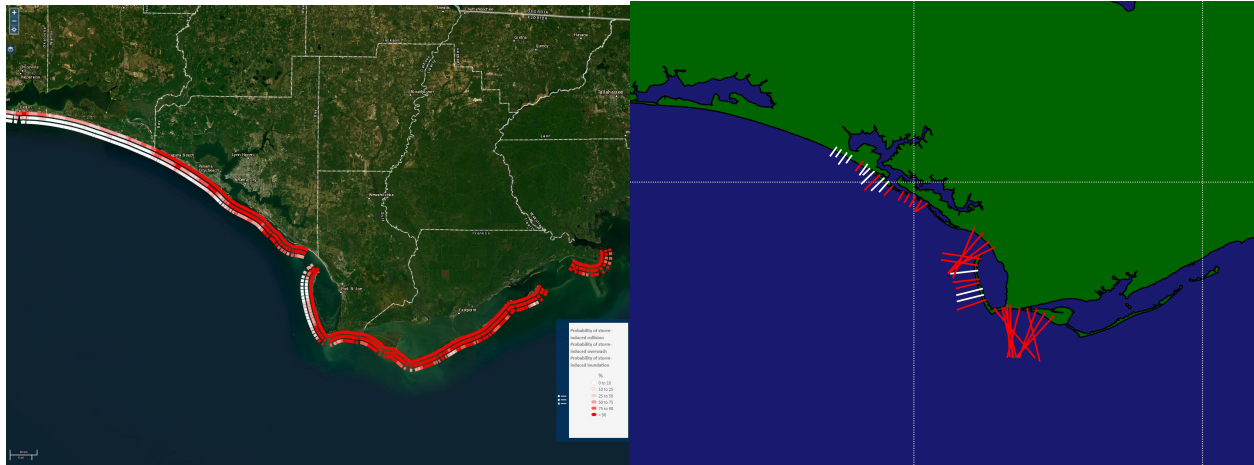


Figure 4.1: CCHP and XBeach impact prediction maps for Michael. Red indicates regions of ‘impact’ predictions and white indicates regions of ‘no impact’ predictions.

are shown in lighter pink or white colors, then it is likely that the region will experience a lower impact.

Our erosion prediction framework uses only two ‘bins’ to classify whether the dune crest is impacted (corresponding to regimes for overwash and inundation) or not (for swash and collision). These impacts are defined by whether water reaches the dune crest index at any time in the XBeach simulation. These two classes can be plotted for all transects (Figure 4.1, right) with a similar color scheme, so that more-extreme changes are shown in red, and lesser changes are shown in white. Because of the difference in the number of classes, and because the CCHP data are not available for public download and therefore cannot be re-plotted on the same map as the XBeach results, we will compare qualitatively the regional predictions given their estimated relative locations.

Comparing the two maps, there is agreement on where we expect to see the greatest impacts and where less erosion is expected. There are 9 XBeach transects near Panama City Beach that are predicted to be in the ‘no impact’ class; these transects align with regions in the CCHP predictions with low probabilities of overwash or inundation. There are also three transects on the west-facing side of Cape San Blas that have ‘no impact’ predictions, which agree with the low probability of inundation in the CCHP. Thus, both forecasts agree that the transects furthest west and along Cape San Blas will see less erosion compared to the surrounding regions. However, from Panama City Beach through Mexico Beach, and from the south-facing side of Cape San Blas to St. Vincent Island, both XBeach and the CCHP predict greater amounts of erosion. The CCHP predicts nearly 100% probability of overwash near Mexico Beach and St. Vincent Island, matching the ‘impact’ predictions for the 14 XBeach transects in those regions.

Table 4.1: Numbers of predicted vs observed impacts at transects during Michael. Impacts are defined as a change in dune crest elevation of larger than 0.2 m. Impacts are quantified at the XBeach transect locations, by using results from the nearest CCHP transect. Colors correspond to the profiles plotted in Figure 4.2.

		Observed	
		Impact	No Impact
Predicted	Impact	25	2
	No Impact	1	11

Thus, both forecasts agree about the general locations that experienced significant erosion during Michael.

In terms of disagreements, taking a closer look at Cape San Blas, there are two XBeach transects (T3655 and T3656) that predict overwash or inundation of the beach and dune where the CCHP does not. These transects are located close to the observed Cape San Blas breach (described in Chapter 2). XBeach is able to predict significant dune impact at the transect location closest to the observed breach, (T3655), whereas the CCHP predicts a low probability of dune overwash or inundation in that same area. This disagreement is encouraging, because it suggests that the morphodynamic predictions may add value beyond what is available in the CCHP. This qualitative assessment shows that XBeach predictions of dune impact can adequately represent regions of vulnerability along the coast.

4.1.2 Quantitative Comparison to Post-Storm Ground Surface

The availability of post-storm lidar data for Michael (Figure 2.1) allows for a more comprehensive validation of the XBeach predictions. In addition to the qualitative comparison of XBeach predicted dune impact to the CCHP (U.S. Geological Survey, 2016), changes in dune crest elevation based on the interpolated post-Michael elevations can be used to verify if dune impact was observed. The observed profile is considered to be impacted when the initial dune crest elevation is lowered by at least 0.2 m. It should be emphasized that the pre-storm ground surface elevations were interpolated from datasets compiled over multiple years before the storm, and thus the XBeach initial conditions may have errors. These errors would then affect any comparison between the XBeach predictions and observations of post-storm ground surface elevations.

By applying the binary dune impact metric to both observations and predictions, the 39 transects can be split into four categories depending on the XBeach predicted dune impact and the observed dune impact (Table 4.1). Out of the 39 XBeach predictions, 36 (about 92 percent) matched the observed profile impact category. Six transects, labeled on the map by their ID

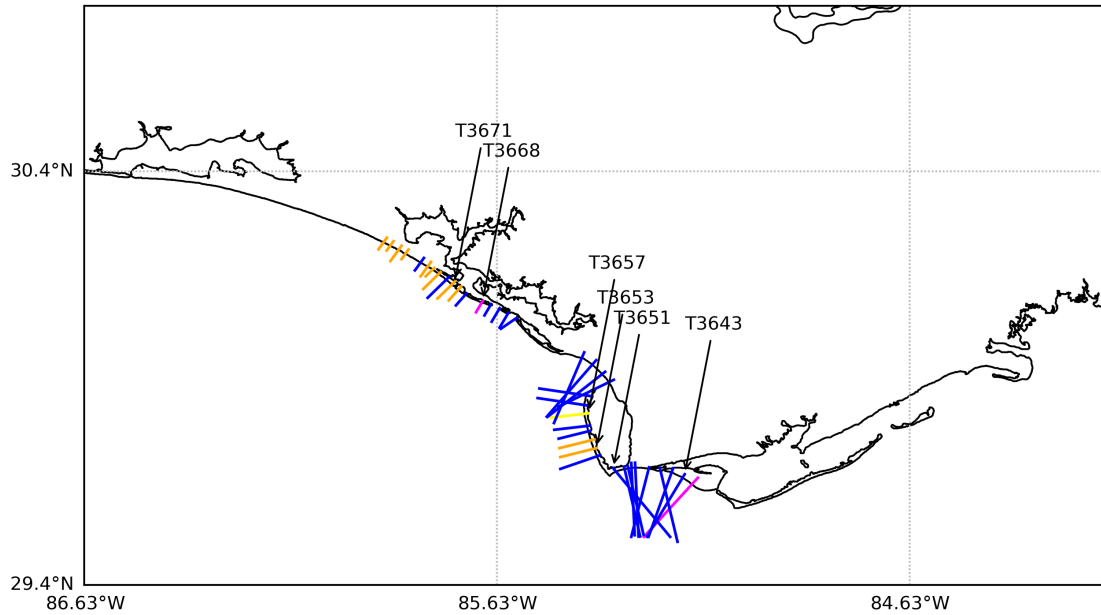


Figure 4.2: Map of predicted vs observed impacts for Michael (with colors to match the categories in Table 4.1). Transects in blue and orange represent matches between predictions and observations, whereas transects in yellow and purple represent mismatches. Labels indicate the selected transects for further analyses (Figure 4.3).

numbers, are selected as examples for all four categories. Of the selected transects, four of the XBeach results closely match the post-Michael observations (T3653, T3671, T3643, and T3651), whereas the final two (T3657 and T6668) are not able to predict the observed impact.

There are several factors that can influence whether the profile will experience overwash or inundation. Starting with the true negative examples, T3653 and T3671 (Figure 4.3a-b) have naturally high dune crests (higher than 6 m), which provided sufficient protection from the storm waves and surge. The storm caused changes to the beach and lower dune, but overwash or inundation was not experienced at these locations. In contrast, the dune crest elevations for T3643 and T3651 were lower than 5 m, which allowed for dune over-topping (Figure 4.3d) or inundation (Figure 4.3c) to be predicted correctly at both locations. At T3643, XBeach predicts the first dune to be removed, with a lowering of the dune crest elevation by more than 1 m; this change is also seen in the observed post-storm elevation. At T3651, the entire dune is removed, with both the predictions and observations showing a lowering of the ground surface by 2 to 3 m. The false negative case (T3657) may be a result of the dune lowering threshold set to 0.2 m for observed dune impacts. In this case, the observed dune face was eroded by the storm, however, it is unlikely that the total water level reaches the nearly 13 m dune crest. This is one potential consequence of setting thresholds to achieve binary metrics. The *BSS* is still generally

positive and favors the under-prediction compared to the over-predicted example. Finally, the false positive case (T3668) demonstrates a complete over-prediction by the XBeach model. This may be a result of the low dune crest elevation or the location of the transect (between the Gulf and St. Andrews Bay).

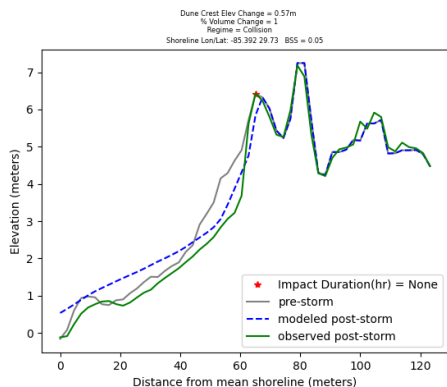
4.2 Forecasts of Storm-Driven Erosion during Ian (2022)

The hindcast for Michael was encouraging, in that the XBeach-predicted dune impacts were similar to forecasts from the CCHP and to observations of the post-storm ground surface, and thus we explore performance in forecasts of Ian. Ian affected the U.S. Gulf and Atlantic coasts in late September 2022, or about 9 months before the writing of this thesis. Although we know anecdotally that post-storm elevation data were collected and are being processed for release, they were not available in significant amounts to aid in the following assessments. Instead, the forecasts for Ian will be evaluated through both qualitative and quantitative comparisons to observed impacts, hindcast simulations, and other hourly impact forecasts.

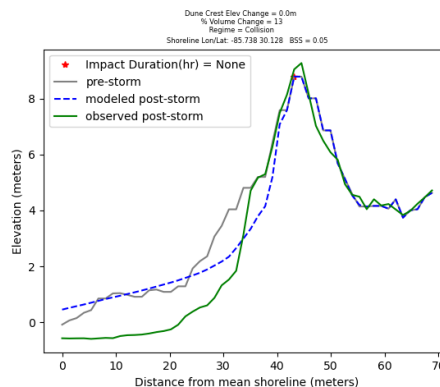
Starting with a general overview of the Ian forecast progression, the forecast and hindcast dune impacts are contrasted to investigate how track uncertainty affects morphodynamic predictions. Based on the forecast and hindcast comparison, several advisories are plotted spatially alongside the associated tracks to evaluate vulnerabilities and select regions for further analysis. Predictions from southwest Florida, southeast Florida, and South Carolina will be compared to qualitative observed erosion and forecasts from the TWLCCFV to evaluate predictive accuracy. One transect from each region is selected to demonstrate the dynamic capabilities of the XBeach model and investigate the role morphology plays in predicting dune impact vulnerability. Analysis of the profile at different times throughout the simulation will provide information on the temporal evolution of the beaches and dunes which is not typically possible due to a lack of observations during storm conditions. From the spatial and temporal model information, we can assess how different factors (location, forecast track uncertainty, etc.) affect erosion during extreme events.

4.2.1 Evolution of Erosion Predictions across Forecast Advisories

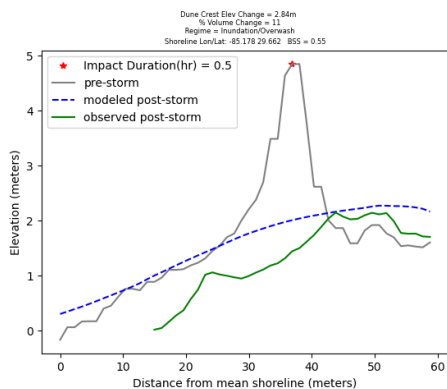
Erosion forecasting for Ian began with the advisory issued at 0600 UTC 23 September and continued through the advisory issued at 1200 UTC 29 September. Depending on the availability of wave and water level information from ADCIRC+SWAN, the frequency of erosion forecasts ranged from daily to every 6 hr, with a total of 25 erosion forecasts over the 7-day period. Because the predicted landfall location varied across the NHC forecast advisories, the erosion



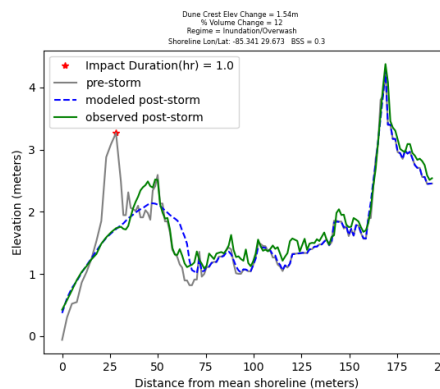
(a) T3653: True negative, no impact predicted or observed



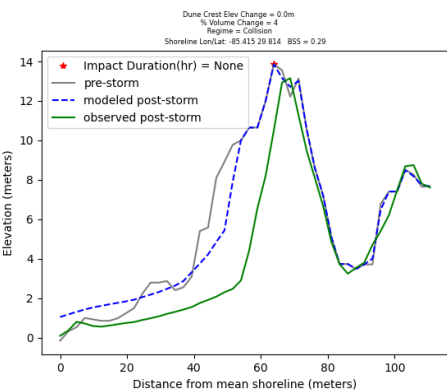
(b) T3671: True negative, no impact predicted or observed



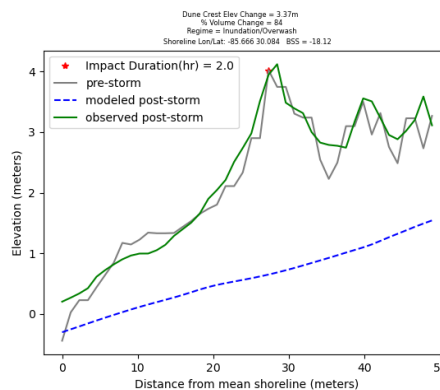
(c) T3643: True positive, impact predicted and observed



(d) T3651: True positive, impact predicted and observed



(e) T3657: False negative, no impact predicted but impact observed



(f) T3668: False positive, impact predicted but no impact observed

Figure 4.3: Examples of XBeach results compared to the observed post-Michael lidar data. Each figure is labeled by the transect ID (with locations shown in Figure 4.2) and the impact comparison category.

prediction framework selected a large set of transects that covered the full region that could be affected by the storm. These transects were selected by using a center location of 29.4843698°N, -81.379159°W, and a radius of 570 km, which identified about 1800 transects ranging from the Florida panhandle to North Carolina.

One research question is related to how uncertainties in storm forecasts were translated into uncertainties in erosion forecasts. There was quite a bit of uncertainty in the storm forecasts, as both the track and intensity were difficult to predict as Ian passed over Cuba and emerged into the Gulf. To evaluate the effect on the erosion forecasts, we compare to a hindcast ‘truth’ for dune impacts everywhere in the region that could be affected by the storm. Thus, the goal of the analyses in this subsection is to investigate how erosion predictions evolved across forecast advisories.

A ‘hindcast’ reanalysis was created by splicing together the forecasts. Segments of 6 hr were selected early in each forecast, after the storm had stabilized but before the larger uncertainties associated with longer forecast horizons. These segments were then combined into a continuous representation of the storm progression. The hindcast-from-forecasts was then applied within ADCIRC+SWAN to recreate the wave and water level conditions from the beginning of the first advisory to the end of the last. The hindcast ADCIRC water level predictions are generally good, with correlation coefficients of $R^2 = 0.83$ to the high water marks and $R^2 = 0.93$ to the gauge peaks (Figure 4.4). Although we cannot use the reanalysis as fact, the strong correlation between the model and observations demonstrates the accuracy of the hydrodynamic predictions to be used for the XBeach hindcast. The XBeach forecast results will be compared to this hindcast-from-forecasts reanalysis (referred to as hindcast going forward) to evaluate how the forecast uncertainties influence the predicted dune impacts.

Figure 4.5a displays the track for the hindcast alongside the National Hurricane Center hindcast. The path of the hindcast matches the qualitative description from the tropical cyclone report (Bucci et al., 2023b) with an initial landfall near Punta Gorda, FL, re-emergence into the Atlantic near Cape Canaveral, FL, and a final landfall near Georgetown, SC. The XBeach predictions (Figure 4.5b) use the ADCIRC+SWAN hindcast results as boundary forcing for the model. For the southwest Florida coast, the transects on the strong side or south of the track saw more erosion than the transects to the north of landfall. This behavior matches qualitative observations of beach erosion conditions from post-Ian reports (e.g. Figure 2.8; Clark et al., 2022). For the Atlantic coast, dune impacts are predicted where the hindcast track re-emerges near Cape Canaveral and further north near the final landfall in South Carolina. There are fewer observations available for these regions, but the impacts align with the observed path of the storm. The hindcast dune impact predictions can be compared to the forecast predictions to understand how the track uncertainties influence the results.

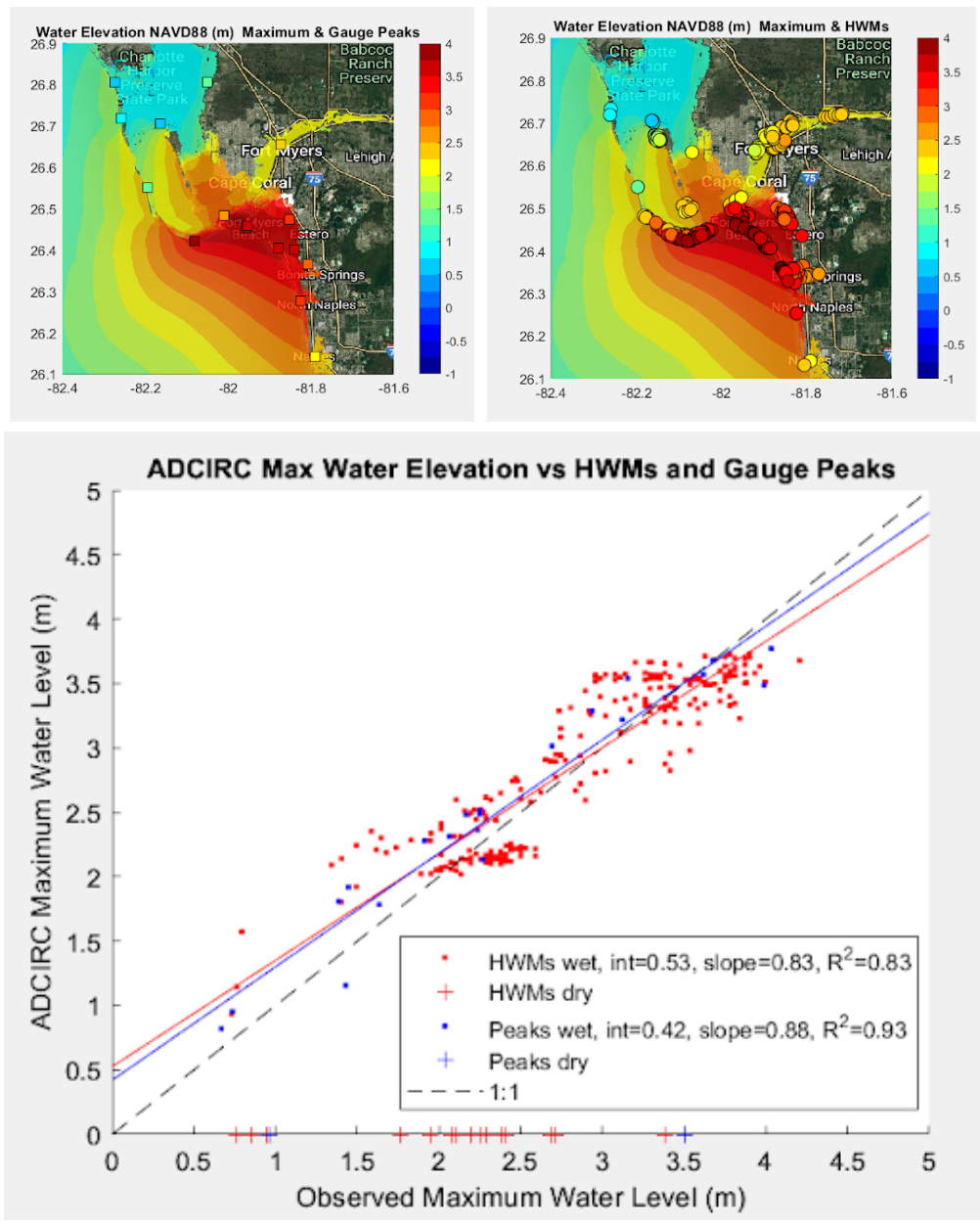
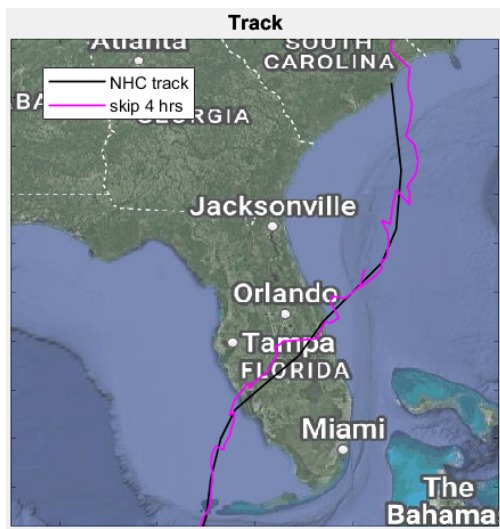
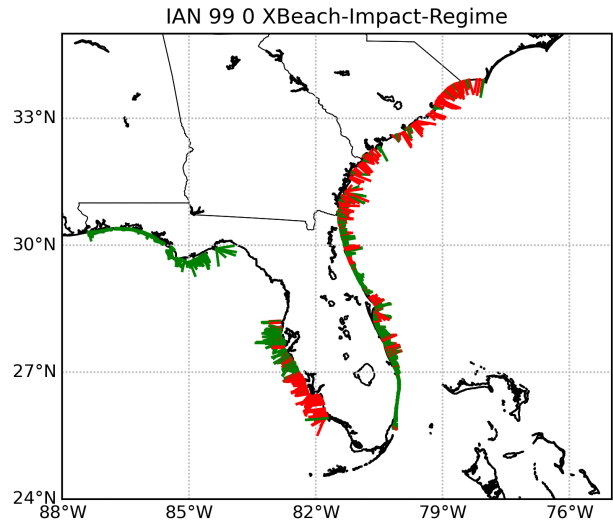


Figure 4.4: Accuracy of hydrodynamic predictions from the hindcast-from-forecasts reanalysis, with subfigures: (upper) contours of ADCIRC peak water levels (m NAVD88) near Fort Myers compared with peaks from (left) gauge observations (m NAVD88) and (right) high water marks (m NAVD88); and (lower) scatter plot of ADCIRC peak water levels vs observed peaks (gauges and high water marks).



(a) Hindcast track



(b) Hindcast dune impact predictions

Figure 4.5: a) Track for hindcast reanalysis compared to NHC best track. b) Dune impact predictions for hindcast simulation where green transects represent 'no impact' or 'collision' predictions, and red transects represent 'impact' or 'overwash/inundation' predictions.

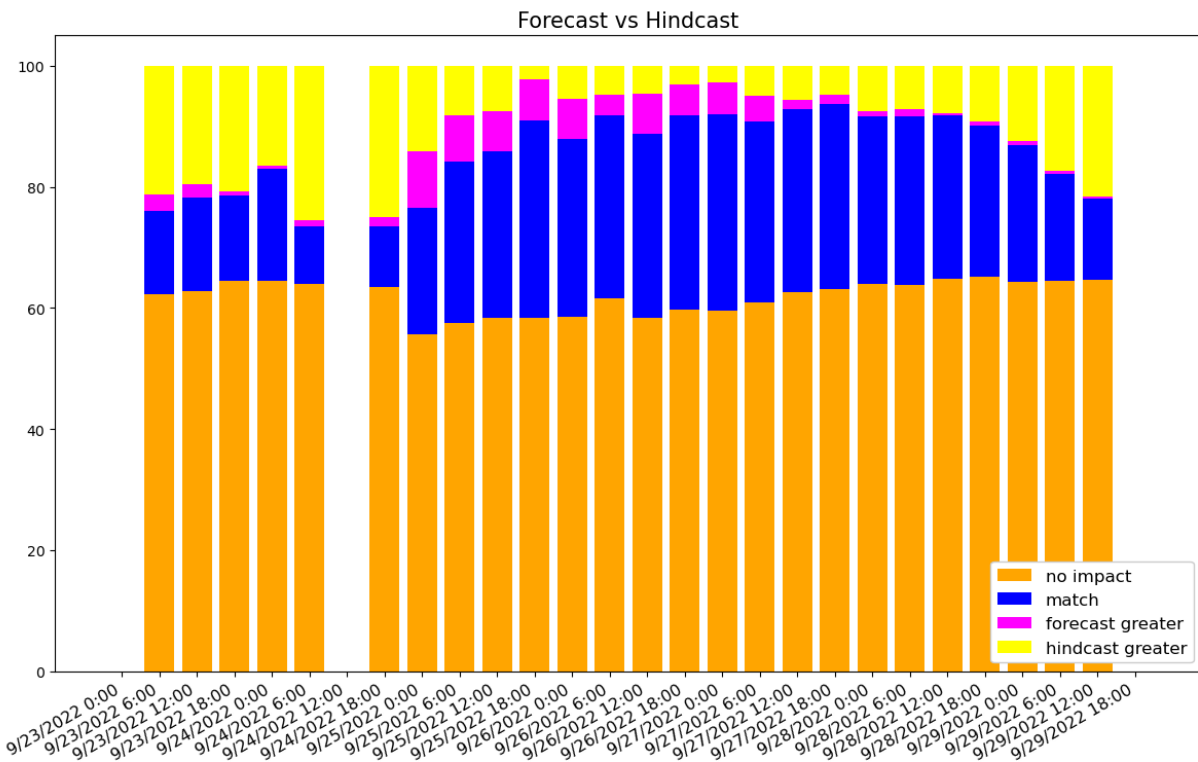
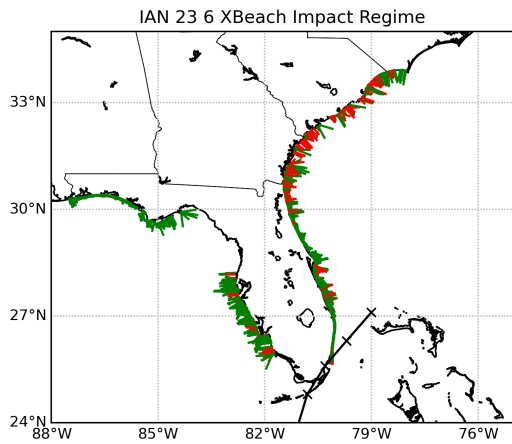


Figure 4.6: Comparison of XBeach-predicted dune impacts between the forecasts and hindcast. The colored bars represent the percentage of transects in each impact category: no impact (orange), match (blue), forecast greater (pink), or hindcast greater (yellow).

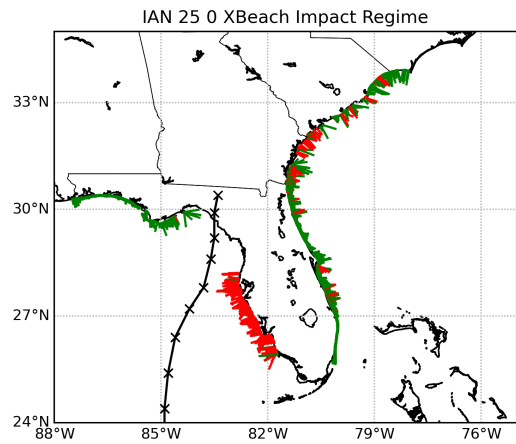
For each forecast advisory and the hindcast, the XBeach predictions at the transects are classified depending on their predicted dune impact. Similar to the hindcast simulation of Michael, the XBeach predictions undergo a binary classification of dune impact, where transects are considered ‘impacted’ when the water level within the XBeach simulation reaches the dune crest. Then the forecasts and hindcasts can be compared. For each transect, each forecast either matches the hindcast (both showing impacts, or both showing no impacts), or there is a mismatch (impact versus no impact) (Figure 4.6). The first takeaway is that most transects (more than 75 percent) show predicted agreement to the hindcast, for all forecasts. The ‘no impact’ category accounts for a majority of the transect agreement across all advisories, however the percentage of matching ‘impact’ transects increase to about 30% in later forecasts. For the transects that don’t match, the trends vary over the forecasts. Earlier forecasts (0600 UTC 23 September through 1800 UTC 24 September) tend to predict lesser impacts compared to the hindcast. Forecasts with greater impacts become common in the days leading up to the observed landfall at 2035 UTC 28 September, and then the forecasts eventually transition to lesser impacts following Ian’s entry into the Atlantic. By the final forecast on 29 September, nearly 20 percent of the XBeach transects predict lesser dune impact than the hindcast. This is likely due to the fact that Ian has already passed a majority of the impacted transects in southwest Florida by 29 September.

The influence the forecast track has on the predicted dune impacts is more apparent for individual advisories (Figure 4.7). Generally, transects located to the east of the track were predicted to have dune impacts, whereas transects located to the west of the track may not have been predicted to have dune impacts. This aligns with the counterclockwise rotation of the storm, which pushes surge and waves on its stronger east side. The forecast for 0600 UTC 23 September (Figure 4.7a) anticipated a landfall approximately 250 km southeast of the observed landfall in Punta Gorda, FL, and thus the storm was not predicted to have a direct effect on southwest Florida’s Gulf coast. The erosion predictions had about 20 percent fewer impacted transects than the hindcast. By the forecast for 0000 UTC 25 September (Figure 4.7b), the anticipated landfall location had shifted more than 400 km to the northwest, which resulted in widespread predictions of dune impact across the Florida Gulf coast and about 10 percent more locations of dune impact than the hindcast. This forecast did not anticipate a secondary landfall along the U.S. Atlantic coast, so about 14 percent of transects predicted less erosion, mainly along the Atlantic coast.

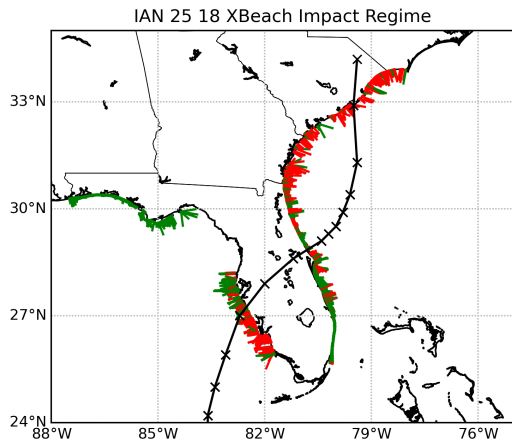
Within the same day, forecasts for 1800 UTC 25 September (Figure 4.7c) align the storm track with the correct landfall location, and thus about 90 percent of the transects match the hindcast impact predictions. The remaining forecasts before landfall, including for 1800 UTC 27 September (Figure 4.7d) and 1200 UTC 28 September (Figure 4.7e), maintain the approximate



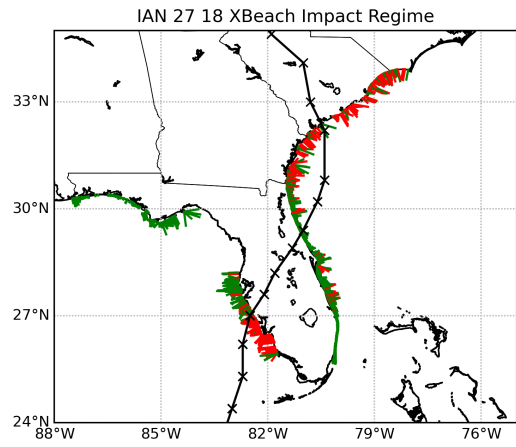
(a) 0600 UTC 23 September



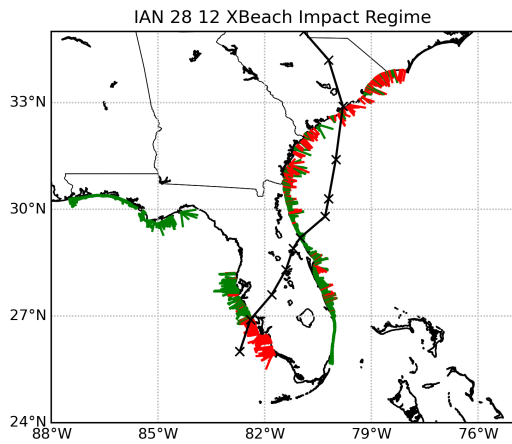
(b) 0000 UTC 25 September



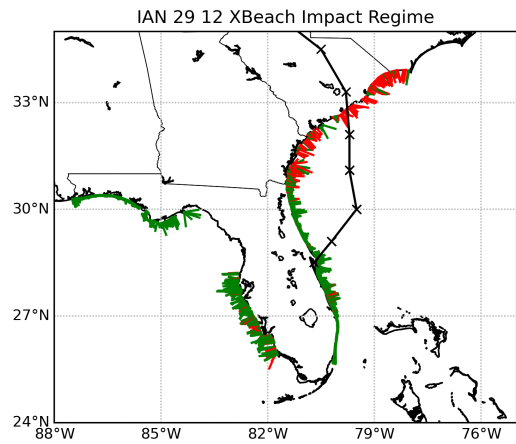
(c) 1800 UTC 25 September



(d) 1800 UTC 27 September



(e) 1200 UTC 28 September



(f) 1200 UTC 29 September

Figure 4.7: Dune impact predictions for Ian forecasts. The approximately 1800 transects are categorized as either ‘impacted’ when water reaches the dune crest (red) or ‘not impacted’ when water levels do not reach the crest index (green).

90-percent match.

After Ian crossed Florida, the XBeach predictions for 1200 UTC 29 September (Figure 4.7f) return to about 80-percent match and 20-percent lesser dune impacts than the hindcast simulation. In these later advisories, because the storm starts in the Atlantic, its effects on the Florida Gulf coast are no longer represented in the XBeach simulations. In the forecasting framework, later advisories will inherently not capture conditions experienced earlier in the storm progression. Transect selection focusing exclusively on future storm impacts can be fixed by updating the specified landfall location and radius of interest for later advisories or switching the transect selection method to adjust depending on the future path. This will be addressed more in future work.

As anticipated, forecast results more closely resemble the hindcast as track accuracy improves in the days leading up to landfall. Forecasts between advisory 1800 UTC 25 September and 1800 UTC 28 September match about 90 percent of the hindcast predicted impacts. Based on the forecast track and dune impact plots, the regions that saw the greatest beach and dune erosion were southwest Florida on the Gulf coast and southeast Florida and South Carolina on the Atlantic coast. The results for these regions will be assessed more thoroughly through multiple qualitative and quantitative comparisons.

4.2.2 Erosion Predictions by Region

Other research questions relate to the accuracy of the erosion predictions relative to other forecast frameworks and to observations during and after the storm. We can compare to the TWLCCFV forecasts, which are well-established and available via public websites and direct downloads. Neither forecast (XBeach or TWLCCVF) can be accepted as ‘truth,’ but the comparison provides insight into the two modeling approaches and how they differ. The TWLCCFV uses an idealized profile that does not change during the storm, whereas XBeach has an interpolated ground surface that evolves throughout the storm. However, by comparing these two forecast models, we can understand how these differences in profile representations affect their predictions of dune impact, especially temporally across and within advisories.

We can also compare to erosion observed in post-storm surveys and aerial imagery. These observations are still being processed and released, and they cannot describe the full erosion as it occurred during the storm. But they can be useful as a truth in select locations. Thus, the goal of the analyses in this subsection is to understand how well the XBeach forecasts perform at specific locations.

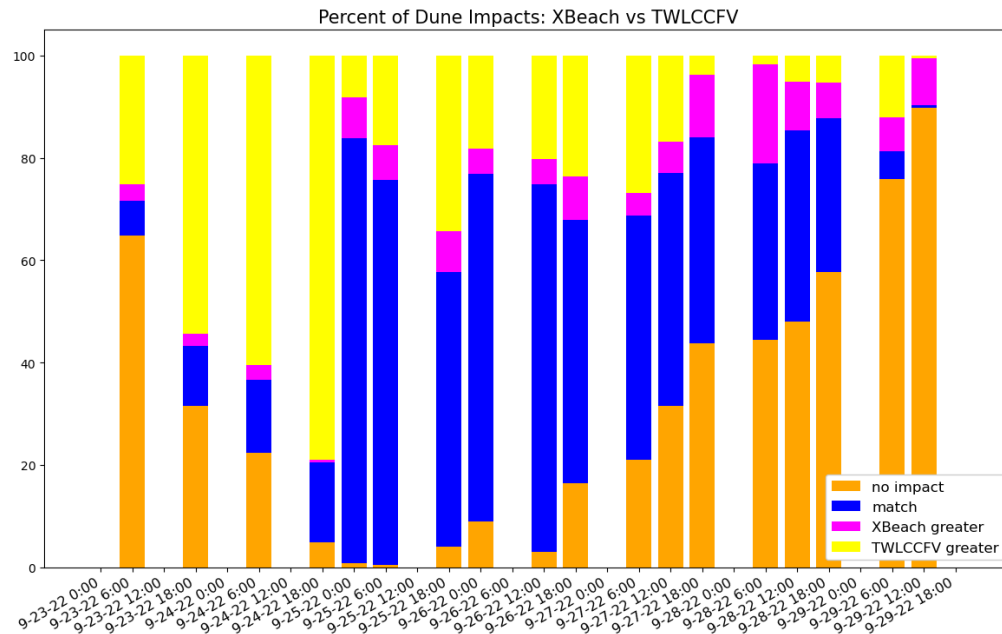


Figure 4.8: For southwest Florida, comparison of predicted dune impacts between XBeach and TWLCCFV forecasts. The colored bars represent the percentage of transects in each impact category: (orange) no impact, (blue) match, (pink) XBeach greater, or (yellow) TWLCCFV greater.

Southwest Florida

Ian made its initial landfall as a Category-4 hurricane in southwest Florida and caused “major dune erosion” along portions of the Gulf coast (Clark et al., 2022). This region was represented for each forecast advisory by more than 450 XBeach transects from north of Clearwater to south of Naples. The first comparison will be a juxtaposition of the XBeach forecasts and the TWLCCFV forecasts for the southwest Florida region, also referred to as region 4 by the TWLCCFV.

Using the same categories as the hindcast comparison, the XBeach impact forecasts are designated as either ‘no impact’, ‘match’, ‘XBeach greater’, or ‘TWLCCFV greater’, depending on the forecasted impact category of the nearest TWLCCFV site (Figure 4.8). In the initial forecast at 0600 UTC 23 September, both forecast models agree that over 60% of locations will not experience dune impact. Over the next 1.5 days, the TWLCCFV begins to predict more dune impacts and by the forecast at 1800 UTC 24 September, the TWLCCFV predicts greater impacts for about 80% of the regional transects. By the next advisory (0000 UTC 25 September), XBeach shifts the majority of its transect predictions, resulting in an 80% ‘match’ between

the two forecast methods. As Ian approaches landfall (about 2000 UTC 28 September), the predictions maintain their high percentage of agreement, but the percentage of ‘no impact’ predictions begin to increase to about 50%. After landfall (forecast 0600 UTC 29 September and 1200 UTC 29 September), about 80% of transects predict ‘no impact’, signaling the storm conditions have passed. It is important to note that the ‘matches’ or ‘no impact’ distinction does not necessarily translate to accuracy, because both forecasts are influenced by uncertainties about the storm. The percentages (Figure 4.8) have to be considered alongside qualitative comparisons to determine the validity and accuracy of both forecast frameworks (Figure 4.9).

We can use qualitative reports and observed water levels to inform decisions on forecast performance. In a post-storm assessment by the Florida Department of Environmental Protection (Clark et al., 2022), maps of beach and dune erosion condition show portions of the coast north of the track or on the weaker side of Ian saw less erosion than the areas to the east of the storm track. Additionally, recorded water levels from Tampa Bay show a major draw-down during the storm (Clark et al., 2022) that is typically expected for areas on the weaker side, whereas storm surge on the strong side of the storm was about 3 m (Clark et al., 2022). With this information in mind, we can critically assess the forecast predictions.

Starting with the forecast for 1800 UTC 24 September (first row in Figure 4.9), the TWLCCFV predicts nearly all transects will be significantly eroded, whereas XBeach predicts little to no erosion for the region, resulting in a low percentage of matching forecasts. This is juxtaposed with the forecasts for 0000 UTC 25 September (second row in Figure 4.9), in which the forecasts have a high ‘match’ percentage because both models predict widespread beach and dune erosion for the entire region. This increase in XBeach predicted impacts between the two advisories only 6 hr apart is likely caused by the sudden shift in the storm track. In the XBeach forecasts based on atmospheric forcing from COAMPS-TC, the track moves closer to the southwest Florida coast, and the XBeach model responds by predicting the majority of the transects will experience dune impacts, much like the TWLCCFV prediction. However, despite the forecast model agreement, they both over-predict the dune impacts, because neither forecast represents the observed divide of less erosion to the north and more erosion to the south of Ian’s landfall near Punta Gorda.

The forecasts for 1800 UTC 27 September (third row in Figure 4.9), and other similar advisories with accurate tracks, do a better job of matching the qualitative observations. Both the TWLCCFV and XBeach predictions forecast less erosion near Clearwater and Tampa Bay and more erosion near Fort Myers and Naples. XBeach tends to predict more dune impacts than the TWLCCFV, but the two forecast models agree for nearly 80 percent of the transects in southwest Florida. Forecasts after the initial U.S. landfall, such as 1200 UTC 29 September (last row of Figure 4.9), are not accurate for southwest Florida because Ian has passed. There is a

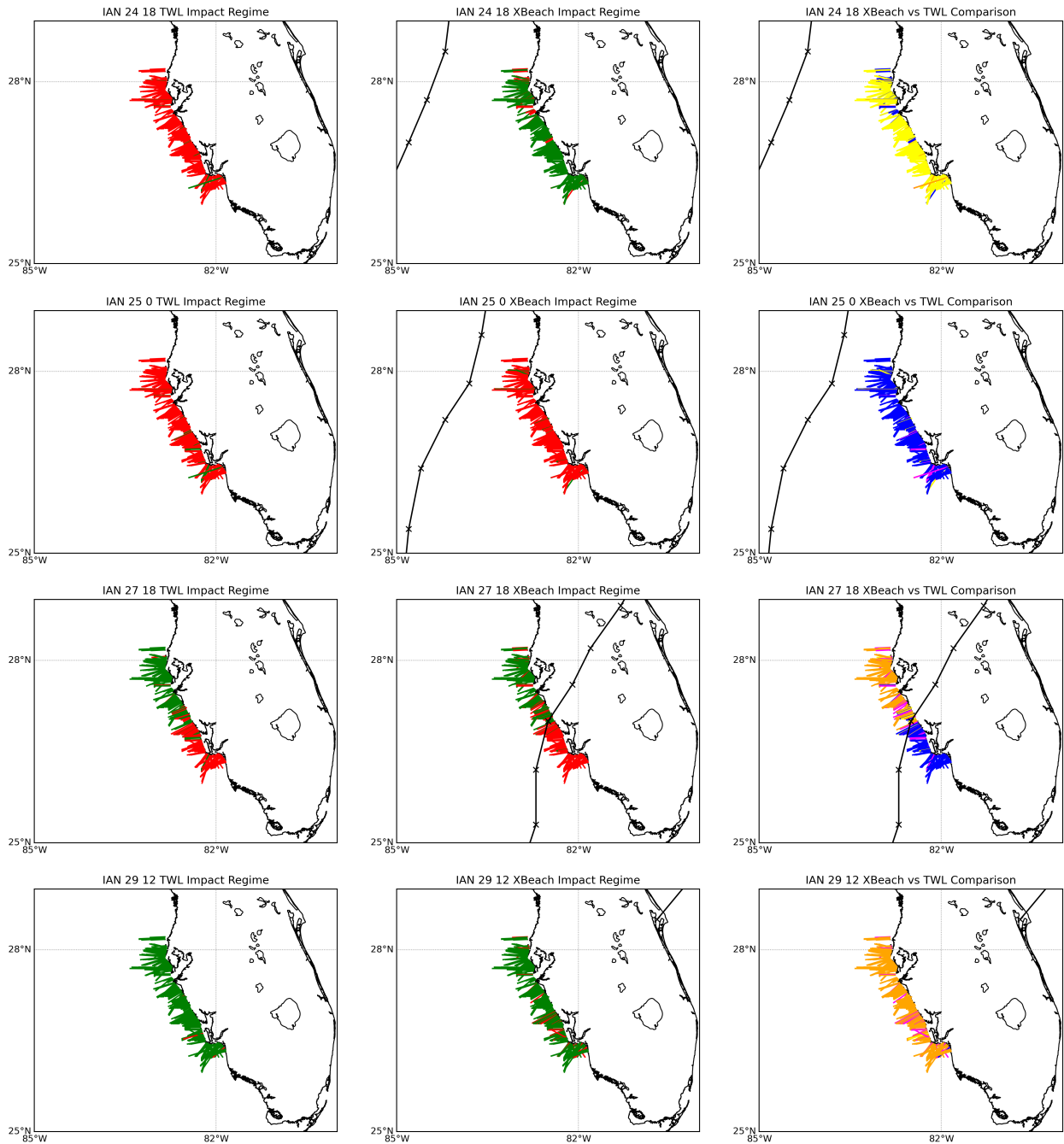


Figure 4.9: For southwest Florida, forecasts of dune impacts for advisories: (first row) 1800 UTC 24 September, (second row) 0000 UTC 25 September, (third row) 1800 UTC 27 September, and (fourth row) 1200 UTC 29 September. Dune impacts are shown for: (first column) the TWLCCFV forecast and (second column) the XBeach forecast, as well as (third column) a comparison between the two. For the two forecast frameworks (first and second columns), the transects are colored based on no predicted dune impacts (green) or predicted dune impacts (red). For the comparison (third column), the transects are colored based on the dune impact category: no impact (orange), match (blue), XBeach greater (pink), or TWLCCFV greater (yellow).

high agreement between the two models, but this does not translate to accuracy because both models can no longer ‘predict’ impacts that have already occurred.

One transect within the southwest Florida region is selected to demonstrate how the addition of dynamic morphology affects if and when dunes impacts are predicted. The transect selected for southwest Florida is T4074, which is located on Estero Island adjacent to the Fort Myers Fishing Pier. Post-Ian aerial photos from NOAA (National Oceanic and Atmospheric Administration, 2022) of this location show visible destruction and complete inundation across the Island. Ideally, the time snaps throughout the XBeach model will provide us with a better understanding of when inundation occurs. The only available source for temporal comparison is the hourly total water level forecasts from the TWLCCFV. One limitation to be aware of is the fact that the nearest TWLCCFV site may use slightly different profile properties (such as dune crest or beach slope) or storm conditions (wave properties and storm surge elevations) to calculate the total water levels and subsequent impacts. However, the TWLCCFV sites are intended to represent the vulnerability of the surrounding area, so the comparison to neighboring deterministic XBeach transects is still informative.

The plots of T4074 in Figure 4.10 show six time snaps from the forecast for 1200 UTC 27 September. The first plot (Figure 4.10a) corresponds to 2300 UTC 27 September, about 11 hr into the approximately 5-day simulation to show the starting conditions before major change occurs. The second plot (Figure 4.10b) corresponds to 0500 UTC 28 September, about 6 hr later when the TWLCCFV forecast first reaches the dune crest. The XBeach simulation predicts dune overwash at 1000 UTC 28 September (Figure 4.10c), about 5 hr after the TWLCCFV. At the same time, the TWLCCFV-predicted water levels are about 2 m. XBeach water levels eventually match the TWLCCFV predictions of about 3 m and completely inundate the profile by 2200 UTC 28 September (Figure 4.10d). Water levels then slowly return to normal in the hours and days following the initial U.S. landfall in Florida, as evident in the final two plots (Figure 4.10e-f). This water would typically flow out into the back bay that is located behind this profile as water levels subsided, but this outflow is prevented by the numerical boundary condition used in the XBeach simulations. This could potentially affect the predicted morphology, which will be discussed in more detail at the end of this chapter.

Although we cannot verify the predicted dynamic morphology through model comparison or temporal observational data, the XBeach model has been validated earlier in this chapter, so going forward we can assume the results for T4074 are realistic. We can use the dynamic information from the XBeach model to better understand the temporal evolution of the profile during the storm. Profile features for 4074 begin to change and smooth as the water reaches the dune crest (Figure 4.10c). This is nearly a day into the simulation for advisory 1200 UTC 27 September and profile changes are minimal considering dune overwash. During the peak of

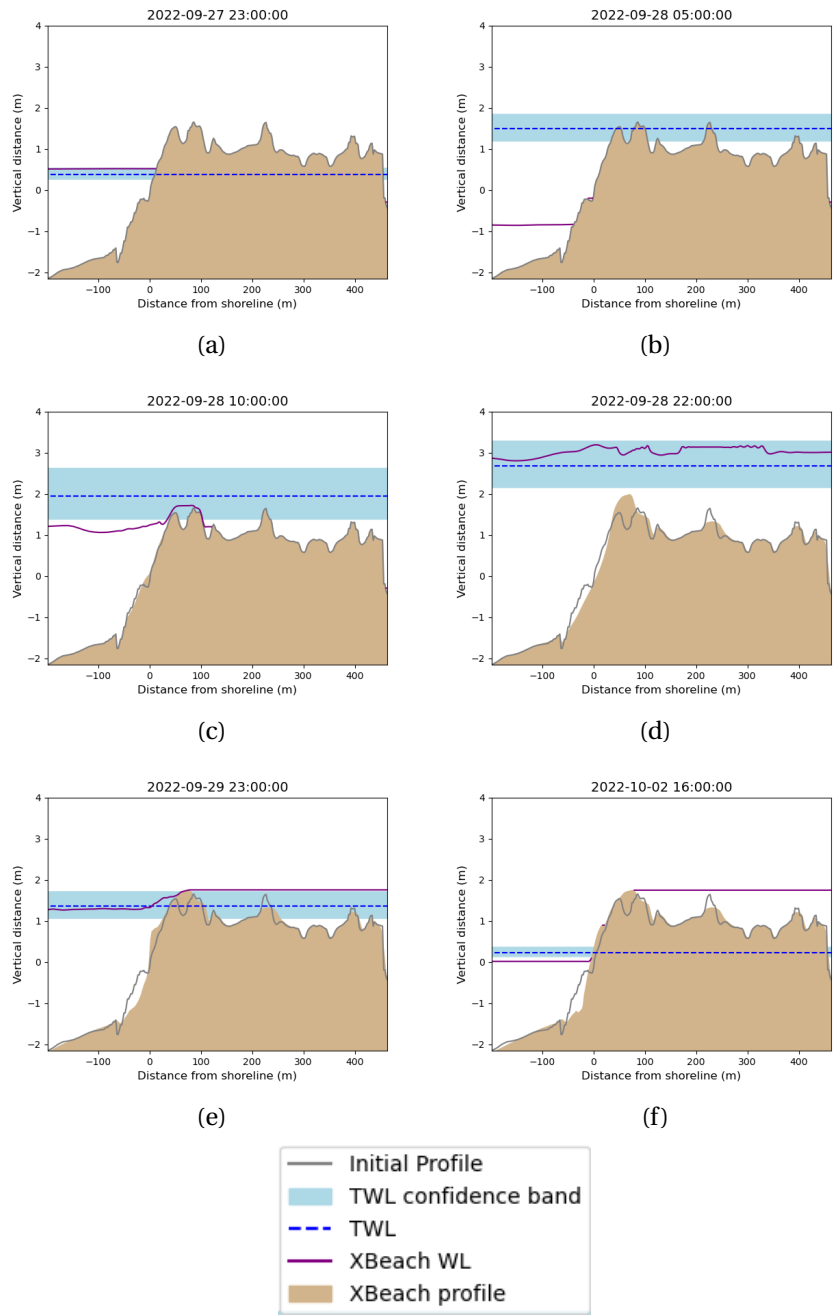


Figure 4.10: XBeach erosion predictions for transect T4074 located on Estero Island adjacent to the Fort Myers Fishing Pier. Times include: 2300 UTC 27 September, 0500 UTC 28 September, 1000 UTC 28 September, 2200 UTC 28 September, 2300 UTC 29 September, and 1600 UTC 2 October. The grey line is the initial XBeach profile and the tan area is the predicted bed levels at a specific time step. The water levels in XBeach are represented as a purple line, and the TWLCCFV predicted TWL (with associated 95% confidence band) are included as a horizontal blue line across the profile.

the storm and profile inundation (Figure 4.10d), the sediment in the offshore bar moves up the profile and combines with the two subaerial dune features, resulting in a higher dune crest than the initial starting profile. As water levels return to normal (Figure 4.10e), the sediment is pulled from the top of the dune and moved to the beach face. A small subaerial mound forms on the beach face while the combined dune is flattened. By the end of the simulation on 2 October (Figure 4.10f), the sediment from the bar is either placed on the beach face or filled between the initial two dune features, however there is no significant scour or volume lost. Although the profile was inundated for multiple hours, the forecasted percent volume change is 21 percent and the predicted dune crest elevation change is 0.08 m. This is informative for evaluating the erosion metrics. The binary dune impact metric seems to better represent the vulnerability of this location, especially the inundation over and behind the dune, compared to the computed volume and crest elevation changes.

The XBeach predictions for this profile can be compared to nearby surveys to validate its accuracy (Figure 4.11). Survey data was shared by Michael Poff from Coastal Engineering Consultants, Inc, who works closely with the local Florida government. Lee County and the town of Fort Myers Beach conduct regular surveys to assess coastal change throughout time. Surveys were conducted in June 2022 and again 12 days following Ian to assess the resulting erosion of beaches and dunes. One of the surveyed profiles is located about 100 m west of T4074 at the same orientation. The pre- and post-storm surveyed profiles will be compared to the XBeach initial and final profiles for validation. The pre-storm survey has a dune crest of nearly 2 m and a post-storm dune crest of about 1 m, whereas the XBeach initial profile has a lower dune crest elevation (1.5 m) that is forecasted to be overtopped but remains around the same elevation. Although XBeach does not predict the same dune crest elevation change, it is difficult to draw a direct conclusion given the different profile locations. Instead, the volume change observed in the pre- and post-Ian surveys can be qualitative evidence of nearby inundation that matches the forecasted dune impact in XBeach simulations.

Southeast Florida

Ian crossed the southeast Florida coast into the Atlantic at 1200 UTC 29 September (Bucci et al., 2023b) as a tropical storm. Although much attention was focused on erosion and flooding near Ian's initial landfall location in southwest Florida, there was also significant erosion and flooding in the southeast. XBeach forecasts were performed along the U.S. Atlantic coast from Miami, FL, to Southport, NC, but our analysis in this subsection will focus on 430 transects from the north end of Volusia County to the south end of Martin County. This subset of the transects on the southeast Florida coast coincides with the transects in region 14 of the TWLCCFV. There is limited qualitative and quantitative observational data available to validate

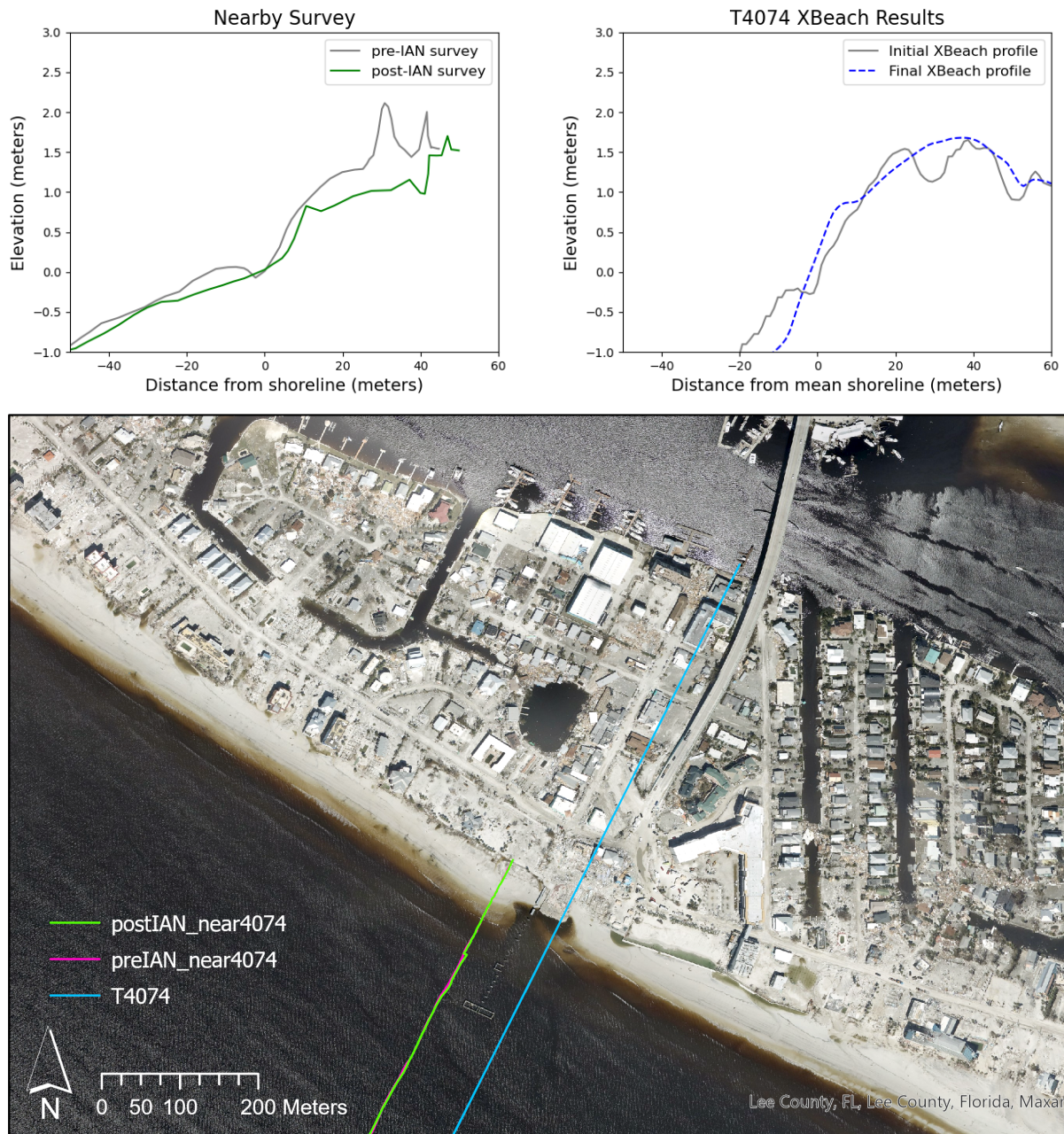


Figure 4.11: Post-Ian aerial photo from NOAA (National Oceanic and Atmospheric Administration, 2022) with the pre- and post-storm survey profiles plotted near transect T4074. The post-Ian aerial photo of the observed coastal change includes two lines depicting where the profiles are located in relation to the shoreline and one another. Above the aerial photo, there are two plots – the surveyed transect (left) and the XBeach transect (right). The plots are limited to the same extent, although the XBeach profile continues much further compared to the surveyed profile.

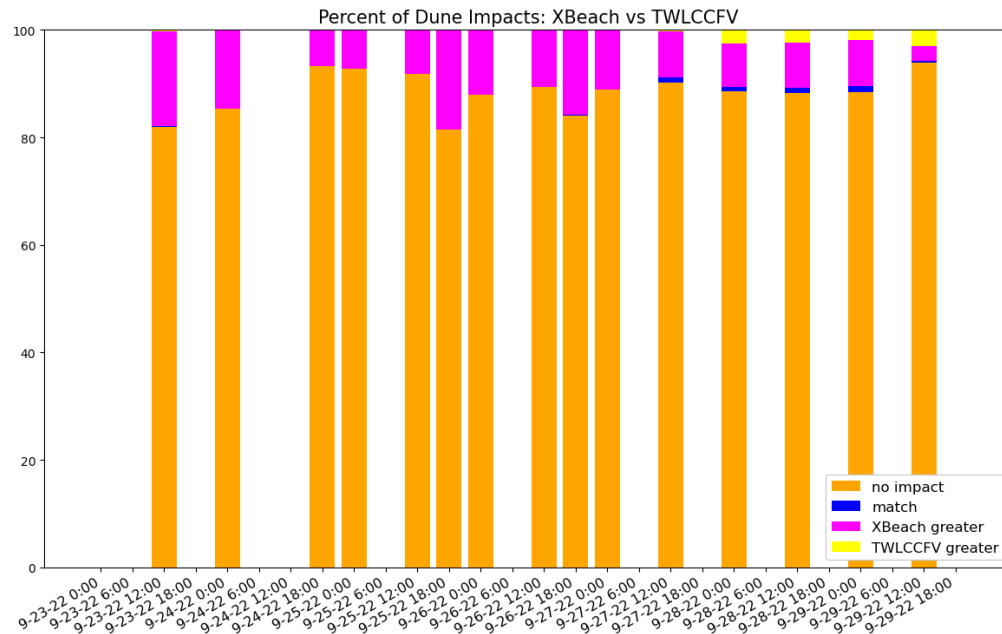


Figure 4.12: For southeast Florida, comparison of predicted dune impacts between XBeach and TWLCCFV forecasts. The colored bars represent the percentage of transects in each impact category: no impact (orange), match (blue), XBeach greater (pink), or TWLCCFV greater (yellow).

the XBeach forecasts in the southeast region of Florida, so the TWLCCFV forecasts will be used as the main source for comparison.

Following the same forecast comparison explained for southwest Florida, the bar chart in Figure 4.12 depicts the percentage of transects in each of the impact categories: 'no impact', 'match', 'XBeach greater', and 'TWLCCFV greater. For southeast Florida, there are fewer TWLCCFV advisories available for the region over the 7-day period, and the advisories that are available show less fluctuation in impact percentages. The forecast models tend to predict 'no impact' 80 to 90% of the time with XBeach typically predicting greater dune impacts for a majority of the advisories. A small percentage of TWLCCFV forecasts in later advisories predict greater impacts, starting with 0000 UTC 28 September and continuing to 1200 UTC 29 September. The southeast Florida region can be summarized with an overall 'no impact' prediction.

The minimal discrepancies between the two models are also visually represented through the spatial maps of the forecasts and comparison. It is harder to verify which forecast is closer to 'truth' because there are fewer observations to cross-reference. The TWLCCFV (left) and XBeach (middle) forecast maps for all three advisories included in Figure 4.13 predict very

limited beach and dune erosion or dune impacts (green) with only a handful of locations forecasted to observe significant erosion (red). Advisories 0000 UTC 24 September and 1200 UTC 28 September have slightly different tracks, but both XBeach forecasts predict dune impacts near Port Canaveral and South Beach. Advisories 1200 UTC 28 September and 1200 UTC 29 September show locations where XBeach predicts less impact than the TWLCCFV, just north of Port Canaveral near the observed eye of the storm. Ian did weaken as it crosses Florida, which could explain why XBeach predicts less erosion in the later forecasts. Overall, the XBeach forecasts closely match the available TWLCCFV forecasts for southeast Florida. The 1800 UTC 28 September forecast will be used going forward to temporally compare the hourly total water level predictions to the dynamic morphology predictions in XBeach.

Transect T2656, located in South Beach, FL, more than 200 km south of where Ian emerged into the Atlantic, is predicted by both XBeach and the closest TWLCCFV site (T4485) to experience no dune impact. This transect is included as an example of a case where the ‘no impact’ predictions match, but XBeach provides additional erosion information we do not get from the TWLCCFV. The forecast at 1500 UTC 28 September (Figure 4.14a) establishes the starting conditions for the simulation. By 0600 UTC 29 September (Figure 4.14b), the XBeach water level overtops an initial peak in the profile and beach face erosion begins. Sediment is pulled from the beach face and settles just offshore. The remaining plots (Figure 4.14c-f) show the continued removal of the initial peak, however elevations behind the dune remain consistent. Water does not overwash the profile so the back of the profile remains dry for the entire simulation. By 0000 UTC 3 October, there is no dune crest lowering or predicted impacts, but 18% of dune volume has been removed. Without the dynamic bed level predictions from XBeach, we would not be able to estimate how much erosion of the dune face took place during Ian at this location. This information is essential for future storm preparation and vulnerability assessment. With nearly a quarter of the dune volume removed, this profile could be more vulnerable to future impacts. An example of this is Hurricane Nicole (2022), which made landfall in southeast Florida only about a month after Ian. Transects were likely weakened by Ian and did not have time to recover. The XBeach forecasts from Ian could have been used to inform the Nicole simulations of recent storm-driven coastal change. Other forecast models would not be able to provide the same information about dune crest lowering or volume change for the profile.

Southeast U.S.

Ian strengthened from a tropical storm to a Category-1 hurricane as it traveled north toward South Carolina (Bucci et al., 2023b). The storm made its final landfall near Georgetown, SC, at about 1800 UTC 30 September. About 130 transects covering South Carolina and some

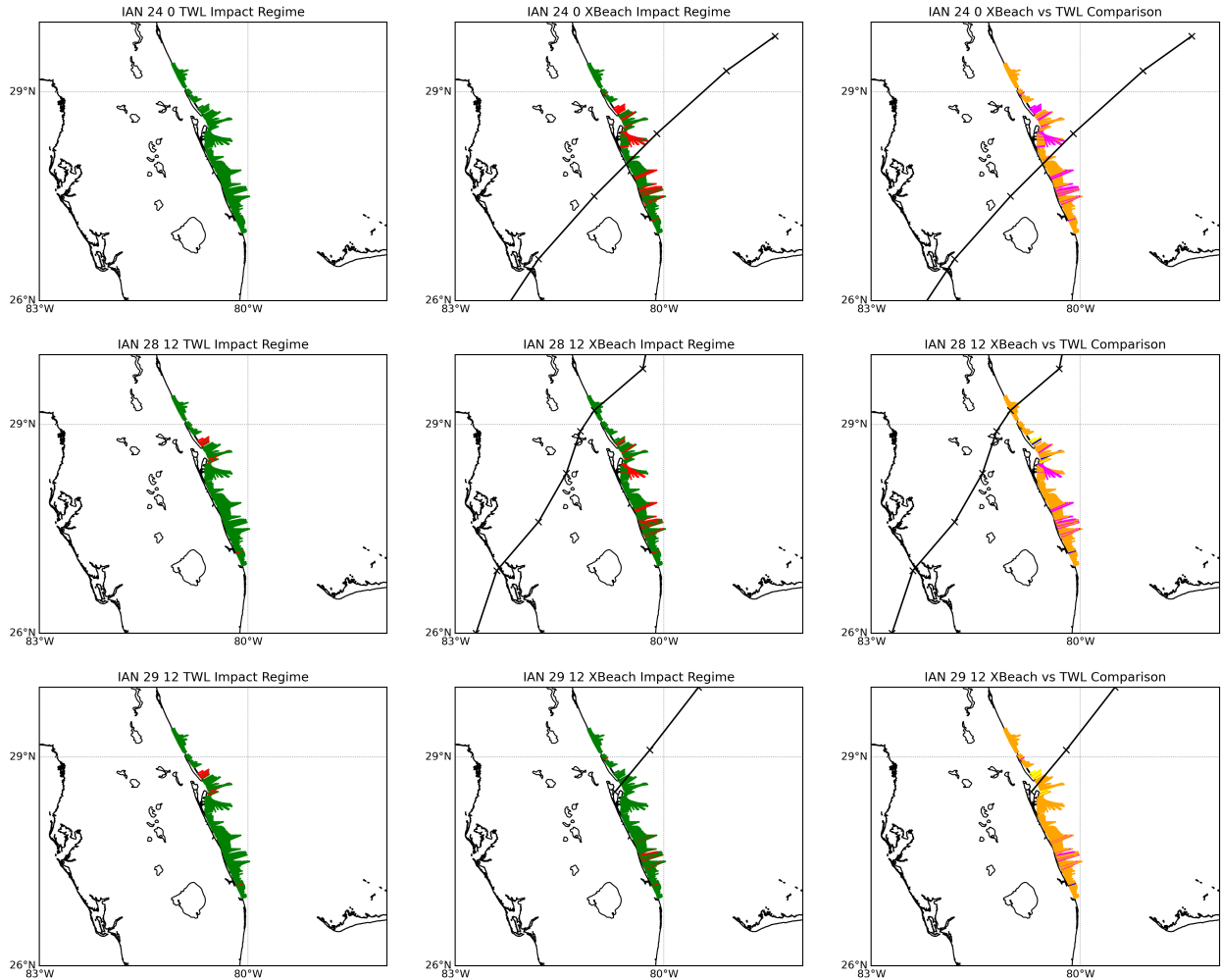


Figure 4.13: For southeast Florida, forecasts of dune impacts for advisories: (first row) 0000 UTC 24 September, (second row) 1200 UTC 28 September, and (third row) 1200 UTC 29 September. Dune impacts are shown for: (first column) the TWLCCFV forecast and (second column) the XBeach forecast, as well as (third column) a comparison between the two. For the two forecast frameworks (first and second columns), the transects are colored based on no predicted dune impacts (green) or predicted dune impacts (red). For the comparison (third column), the transects are colored based on forecast impact categories: no impact (orange), match (blue), XBeach greater (pink), or TWLCCFV greater (yellow).

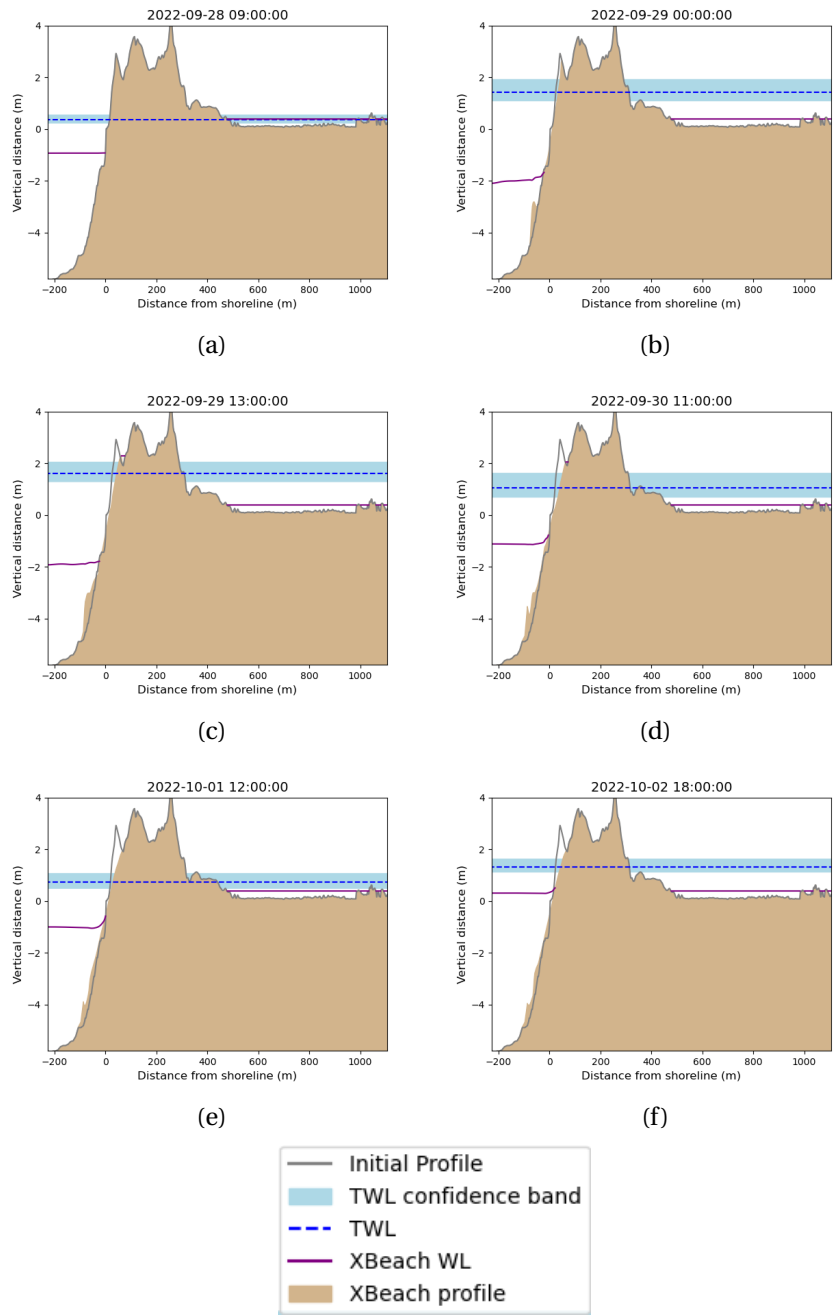


Figure 4.14: XBeach results at 6 time snaps during the 1200 UTC 28 September forecast for transect 2656 located in South Beach, FL. Times include: 0900 UTC 28 September, 0000 UTC 29 September, 1300 UTC 29 September, 1100 UTC 30 September, 1200 UTC 1 October, and 1800 UTC 2 October. The grey line is the initial XBeach profile and the tan area is the predicted bed levels at a specific time step. The water levels in XBeach are represented as a purple line and the TWLCCFV predicted TWL (with associated 95% confidence band) are included as a horizontal blue line across the profile.

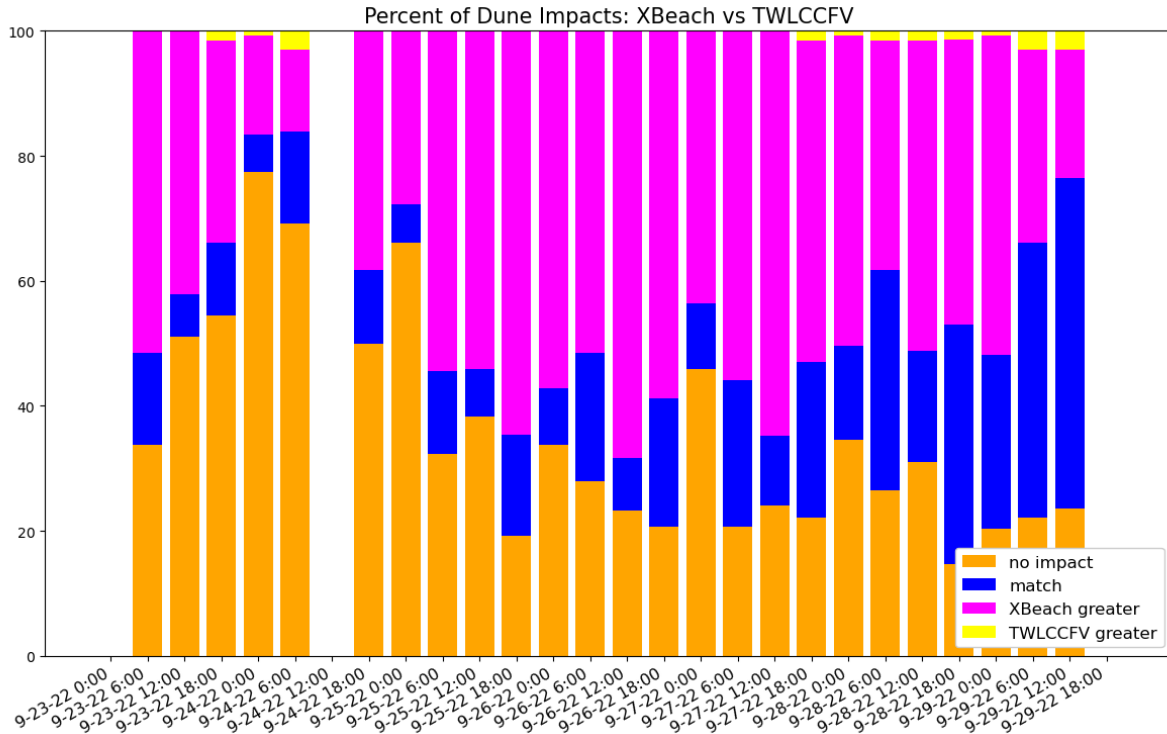


Figure 4.15: For the southeast U.S., comparison of predicted dune impacts between XBeach and TWLCCFV forecasts. The colored bars represent the percentage of transects in each forecast impact category: no impact(orange), match (blue), XBeach greater (pink), and TWLCCFV greater (yellow).

additional portions of North Carolina and Georgia are selected to represent the erosion predictions for the final days of the storm. Much like the southwest Florida region, there are few observations for comparison, so the TWLCCFV will be a major focus of this results section. The 130 transects cover regions 9 and 11 in the TWLCCFV, however both regions are not always available for each advisory. Out of the 25 XBeach forecasts, 11 simulations have both TWLCCFV regions available for comparison while the remaining 14 only have transects from region 9. The forecast comparison follows the same ‘no impact’, ‘match’, ‘XBeach greater’, or ‘TWLCCFV greater’ classifications explained for the other two regions (Figure 4.15).

Compared to the other regions, the southeast U.S. forecasts do not agree as well. Percentage of transects that agree is typically less than 80 percent. The forecast for 0000 UTC 24 September has one of the highest percentages of transects that agree between forecast methods, but the majority of the predictions are ‘no impact’ (77 percent) as a result of the shifted track. XBeach predicts greater impacts than the TWLCCFV for a majority of the advisories after 0600 UTC 25 September. As the storm progresses and travels closer to final landfall, the percentage of matching dune impact predictions increases to more than 50 percent at 1200 UTC 29 September.

This reflects early XBeach impact predictions that were later agreed upon by the TWLCCFV. These percentages of matching, greater, or lesser impacts will be represented spatially to evaluate how the track uncertainties play a role in the dune impact predictions (Figure 4.15).

The advisory with the most ‘no impact’ predictions is 0000 UTC 24 September (first row in Figure 4.15). Both the TWLCCFV and XBeach predicted little to no dune impacts because the storm was not projected to pass near this region. This track inaccuracy results in fewer predicted impacts along the southeast U.S. coast. The advisory with the smallest percentage of matching forecast predictions is 1200 UTC 26 September (second row in Figure 4.15). Although XBeach predicts greater impacts than the TWLCCFV for nearly 70% of transects, the track location is more accurate than the advisory on 24 September (first row). The same goes for the 1200 UTC 28 September advisory (third row in Figure 4.15). With limited to no observational data for this region, it is difficult to determine whether the XBeach predictions of more dune impacts than the TWLCCFV is more accurate or not.

Forecast 0000 UTC 28 September is selected for further analysis. For this forecast in the southeast U.S., about 50 percent of the XBeach predictions match those of the closest TWLCCFV sites. At transect 1173, located on Oak Island, the nearest TWLCCFV site disagrees with the forecasted dune impact prediction, but the timing of morphology aligns closely with the peak of the storm.

The first plot establishes the initial conditions 20 hours after the start of the 0000 UTC 28 September advisory (Figure 4.16a). XBeach predicts the approximately 4-m dune will be overtopped about a full day later (Figure 4.16b) at 1900 UTC 29 September, but minimal water spills over the dune and no elevation changes occur. Water levels lower to about -2 m at the start of 30 September before returning to about 2.5 m at 0800 UTC 30 September (Figure 4.16c). The waves and surge start to scarp the upper dune face and create a steep beach face. At 1900 UTC 30 September, the dune crest is inundated about an hour after the observed landfall (Figure 4.16d). At the exact same time, the TWLCCFV predicts a slight increase in TWL elevation to about 2 m, however this is almost a full meter below the XBeach water levels. After the peak of the storm, the remaining two plots are included to display the differences between the predicted total water levels for XBeach and TWLCCFV (Figure 4.16e) and show the final XBeach predicted transect (Figure 4.16f). Focusing specifically on the TWLs, XBeach has much higher highs and much lower lows compared to the other forecast model. Additionally, there seems to be a lag where TWLCCFV shifts transitions between rising and falling much faster than XBeach. The lag and overall differences between the forecasted TWLs will be discussed in the next section.

This transect was included because there is a discrepancy between the two forecasting approaches. XBeach predicts dune inundation, whereas the TWLCCFV does not. Either case

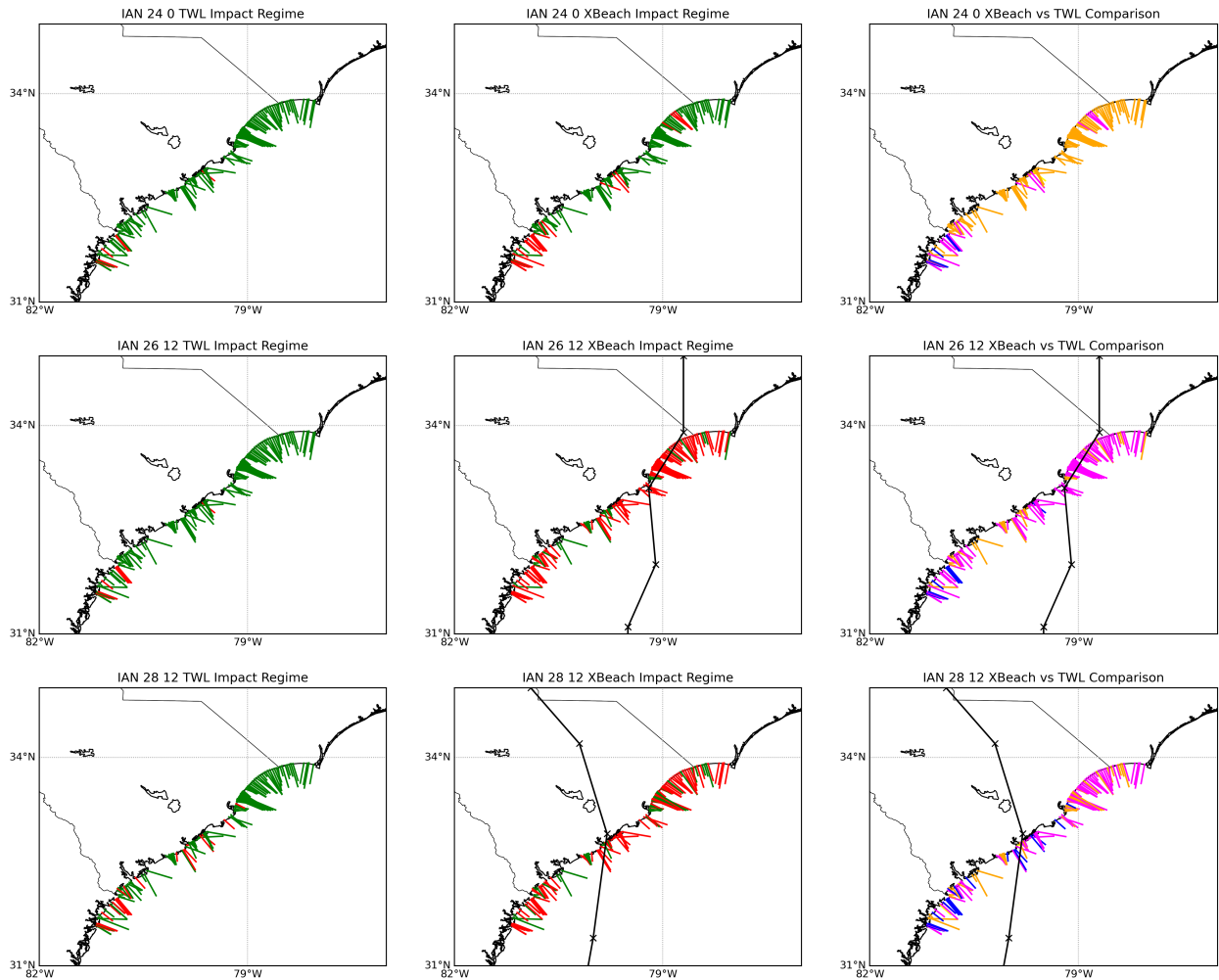


Figure 4.16: For the southeast U.S., forecasts of dune impacts for advisories: (first row) 0000 UTC 24 September, (second row) 1200 UTC 26 September, and (third row) 1200 UTC 28 September. Dune impacts are shown for: (first column) the TWLCCFV forecast and (second column) the XBeach forecast, as well as (third column) a comparison between the two. For the two forecast frameworks (first and second columns), the transects are colored based on no predicted dune impact (green) or predicted dune impact (red). For the comparison (third column), the transects are colored based on the dune impact category: (orange) no impact, (blue) match, (pink) XBeach greater, or (yellow) TWLCCFV greater.

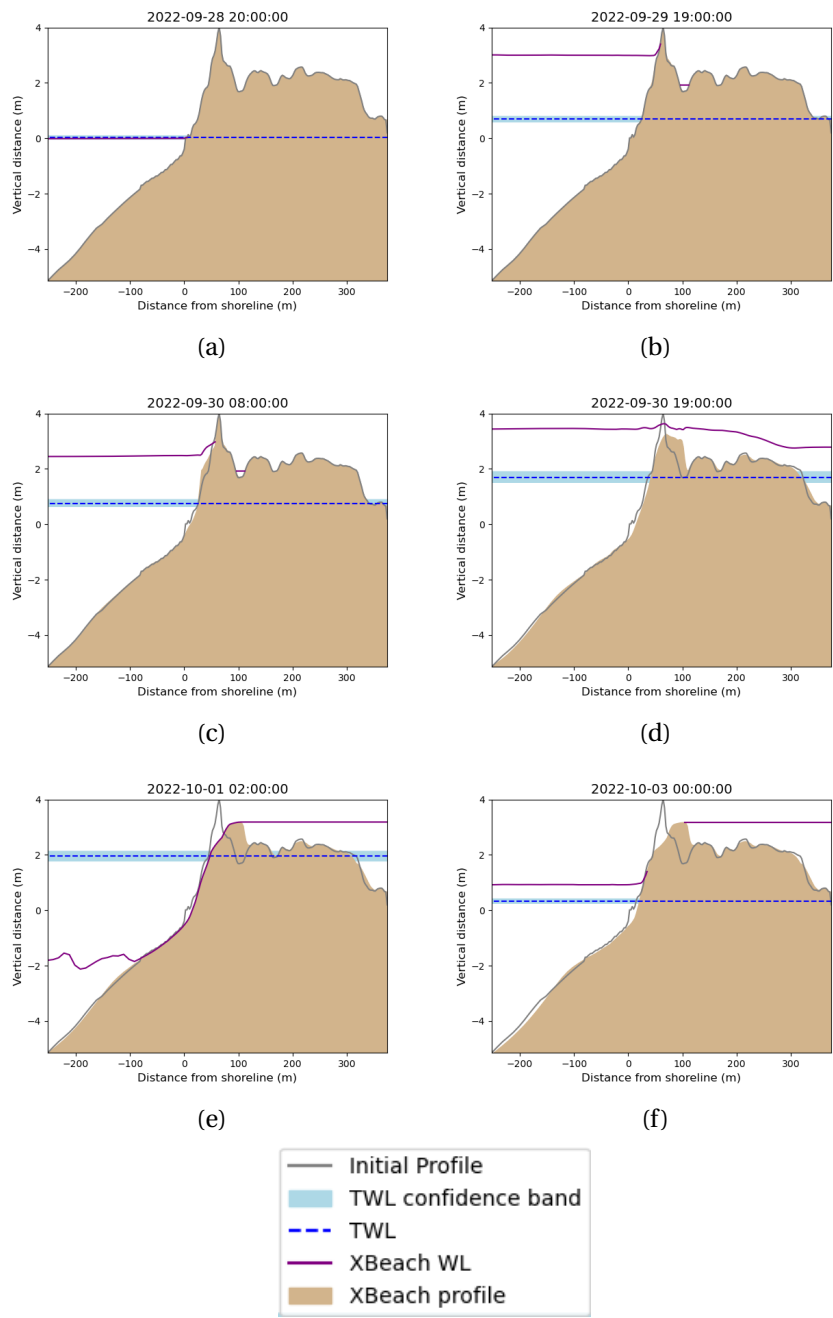


Figure 4.17: XBeach results at six time snaps during the 0000 UTC 28 September forecast for transect 1173 located on Oak Island NC. Times include: 2000 UTC 28 September, 1900 UTC 29 September, 0800 UTC 30 September, 1900 UTC 30 September, 0200 UTC 1 October, and 0000 UTC 3 October. The grey line is the initial XBeach profile and the tan area is the predicted bed levels at a specific time step. The water levels in XBeach are represented as a purple line and the TWLCCFV predicted TWL (with associated 95% confidence band) are included as a horizontal blue line across the profile.

is plausible given limited observational data availability, but we can use the XBeach results to learn more about the profile evolution throughout the storm. The most notable change happens when the transect is inundated at 1900 UTC 30 September. This aligns with the timing of Ian's final landfall and the observed peak surge (Figure 3.4b). The high total water levels push the dune back and round the top of the crest. As water levels return to a normal range, sediment from the smoothed dune is pulled offshore and onto the beach face. By the end of the simulation, the beach returns to a similar slope, however the dune is lowered and relocated further back. XBeach predicts a 1.6-m dune crest elevation change and a 27-percent volume change. This forecast information about the profile evolution and scale of erosion would not be possible without the dynamic morphology component in XBeach.

4.3 Discussion

This section will use the XBeach predictions to propose answers to our remaining research questions (Chapter 2). We will address the accuracy and effectiveness of the XBeach modeling framework. Then, after establishing the XBeach model and associated framework are capable of predicting storm-driven erosion, we will analyze what we have learned from the dynamic morphological models of two extreme events. Finally, we will discuss some of the remaining challenges for this forecast framework. Some of the challenges will lead directly into future work, which will be discussed in the final chapter.

4.3.1 Lessons Learned about Deterministic Forecasting

Previous studies have used XBeach for real-time forecasting of storm-driven erosion (e.g. Baart et al., 2003, 2016; Harley et al., 2011; Vousdoukas et al., 2012), but their study areas were limited to single locations. By attempting to represent all sandy beach/dune systems along the U.S. Atlantic and Gulf coasts, we learned several lessons about real-time forecasting with a deterministic morphological model. These lessons are related to: (a) the use of a single set of input parameters, calibrated in other studies; (b) the computational efficiency of the XBeach simulations; and (c) the communication of erosion predictions with a binary classification of dune impact or no dune impact.

Parameter calibration can be time consuming and lead to over-calibration, which can limit the model's applicability (Simmons et al., 2019). However, relying entirely on default XBeach parameters can produce unskillful results (Simmons et al., 2019). Adjustments to influential parameters, such as γ and f_{acua} , can improve model skill (Simmons et al., 2017). We selected a single set of model parameters, based on recent studies related to optimizing calibra-

tions, and implemented them for simulations over a wide region. Most of the parameters were tested for 2D models at two locations at either end of the U.S. Atlantic coast (Fire Island, NY and Matanzas, FL, van der Lugt et al., 2019), and thus model validation is required to verify the parameters are appropriate for 1D models and elsewhere along the U.S. coast. A hindcast simulation of Michael is evaluated to determine the model accuracy before forecast implementation. The available post-storm lidar allows for multiple qualitative and quantitative assessments of the XBeach predicted erosion and the metrics used to represent the results. Several transects were able to produce ‘excellent’ *BSS*, and more than 90 percent of the XBeach predictions matched the observed dune impacts based on changes to dune crest elevations. Despite the initial parameter calibration for the Atlantic, the Michael simulations on the Gulf coast were able to predict where the dune impact occurred. This was promising and allowed us to apply the same versatile set of parameters to real-time forecasting.

We built a flexible, efficient forecasting framework that can produce hundreds of 1D model results in a reasonable amount of time and represent the full range of forecast variations. To represent a wider study area, more than 4000 transects are updated with recent ground surface information in preparation for the hurricane season. Transects are selected for morphological modeling depending on the user-specified landfall location and region of interest. This flexibility allows the user to adjust where or how many transects will be modeled depending on recent storm track progression. For Ian, an extensive radius and consistent landfall location was specified resulting in nearly 1800 simulations per advisory from the Florida Panhandle to the southern edge of North Carolina. Despite the large quantity of XBeach simulations, the entire process from initiation to publishing results typically took less than 70 minutes (assuming little to no competition for computing resources). The HPC resources and maximum time allotments help to reduce computational time and ensure forecast efficiency. This framework requires significantly less computational time compared to 2D morphological modeling (Bart et al., 2011) while representing a wider region of the coast, demonstrating the overall efficiency.

The model outputs must be combined with an effective method to process the output data and communicate the spatial and temporal predictions. Multiple erosion metrics, both qualitative and quantitative, were selected to communicate the results at different scales. A binary dune impact metric was selected as the primary erosion signaling method because it was easy to communicate to a wider audience and it allowed for forecast model comparisons. Similar categorical impact regime approaches are a common practice for predicting coastal erosion (Sallenger, 2000; Stockdon et al., 2006), however the binary dune impact decision reduces the potential categories by half. The dune impact predictions are accompanied by additional quantified metrics (e.g. dune crest change, percent volume change) that provide supplemental information about the scale of predicted erosion within the two categories.

During Ian, there was a general agreement in the regions of predicted dune impacts between the XBeach and empirical forecasts for dune impacts. The agreements closer to landfall also aligned with qualitative observations from reports. The supplemental quantitative metrics add a range of predicted erosion beyond what is possible with the traditional 4-regime impact scale (Sallenger, 2000). This encourages the use of a binary dune impact metric with supplemental erosion quantification to represent coastal vulnerability during real-time forecasting.

4.3.2 Lessons Learned about Beach/Dune Erosion during Storms

With the model accuracy established, the XBeach forecasts for Ian can be assessed to learn several lessons about coastal change and storm evolution. These lessons are related to: (a) the relationship between storm track uncertainties and erosion predictions, and (b) how to identify the timing of dune impact.

Despite the high skill of COAMPS-TC, especially relative to other atmospheric forecasts during Ian, its forecasts still had uncertainties about the track and projected landfall location in southwest Florida. These uncertainties affected the erosion predictions, as suggested by previous studies (Baart et al., 2016; Sherwood et al., 2022). By comparing with a hindcast and with limited observations, we can quantify how the erosion predictions changed across forecasts. As anticipated, later forecasts with improved storm tracks better predicted dune impacts based on qualitative observational data. This trend of improved predictions closer to landfall is present as the storm moved through the three regions. In southwest Florida, the dune impact predictions improve as the track converges, with fewer ‘impact’ transects to the north of the eventual landfall location. This trend aligns with qualitative observations of coastal erosion during Ian for this region. For southeast Florida, XBeach and the TWLCCFV generally agreed that more than 80 percent of the transects in this region would not experience dune impacts. However, XBeach is able to provide additional erosion metrics, such as percent volume change, which help to inform future vulnerability assessment. There was less agreement between the XBeach and TWLCCFV forecast predictions for the southeast Atlantic coast. XBeach generally predicted greater dune impacts than the TWLCCFV for most forecasts, but the forecast models converged to a nearly 80-percent agreement. In later forecasts, the TWLCCFV began to predict more impacted locations and agree with the dune impact predictions made several advisories earlier by XBeach. Without observations, neither forecast can be interpreted as ‘truth’, but we can see forecast improvements via model convergence for advisories closer to the timing of the regional landfall. The time of convergence is about three days before landfall, which aligns with the conclusions of previous studies comparing forecast lead time and morphological modeling skill (Baart et al., 2016).

We can use the XBeach forecasts, which include morphodynamics, to explore differences from (and possible advantages relative to) the TWLCCFV forecasts, which rely on a static ground surface. Both forecasts can predict the dune impact regimes, by using TWL to identify regimes via Sallenger (2000), but XBeach can also predict the actual changes to the dune crest elevation. Depending on the threshold (TWL or actual dune crest change), the forecasts may vary in their predictions of dune impacts.

For a water-level threshold (Figure 4.18a), the timing of dune impact is selected as the first time step in the XBeach simulation when water reaches the dune crest, essentially relying on the hydrodynamics of the model to trigger the dune impact decision. As expected, transects on the southwest Florida coast closer to observed landfall are forecasted to experience dune impacts within 10 hours (before or after landfall), but transects in South Carolina predict dune impacts more than 40 hours later. This aligns with the general progression and track of the storm. There is a spatial trend where transects on the strong side (south of the track in southwest Florida) predict dune impact before the regional landfall, whereas transects on the weak side (north of the track in southwest Florida) predict after the regional landfall. There are a few locations in southeast Florida that experience dune impact much later than the surrounding locations. The cause of these late predictions is unknown, given that Ian has already passed this region. The hourly TWLCCFV predictions could create a similar map based purely on a water-level threshold, but it is unable to signal erosion based on dynamic morphological change.

For a morphodynamic threshold (Figure 4.18b) the timing of dune crest impact can be identified as the time step when the dune crest elevation is changed by more than 0.2m. This is a direct route to impact categorization. Timing of dune crest elevation change over a 0.2 m threshold signals significant dune erosion, whereas the water-level threshold does not provide direct information about erosion. Both the water-level and morphodynamic thresholds result in similar spatial trends. A key difference between the maps is the handfuls of transects in southeast and southwest Florida that predict dune crest elevation changes much later in the simulation (more than 40 hours after initial landfall) than with the water-level threshold. This could be a result of several factors. Most likely, the delay in dune crest elevation changes is related to additional ground surface information included in XBeach, such as bed friction information. Large bed friction values at the dune crest could potentially prevent dune crest lowering while the total water levels still overwash or inundate the transect. Without temporal observations of hydrodynamics and coastal change, it is impossible to determine which threshold provides the more accurate time estimate of storm impact. The general similarity between the two models signifies the effectiveness of the water-level threshold implemented in the modeling framework.

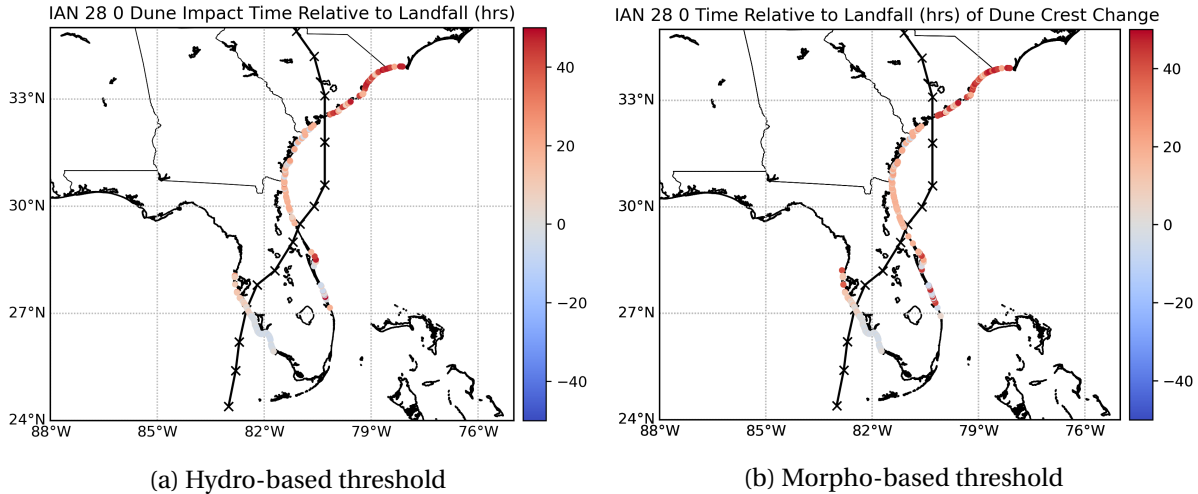


Figure 4.18: Timing of dune impact, represented as hours relative to Ian’s initial landfall in southwest Florida at 2000 UTC 28 September. Panels identify the timing of dune impact via thresholds of: (a) when water levels reach the dune crest, or (b) when the dune crest elevation is changed by more than 0.2 m. Lighter colors indicate impacts predicted closer to the observed landfall. Negative or blue colors indicate dune impacts before 0000 UTC 28 September, and positive or red colors indicate dune impacts after the initial landfall.

4.3.3 Remaining Challenges

The modeling framework described in this thesis was implemented to predict the erosion of beaches and dunes along the U.S. Atlantic and Gulf coast for Michael and Ian. The XBeach 1D models are successful in predicting locations of significant dune erosion along large stretches of the coast. This section will discuss the remaining challenges for the modeling framework. The challenges include: (a) automating the entire modeling process; (b) effectively communicating erosion risk without oversimplifying or misrepresenting the model results; (c) parameter calibration to replace the ‘wall’ back-boundary condition; and (d) sensitivity testing to better understand temporal discrepancies between forecast models and observational data.

The current model framework requires a user to initiate the scripts and provide storm track information for each advisory simulation. To produce timely forecast results, this semi-automated approach relies heavily on the promptness of the user. To ensure reliable and consistent predictions every 6 hr (or as soon as the ADCIRC+SWAN forecast results are available), the framework would need to be fully automated. This includes adjusting the transect selection from user-specified information to a track-dependant method. This automation may also avoid excess computation and unrepresentative simulations by only selecting transects within the future forecast cone.

Observations for real-time forecasting are often challenging to obtain. The majority of our

predictive evaluation is comparison to other forecast models. A comparison requires both of our models to be using similar scales and metrics. For this reason, a focus of this thesis has been analyzing how well dune impact categorization represents coastal vulnerability to storm-driven erosion. However, this binary categorization significantly reduces the information produced by the model, and it could misrepresent the observed changes. For example, if the dune crest elevation is lowered by dynamic morphology and the TWL reaches the dune crest index (which is now more attainable), the profile would be flagged as impacted without observed overwash or inundation. While binary dune impact prediction is generally successful in identifying vulnerable regions, the metric may oversimplify the results and lead to misrepresentation in some cases.

A ‘wall’ back-boundary condition is applied to all forecasts to prevent unrealistic over-erosion and complete subaerial volume removal. This parameter was added after several Michael test cases became unstable during profile inundation. Multiple other approaches were attempted, including non-erodible layers and setting the back boundary water elevation to zero, but they were not effective in maintaining a realistic subaerial profile volume. Unfortunately, the wall boundary condition causes water to pool behind the dune and remain there for the rest of the storm duration. This likely affects the morphodynamics of the profile when overwash or inundation occurs. Additionally, the no-flux wall causes water levels in the back of the domain to not fluctuate during the simulation. This means the XBeach simulations do not consider outwash or other processes for profiles located between the ocean and a bay. More calibration and other test cases are necessary to remove the ‘wall’ back-boundary condition while maintaining model stability.

A key challenge and motivator for future work is to improve predictions on every individual transect. While XBeach and TWLCCFV typically match in their overall prediction of dune impact, there are some temporal discrepancies. As an example, we consider observations and forecasts of water levels near Naples, FL (Figure 4.19). Even in the water levels, there are successes and challenges, which would then translate to discrepancies in erosion predictions.

NOAA station 8725110 (green line in Figure 4.19) is located along the open coast near Naples, FL, and it observed the storm’s effects on water levels before landfall. The tides oscillate between +/- 0.5 m (NAVD88) during 27 September and the first half of 28 September, but then the water levels rise rapidly to an observed peak of about 2 m. The station failed as the storm made landfall (National Oceanic and Atmospheric Administration, 2023e). The ADCIRC forecast on 0000 UTC 27 September matches the observations in timing and amplitude during 27 September, but then overpredicts during the first tidal cycle on 28 September. The effects of wave setup (via coupling with SWAN) are evident in the ADCIRC predictions. At an offshore location (red line in Figure 4.19) corresponding to the XBeach transect boundary, the ADCIRC

peak water level of about 1.7 m is reasonably close to the observed peak, but it occurs several hours before landfall. At a nearshore location (pink line in Figure 4.19), the ADCIRC peak water level of about 2.2 m is higher due to wave setup at the coast.

While the ADCIRC predictions can show the effects of wave setup, the TWLCCFV predictions can show the effects of wave runup. For this forecast, TWLCCFV water levels are plotted for their case with 'tidewindsetup' (black line in Figure 4.19) and TWL (blue line). The TWLCCFV-predicted TWL jumps from 0.5 to 2 m when forecasted wave heights spike at the beginning of 28 September. This is almost 12 hours before the observed spike in water elevations, and about 1 m higher than the case without wave runup. The peak TWL is about 2.25 m at 1700 UTC 28 September before wave heights gradually decrease over the upcoming days. The inclusion of wave runup is one factor why the ADCIRC and TWLCCFV water levels are different, but it does not explain the mismatch when runup is excluded. Another factor may be the different sources for atmospheric forcing. Although the TWLCCFV uses ADCIRC- and SWAN-based models for Ian (ESTOFS and NWPS, U.S. Geological Survey, 2023b), the atmospheric forcing for those models is different than COAMPS-TC (Chen et al., 2003). This difference in atmospheric forcing may then translate to different waves and water levels in the TWLCCFV forecasts.

The XBeach water levels show different behavior. At its offshore boundary, the XBeach water levels (yellow line in Figure 4.19) follow closely to the ADCIRC water levels (red line) from which they were interpolated, especially a close match to the peak water level of about 1.7 m. The exception is during the first half of 28 September when the XBeach water levels are lower and closer to the observations. However, XBeach water levels in the nearshore, evaluated about 1 m offshore of transect T4071, lag the ADCIRC-predicted peak of the water levels by about 3 hr consistently during this time period. The cause of this lag is unknown, but it may be caused by the long length of the XBeach transect, which extends 25 km offshore. Based on temporal plots (not shown) of water levels across the entire transect, the water level changes at the boundary seem to propagate slower than they should through the domain, resulting in water level differences between the offshore boundary and nearshore. Shorter transects (about 3 m) from other test cases do not show the same temporal lag. Previous XBeach calibration studies used profiles that were 5 km or less (Simmons et al., 2019), however XBeach documentation does not provide a suggested length range. Additionally, the XBeach nearshore forecasted water levels have greater peaks, with a maximum water elevation of nearly 3 m at 2000 UTC 28 September. The cause of the steep water elevation changes is currently unknown. It should be mentioned that the water elevations for XBeach include tide, surge, and wave setup, so infragravity wave representation in the model may play a role in the steep nearshore water level peaks. Further transect length sensitivity analysis and general hydrodynamic assessment is required to better understand these temporal and elevation discrepancies.

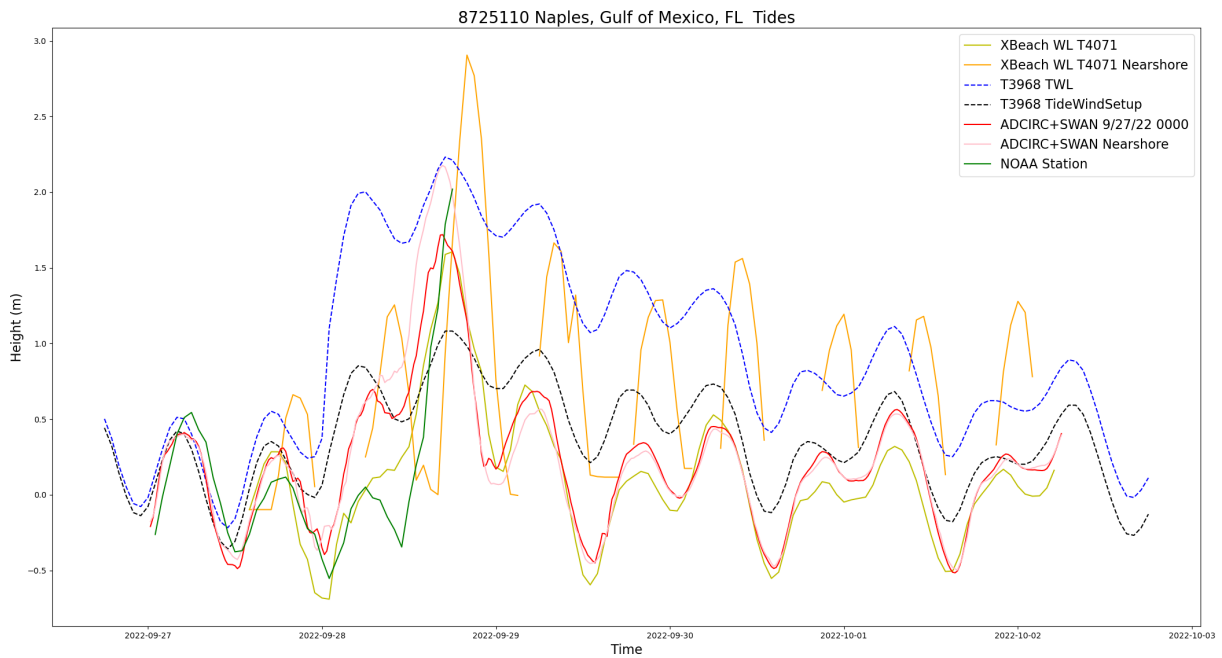


Figure 4.19: Water level time series in NAVD88 for forecasts or observations at 0000 UTC 27 September. The dashed lines are from the TWLCCFV api, with the blue and black color indicating the hourly TWL and ‘tidewindsetup’ forecasts respectively (U.S. Geological Survey, 2023b). Observational water levels from Station 8725110- Naples, FL are included in green (before damage during the peak of Ian). The red and pink lines are ADCIRC forecasted water levels at the tide gauge and a location closer to shore (-82.0335,26.436) respectively. XBeach water elevations at the offshore origin in yellow and at the shoreline in orange for the closest transect to the tide gauge (T4071).

CHAPTER

5

CONCLUSIONS AND FUTURE WORK

Beaches and dunes help to protect our coastal communities during extreme events by acting as a barrier between storm conditions and local infrastructure or property. It is important to forecast which regions of the coast are vulnerable to storm impacts and inform local stakeholders or decision-makers about predicted impacts. This research aims to build an accurate and efficient modeling framework that can predict spatial and temporal erosion and effectively communicate the forecasts to a broad audience. The framework is first validated with a hindcast simulation of Michael (2018), which demonstrates the model's ability to predict which regions of the coast are anticipated to experience significant storm-driven erosion and dune impacts. The validated framework is then implemented for real-time forecasting during Ian (2022). The results are compared to an established forecast model to understand how the dynamic morphology and high-resolution ground surface information in the XBeach model affect the predictions of storm impacts. The dynamic aspect of the XBeach model allows us to understand how the storm progresses and how the transect evolves in response when temporal observational data are not available. This work improves our ability to forecast coastal change and expands our knowledge of storm-driven morphodynamics as a whole. The major conclusions of this study are:

- *The modeling framework is accurate and efficient for real-time forecasting of coastal erosion.* The XBeach models are able to accurately predict about 90% of the observed

dune impacts for Michael. The entire forecasting process from preparation to evaluation for about 1800 simulations is typically completed in under 70 minutes, verifying the efficiency of the framework.

- *Dynamic morphology affects the predicted dune impacts.* Erosion throughout the model can weaken or lower the dune earlier in the storm duration. When compared to the TWLCCFV, the dynamic XBeach forecasts can differ in the timing of impact or dune impact category. This could potentially be a result of the morphodynamics in the model.
- *XBeach provides valuable information about the storm not previously available.* The high-resolution ground surface information allows for additional computations, such as dune crest elevation and percent volume change, that are not possible for empirical forecast approaches. Observations of ground surface evolutions throughout Ian are unavailable, so the dynamic XBeach models provide bed-level predictions to represent erosion throughout the storm.

There are multiple ways the forecasts can be improved or expanded upon for future work:

- *Full automation of the modeling framework.* Currently, forecasts are initiated manually and require user-specified information about the forecast track. By automating the initial transect selection based on the forecasted landfall location, there is less user responsibility and the forecast will innately become more efficient.
- *Distinguish between dune overwash and inundation in categorization.* A binary dune impact categorization is currently used to represent vulnerable locations along the coast. Other forecast models use three to four categories to present storm impacts. Splitting the dune impact prediction categories would provide more information about the scale of predicted storm-driven erosion.
- *Remove back boundary conditions.* XBeach tends to remove all subaerial sand when inundation occurs to a depth that is unrealistic. To avoid this, a back wall boundary was implemented as a short-term fix for this issue, however this causes water to pool behind the dune and prevents flow out of the back boundary. To remove this boundary condition, a full-scale calibration is required to avoid unrealistic scour from the profile.
- *Sensitivity analysis to understand water level lag.* In the discussion, we highlight a lag in the XBeach predicted water levels in comparison to other observational or forecast data. This could be a result of several factors. Further testing and analysis is required to understand and avoid this issue.

- *Trigger a more robust 2D XBeach model.* While the 1D model is able to capture cross-shore sediment transport, a 2D model could include the alongshore component of coastal change during extreme events. The established 1D framework can be used to trigger 2D models in the more susceptible locations.

To better understand and represent coastal erosion along the U.S. Atlantic and Gulf coasts, further analysis and improvements to the created forecasting framework are essential. A majority of these suggestions were attempted, however time constraints prevented the amount of attention required. With more time and development, this modeling approach can provide additional information about predicted coastal erosion that is not typically available in real-time forecasting. This will allow us to better prepare for extreme events and protect coastal communities from storm-driven erosion along the U.S. Atlantic and Gulf coast, and potentially other locations as well.

BIBLIOGRAPHY

- Anderson, J. R. et al. (1976). *A Land Use and Land Cover Classification System for Use with Remote Sensor Data*. Tech. rep. 964. Geological Survey Professional Paper.
- Baart, F et al. (2003). “Real-time forecasting of morphological storm impacts: A case study in the Netherlands”. In: *Journal of Coastal Research* 56, pp. 1617–1621.
- Baart, F et al. (2011). “Confidence in real-time forecasting of morphological storm impacts”. In: *Journal of Coastal Research* SI 64, pp. 1835 –1839.
- Baart, F et al. (2016). “Morphological impact of a storm can be predicted three days ahead”. In: *Computers & Geosciences* 90, pp. 17–23.
- Beuzen, T et al. (2019a). “Controls of variability in berm and dune storm erosion”. In: *Journal of Geophysical Research: Earth Surface* 124, 2647—2665.
- Beuzen, T et al. (2019b). “Ensemble models for machine learning: an example of wave runup and coastal dune erosion”. In: *Natural Hazards Earth System Science* 19, 2295—2309.
- Beven, J and Lalaka (2023). *National Hurricane Center Tropical Cyclone Report, Hurricane Nicole (AL172022) 7-11 November 2022*. Tech. rep. [Retrieved 23 May 2023]. National Hurricane Center.
- Beven, J. L. et al. (2019a). *National Hurricane Center Tropical Cyclone Report, Hurricane Michael (AL142018) 7-11 October 2018*. Tech. rep. [Retrieved 10 May 2021]. National Hurricane Center.
- (2019b). *Tropical Cyclone Report, Hurricane Michael, 7-11 October 2018*. Tech. rep. National Hurricane Center.
- Bilskie, M. V. et al. (2020). “Unstructured finite element mesh decimation for real-time Hurricane storm surge forecasting”. In: *Coastal Engineering* 156, p. 103622.
- Bilskie, M. V. et al. (2022). “Real-Time Simulated Storm Surge Predictions during Hurricane Michael (2018)”. In: *Weather and Forecasting* 37, pp. 1085 –1102.
- Blanton, B. O. and R. A. Luettich (2008). *North Carolina Coastal Flood Analysis System: Model Grid Generation*. Tech. rep. TR-08-05. Renaissance Computing Institute.
- Blanton, B. O. et al. (2012). “Urgent Computing of Storm Surge for North Carolina’s Coast”. In: *Proceedings of the International Conference on Computational Science*. Vol. 9, pp. 1677–1686.
- Booij, N et al. (1999). “A third-generation wave model for coastal regions, Part I, Model description and validation”. In: *Journal of Geophysical Research* 104, pp. 7649–7666.
- Bosboom, J et al. (2014). “On the perception of morphodynamic model skill”. In: *Coastal Engineering* 94, pp. 112–125.

- Bucci, L et al. (2023a). *National Hurricane Center Tropical Cyclone Report, Hurricane Ian (AL092022) 23-30 September 2022*. Tech. rep. [Retrieved 10 April 2023]. National Hurricane Center.
- (2023b). *Tropical Cyclone Report for Hurricane Ian, 23 September – 30 September 2022*. Tech. rep. National Hurricane Center.
- Canizares, R and J. L. Irish (2008). “Simulation of storm-induced barrier island morphodynamics and flooding”. In: *Coastal Engineering* 55, pp. 1089–1101.
- CERA Historical Storm Archive (2023). <https://historicalstorms.coastalrisk.live/>. [Retrieved 6 April 2023].
- Chen, S et al. (2003). *COAMPS™ Version 3 Model Description - General Theory and Equations*. Tech. rep. NRL/PU/7500–04-448. Naval Research Laboratory.
- Cho, M et al. (2012). “Comparative Study on the Numerical Simulation of Bathymetric Changes under Storm Condition”. In: *Journal of Coastal Research* SI 91, pp. 106–110.
- CIRES (2014). *Continuously Updated Digital Elevation Model (CUDEM) - 1/9 Arc-Second Resolution Bathymetric-Topographic Tiles*. https://coast.noaa.gov/htdata/raster2/elevation/NCEI_ninth_Topobathy_2014_8483/. Accessed 15 July 2021.
- Clark, R et al. (2022). *Hurricane Ian & Hurricane Nicole Preliminary Post-Storm Beach Conditions and Coastal Impact Report*. Tech. rep. Florida Department of Environmental Protection.
- Coastal Emergency Risks Assessment (2019). <https://cera.coastalrisk.live/>. [Retrieved 28 May 2019].
- Dietrich, J. C. et al. (2011a). “Hurricane Gustav (2008) Waves and Storm Surge: Hindcast, Validation and Synoptic Analysis in Southern Louisiana”. In: *Monthly Weather Review* 139 (8), pp. 2488–2522.
- Dietrich, J. C. et al. (2011b). “Modeling Hurricane Waves and Storm Surge using Integrally-Coupled, Scalable Computations”. In: *Coastal Engineering* 58, pp. 45–65.
- Dietrich, J. C. et al. (2018). “Sensitivity of Storm Surge Predictions to Atmospheric Forcing During Hurricane Isaac”. In: *Journal of Waterway, Port, Coastal and Ocean Engineering* 144 (1).
- Fleming, J et al. (2008). “A Real Time Storm Surge Forecasting System Using ADCIRC”. In: *Estuarine and Coastal Modeling (2007)*, pp. 893–912.
- Galappatti, R and C. B. Vreugdenhil (1985). “A depth integrated model for suspended transport”. In: *Journal of Hydraulic Engineering* 23 (4), pp. 359–377.
- Gharagozlou, A et al. (2020). “Storm-Driven Erosion and Inundation of Barrier Islands from Dune- to Region-Scales”. In: *Coastal Engineering* 158.103674.
- Gharagozlou, A et al. (2022). “Emulator for Eroded Beach and Dune Profiles due to Storms”. In: *Journal of Geophysical Research: Earth Surface*.

- Harley, M et al. (2011). “Evaluation of XBeach predictions for a real-time warning system in Emilia-Romagna, Northern Italy”. In: *Journal of Coastal Research* (Special Issue 64: PROCEEDINGS OF THE 11th INTERNATIONAL COASTAL SYMPOSIUM ICS 2011), pp. 1861–1865.
- Harter, C and J Figlus (2017). “Numerical modeling of the morphodynamic response of a low-lying barrier island beach and foredune system inundated during Hurricane Ike using XBeach and CSHORE”. In: *Coastal Engineering* 120, pp. 64–74.
- Himmelstoss, E et al. (2017). “National Assessment of Shoreline Change—summary statistics for updated vector shorelines and associated shoreline change data for the Gulf of Mexico and southeast Atlantic coasts”. In: *USGS Data Release*.
- Jager, W. S. et al. (2018). “A Bayesian network approach for coastal risk analysis and decision making”. In: *Coastal Engineering* 134, April, pp. 48–61.
- Johnson, B. D. et al. (2012). *Cross-Shore Numerical Model CSHORE for Waves, Currents, Sediment Transport and Beach Profile Evolution*. Tech. rep. TR-12-22. Vicksburg, Mississippi: Coastal Engineering Research Center, U.S. Army Engineer Waterways Experiment Station.
- Kalligeris, N et al. (2020). “Calibration and assessment of process-based numerical models for beach profile evolution in southern California”. In: *Coastal Engineering* 158, p. 103650.
- Knutson, T (2023). *Global Warming and Hurricanes: An Overview of Current Research Results*. <https://www.gfdl.noaa.gov/global-warming-and-hurricanes/>. [Retrieved 15 May 2023].
- Kobayashi, N (2016). “Coastal Sediment Transport Modeling for Engineering Applications”. In: *Journal of Waterway, Port, Coastal, and Ocean Engineering* 142.6, p. 03116001.
- Larson, M and N Kraus (1989). *SBEACH: numerical model for simulating storm-induced beach change. Report 1: Empirical Foundation and Model Development*. Tech. rep. CERC-89-9. Vicksburg, Mississippi: US Army Engineer Waterways Experiment Station.
- Luetlich, R. A. et al. (1992). *ADCIRC: An Advanced Three-Dimensional circulation model for shelves coasts and estuaries, report 1: Theory and methodology of ADCIRC-2DDI and ADCIRC-3DL*. Tech. rep. United States Army Corps of Engineers.
- McCall, R. T. et al. (2023). “Accounting for directional wave spreading effects on infragravity wave growth in a 1d dune erosion model”. In: *Coastal Sediments 2023*.
- Mickey, R. C. and D. L. Passeri (2022). “A Database of Topo-Bathy Cross-Shore Profiles and Characteristics for U.S. Atlantic and Gulf of Mexico Sandy Coastlines”. In: *Data* 7, p. 92.
- Mitasova, H et al. (1996). “Modelling topographic potential for erosion and deposition using GIS”. In: *International Journal of Geographical Information Systems* 10.5, pp. 629–641.
- Multi-Resolution Land Characteristics Consortium (2019). *MRLC Viewer*.

- National Geodetic Survey (2016). *2016 NOAA NGS Topobathy Lidar: St. Joe (FL)*. <https://www.fisheries.noaa.gov/inport/item/48179>. [Retrieved 16 May 2023].
- National Hurricane Center (2021). *Storm Surge Overview*. <https://www.nhc.noaa.gov/surge/>. [Retrieved 10 May 2021].
- National Oceanic and Atmospheric Administration (2021). *Storm Surge and Tide Operational Forecast*. <https://polar.ncep.noaa.gov/estofs/>. [Retrieved 1 March 2021].
- (2022). *2022 NOAA NGS Emergency Response Imagery: Hurricane Ian*. <https://storms.ngs.noaa.gov/storms/ian/index.html>. [Retrieved 15 May 2023].
- (2023a). *Nearshore Wave Prediction System*. <https://polar.ncep.noaa.gov/nwps/>. [Retrieved 15 May 2023].
- (2023b). *NOAA Economics and Demographics*. <https://coast.noaa.gov/states/fast-facts/economics-and-demographics.html>. [Retrieved 15 May 2023].
- (2023c). *NOAA Hurricane Costs*. <https://coast.noaa.gov/states/fast-facts/hurricane-costs.html>. [Retrieved 15 May 2023].
- (2023d). *Probabilistic Tropical Storm Surge 3.0*. <https://slosh.nws.noaa.gov/psurge/>. [Retrieved 15 May 2023].
- (2023e). *Tides and Currents*. <https://tidesandcurrents.noaa.gov/>. [Retrieved 23 May 2023].
- (2023f). *WAVEWATCH III Model Description*. <https://polar.ncep.noaa.gov/waves/wavewatch/>. [Retrieved 23 May 2023].
- National Weather Service (2019). *Catastrophic Hurricane Michael Strikes Florida Panhandle, October 10, 2018*. <https://www.weather.gov/tae/HurricaneMichael2018>. [Retrieved 18 May 2023].
- OCM Partners (2010). *2010 USACE NCMP Topobathy Lidar: Gulf Coast (AL, FL)*. <https://www.fisheries.noaa.gov/inport/item/50083>. [Retrieved 16 May 2023].
- (2015). *2015 USACE NCMP Topobathy Lidar: Florida Gulf Coast*. <https://www.fisheries.noaa.gov/inport/item/49720>. [Retrieved 16 May 2023].
- (2018). *2018 USACE FEMA Post-Michael Topobathy Lidar: Florida Panhandle*. <https://www.fisheries.noaa.gov/inport/item/54682>. [Retrieved 16 May 2023].
- Passeri, D. L. et al. (2018). “The influence of bed friction variability due to land cover on storm-driven barrier island morphodynamics”. In: *Coastal Engineering* 132, pp. 82–94.
- pyproj* (2023). <https://pypi.org/project/pyproj/>. [Retrieved 15 May 2023].
- rasterio* (2023). <https://rasterio.readthedocs.io/en/stable/intro.html>. [Retrieved 15 May 2023].
- Roelvink, D et al. (2009). “Modelling storm impacts on beaches, dunes and barrier islands”. In: *Coastal Engineering* 56, pp. 1133–1152.

- Roelvink, D et al. (2010). *XBeach Model Description and Manual*. Tech. rep. UNESCO-IHE Institute for Water Education, Deltares and Delft University of Technology.
- Roelvink, J. A. (1993). “Dissipation in random wave groups incident on a beach”. In: *Coastal Engineering* 19, pp. 127–150.
- Roelvink, J. A. and G. V. Banning (1994). “Design and development of Delft3D and application to coastal morphodynamics”. In: International Association for Hydraulic Research, Rotterdam, 451—455.
- Ruggiero, P et al. (2001). “Wave runup, extreme water levels and the erosion of properties backing beaches.” In: *Journal of Coastal Research* 17(2), 407—419.
- Sallenger, A. H. (2000). “Storm impact scale for barrier islands”. In: *Journal of Coastal Research* 16 (3), pp. 890–895.
- Santos, V. M. et al. (2019). “Combining numerical and statistical models to predict storm-induced dune erosion”. In: *Journal of Geophysical Research: Earth Surface* 124, 1817–1834.
- Schweiger, C et al. (2020). “Spatial and temporal evaluation of storm-induced erosion modelling based on a two-dimensional field case including an artificial unvegetated research dune”. In: *Coastal Engineering* 161, p. 103752.
- Sherwood, C. R. et al. (2022). “Modeling the morphodynamics of coastal responses to extreme events: what shape are we in?” In: *Annual review of marine science* 14, pp. 457–492.
- Simmons, J. A. et al. (2017). “Calibrating and assessing uncertainty in coastal numerical models”. In: *Coastal Engineering* 125, 28–41.
- Simmons, J. A. et al. (2019). “Calibration data requirements for modeling subaerial beach storm erosion”. In: *Coastal Engineering* 152.103507.
- Splinter, K. D. and M. L. Palmsten (2012). “Modeling dune response to an East Coast Low”. In: *Marine Geology* 329–331, pp. 46–57.
- Splinter, K. D. et al. (2014). “A relationship to describe the cumulative impact of storm clusters on beach erosion”. In: *Coastal Engineering* 83, pp. 49–55.
- Stockdon, H. F. et al. (2006). “Empirical parameterization of setup, swash, and runup”. In: *Coastal Engineering* 53, pp. 573–588.
- Stockdon, H. F. et al. (2023). “Operational forecasts of wave-driven water levels and coastal hazards for US Gulf and Atlantic coasts”. In: *Communications Earth amp; Environment* 4.1.
- Thomas, A et al. (2019). “Influence of Storm Timing and Forward Speed on Tide-Surge Interactions during Hurricane Matthew”. In: *Ocean Modelling* 137, pp. 1–19.
- U.S. Geological Survey (2016). *Coastal Change Hazards Portal*. <http://marine.usgs.gov/coastalchangehazardsportal/>. [Retrieved 18 July 2016].
- (2023a). *Coasts, Storms, and Sea Level Rise*. <https://www.usgs.gov/science/science-explorer/climate/coasts-storms-and-sea-level-rise>. [Retrieved 23 May 2023].

- U.S. Geological Survey (2023b). *USGS Total Water Level and Coastal Change Forecast Viewer*. <https://coastal.er.usgs.gov/hurricanes/research/twlviewer/>. [Retrieved 16 May 2023].
- (2023c). *Wave runup (R) is the time-varying elevation of water level at the sho*. <https://www.usgs.gov/media/images/wave-runup-r-time-varying-elevation-water-level-sho>. [Retrieved 23 May 2023].
- USGS (2019). *NLCD 2019 Land Cover (CONUS)*. [Retrieved 23 May 2022].
- USGS (2023). <https://www.usgs.gov/faqs/what-digital-elevation-model-dem>. [Retrieved 17 April 2023].
- van der Lugt, M. A. et al. (2019). “Morphodynamic modeling of the response of two barrier islands to Atlantic hurricane forcing”. In: *Estuarine, Coastal and Shelf Science* 229.106404.
- van Thiel de Vries, J. S. M. (2010). “Dune erosion during storm surges”. PhD thesis. Delft, The Netherlands: Delft University of Technology.
- Vousdoukas, M. I. et al. (2012). “Toward reliable storm-hazard forecasts: XBeach calibration and its potential application in an operational early-warning system”. In: *Ocean Dynamics* 62, pp. 1001–1015.
- Water Resource Management, D. of (2019). *Hurricane Michael Post-Storm Beach Conditions and Coastal Impact Report*. Tech. rep. Florida Department of Environmental Protection.
- Westerink, J. J. et al. (2008). “A Basin to Channel Scale Unstructured Grid Hurricane Storm Surge Model Applied to Southern Louisiana”. In: *Monthly Weather Review* 136 (3), pp. 833–864.

APPENDIX

APPENDIX

A

APPENDIX

A.1 XBeach Parameters

This is an example of the parameter file for transect 4074 (Fort Myers,FL) during a forecast at 0600 UTC 27 September 2022:

%%%% This is for Transect 4074

%% Bed composition parameters %%

D50 = 0.000225

%% Flow boundary condition parameters %%

front = abs_1d
back = wall
tidetype = velocity

%% Flow parameters %%

bedfriction = manning
bedfricfile = T4074_bedfric.txt
nuhfac = 0

%% General %%

alfaD50 = 0.400000
deltahmin = 0.100000
droot = 0.500000
dstem = 0.500000
dtheta_s = 10
dynamicroughness = 1
fixedavaltime = 0
gridform = xbeach
oldTmin = 0
oldhmin = 0
single_dir = 1
wavemodel = surfbeat
wbctype = jonstable

%% Grid parameters %%

depfile = y_file_tnsct_4074.txt
posdwn = 0
nx = 2463
ny = 0
alfa = 63.393904607779284
vardx = 1
xfile = x_file_tnsct_4074.txt
thetamin = 116.60609539222071
thetamax = 296.6060953922207
thetanaut = 1

%% Model time %%

tstop = 448800

%% Morphology parameters %%

morfac = 5
morstart = 1800
wetslp = 0.180000
struct = 0

%% Physical processes %%

sedtrans = 1
morphology = 1

%% Roller parameters %%

beta = 0.080000

%% Sediment transport parameters %%

waveform = vanthiel
facSk = 0.150000
facAs = 0.250000

%% Tide boundary conditions %%

zs0file = wl_4074.txt
tideloc = 1

%% Wave breaking parameters %%

break = roelvink_daly
gamma = 0.460000
gamma2 = 0.340000
alpha = 1.380000

%% Wave numerics parameters %%

wavint = 3600

%% Wave-spectrum boundary condition parameters %%

bcfile = wv_4074.txt

%% Output variables %%

outputformat = netcdf
tintm = 3600
tintp = 1
tintg = 3600
tstart = 0

nglobalvar = 3
zb
zs
H